

SUPPORTING INFORMATION

A Rh-Catalyzed Cycloisomerization/Diels-Alder Cascade Reaction of 1,5-Bisallenes for the Synthesis of Polycyclic Heterocycles

Albert Artigas, Jordi Vila, Agustí Lledó, Miquel Solà, Anna Pla-Quintana, Anna Roglans.

Institut de Química Computacional i Catàlisi (IQCC) and Departament de Química,
Universitat de Girona (UdG), Facultat de Ciències, C/ Maria Aurèlia Capmany, 69, 17003-
Girona, Catalunya, Spain.

TABLE OF CONTENTS

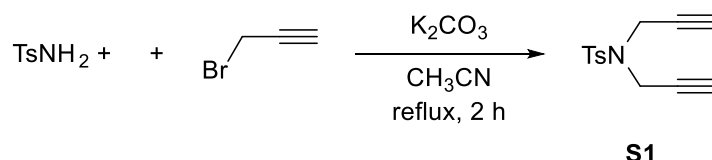
• General materials and methods.....	S4
• Scheme S1. Synthesis of diyne S1.....	S5
• Scheme S2. Synthesis of bisallenes 1a-b.....	S5
• Table S1. Optimization of the rhodium(I)-catalyzed cycloaddition of bisallene 1a with alkene 2a.....	S7
• Synthesis of compounds 3aa-3bj.....	S9
• Scheme S3. General procedure for the synthesis of product 3aa.....	S9
• Compound 3ab.....	S10
• Compound 3ac.....	S10
• Compound 3ad.....	S11
• Compound 3ae.....	S11
• Compound 3af.....	S12
• Compound 3ag.....	S12
• Compound 3ah.....	S13
• Compound 3ai.....	S13
• Compound 3aj.....	S14
• Compound 3ak.....	S14
• Compound 3al.....	S15
• Compound 3am.....	S15
• Compound 3ba.....	S16
• Compound 3bg.....	S16
• Compound 3bj.....	S17
• Scheme S4. Mechanistic experiments using compound 5a and ethyl acrylate 2a.....	S18
• Scheme S5. Mechanistic experiments using compound 5a, ethyl acrylate 2a and Rh(I) catalyst.....	S18
• Scheme S6. Mechanistic experiments using compound 1a and Rh(I) catalyst.....	S19
• ¹ H and ¹³ C NMR spectra.....	S20
• Diyne S1.....	S20
• Bisallene 1a.....	S22
• Bisallene 1b.....	S24
• Product 3aa.....	S26
• Product 3ab.....	S37
• Product 3ac.....	S39
• Product 3ad.....	S43
• Product 3ae.....	S47
• Product 3af.....	S50
• Product 3ag.....	S53
• Product 3ah.....	S56
• Product 3ai.....	S59

• Product 3aj.....	S62
• Product 3ak.....	S65
• Product 3al.....	S68
• Product 3am.....	S71
• Product 3ba.....	S74
• Product 3bg.....	S77
• Product 3bj.....	S86
• Product 4a.....	S89
• Product 5a.....	S95
• Product 6a.....	S97
• HPLC	S106
• Figure S1. HPLC trace of compound 3aa obtained using (±)-BINAP as a phosphine ligand.	S106
• Figure S2. HPLC trace of compound 3aa obtained under optimal conditions, using (<i>R</i>)- DTBM-Segphos as a phosphine ligand.	S106
• Crystal structure of compound 3am.....	S107
• Figure S3: ORTEP representation of compound 3am with probability level of 30%.	S107
• Table S2. Sample and crystal data for 3am.	S108
• Table S3. Data collection and structure refinement for 3am.....	S108
• Table S4. Atomic coordinates and equivalent isotropic atomic displacement parameters (Å ²) for 3am.	S109
• Computational methods.....	S110
• Figure S4. Molecular structures of (a) TS A1A2, (b) TS A2A3, (c) TS A3A4, (d) TS A3'B1, (e) TS A5-3aa' and (f) TS A5-3aa. Distances are given in Angstroms (Å). Hydrogen atoms not shown for clarity.	S111
• Figure S5. M06L-D3/cc-pVTZ-PP/SMD(76% THF, 24% CH ₂ Cl ₂)/B3LYP-D3/cc-pVDZ-PP Gibbs energy profile for the tandem cycloisomerisation/Diels-Alder cycloaddition of 1,5- bisallene 1a and ethyl acrylate catalysed by [Rh(BINAP)] ⁺ . Alternative reaction path: Diels- Alder cycloaddition involving intermediate A4.	S112
• Figure S6. M06L-D3/cc-pVTZ-PP/SMD(76% THF, 24% CH ₂ Cl ₂)/B3LYP-D3/cc-pVDZ-PP Gibbs energy profile for the tandem cycloisomerisation/Diels-Alder cycloaddition of 1,5- bisallene 1a and ethyl acrylate catalysed by [Rh(BINAP)] ⁺ . Alternative reaction path: Diels- Alder cycloaddition involving intermediate A3.	S113
• Figure S7. M06L-D3/cc-pVTZ-PP/SMD(76% THF, 24% CH ₂ Cl ₂)/B3LYP-D3/cc-pVDZ-PP Gibbs energy profile for the tandem cycloisomerisation/Diels-Alder cycloaddition of 1,5- bisallene 1a and ethyl acrylate catalysed by [Rh(BINAP)] ⁺ . Alternative reaction path: Diels- Alder cycloaddition involving intermediate A2.	S114
• Figure S8. (a) M06L-D3/cc-pVTZ-PP/SMD(76% THF, 24% CH ₂ Cl ₂)/B3LYP-D3/cc-pVDZ- PP Gibbs energy profile for the transformation of intermediate C1 into intermediate A2 catalysed by [Rh(BINAP)] ⁺ . (b) Molecular structure of TS C1A2. Distances are indicated in Angstroms (Å). ΔG relative to 1a + catalyst. Hydrogen atoms suppressed for clarity.	S115
• Computational data	S116
• References.....	S116

General materials and methods

Unless otherwise noted, materials were obtained from commercial suppliers and used without further purification. CH₂Cl₂ and THF were dried under nitrogen by passing through solvent purification columns (MBraun, SPS-800). Reaction progress during the preparation of all compounds was monitored using thin layer chromatography on Macherey-Nagel Xtra SIL G/UV254 silica gel plates. Solvents were removed under reduced pressure with a rotary evaporator. Reaction mixtures were chromatographed on silica gel. All ¹H and ¹³C NMR spectra were recorded on a Bruker ASCEND 400 spectrometer equipped with a 5 mm BBFO probe using CDCl₃ as a deuterated solvent. Chemical shifts for ¹H and ¹³C NMR are reported in ppm (δ) relative to residual solvent signals. Coupling constants are given in Hertz (Hz). ¹H and ¹³C NMR signals were assigned based on 2D-NMR HSQC, HMBC, COSY and NOESY experiments. Mass spectrometry analyses were recorded on a Bruker micrOTOF-Q II mass spectrometer (high resolution), equipped with electrospray ion source. The instrument was operated in the positive ESI (+) ion mode. IR spectra were recorded on an Agilent Cary 630 FT-IR spectrometer equipped with an ATR sampling accessory. The X-ray intensity data were measured on a three-circle diffractometer system equipped with a Ceramic x-ray tube (Mo Kα, λ = 0.71073 Å) and a doubly curved silicon crystal Bruker Triumph monochromator. Melting points were measured in a SMP10 apparatus from Stuart without any correction. High performance liquid chromatography (HPLC) was performed using a CHIRALPAK IA column (4.6 x 250 mm, 5 μm) on an Agilent Technologies 1260 Infinity instrument, equipped with a quaternary pump G1311C, an auto sampler G1329B, a thermostatic column compartment G1316A and a variable wavelength UV-Vis detector G1314F.

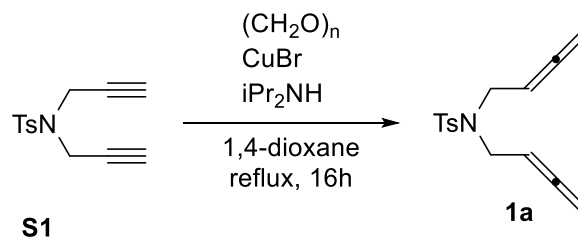
Scheme S1. Synthesis of diyne **S1**



In a 100 mL round-bottom flask equipped with a reflux condenser and a magnetic stirrer, a mixture of 4-methylbenzenesulfonamide (1 g, 5.84 mmol), K_2CO_3 (4.80 g, 34.73 mmol) and propargyl bromide (1.45 mL, 80 % in toluene, 1.60 mg, 13.42 mmol) in acetonitrile (60 mL) was stirred at 80 °C for 2 h until completion (TLC monitoring). The reaction mixture was allowed to cool to room temperature, the solids were filtered off and the filtrate was concentrated under reduced pressure to provide a yellowish oil which was purified by column chromatography (SiO_2 , 40–60 μ m, Hexanes/ CH_2Cl_2 1:1 v/v) to afford diyne **S1** (1.33 g, 92% yield), as a colourless solid.

MW ($C_{13}H_{13}NO_2S$): 247.3 g/mol; **Rf**: 0.33 (Hexanes/ CH_2Cl_2 1:1); **1H NMR (400 MHz, $CDCl_3$) δ (ppm)**: 2.14 (t, J = 2.4 Hz, 2H), 2.41 (s, 3H), 4.15 (d, J = 2.4 Hz, 4H), 7.28 (d, J = 8.4 Hz, 2H), 7.70 (d, J = 8.4 Hz, 2H); **^{13}C NMR (101 MHz, $CDCl_3$) δ (ppm)**: 21.67, 36.27, 74.17, 76.24, 127.96, 129.67, 135.22, 144.11.; **ESI-MS (m/z)**: $[M+H]^+ = 248.0$. Spectral data in accordance with literature values.¹

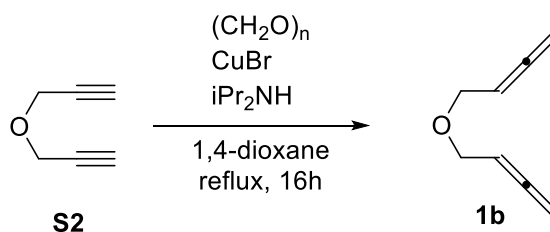
Scheme S2. Synthesis of bisallenenes **1a-b**



In a 250 mL round-bottom flask equipped with a reflux condenser and a magnetic stirrer, a suspension of diyne **S1** (6 g, 24.26 mmol), paraformaldehyde (3.64 g, 121.3 mmol) and CuBr (3.48 g, 24.26 mmol) in 1,4-dioxane (100 mL) was stirred and heated at reflux. Diisopropylamine (13.60 mL, 9.82 g, 97.04 mmol) was then added and the resulting mixture was stirred at reflux for 16 h until completion (TLC monitoring). The reaction mixture was allowed to cool to room temperature, filtered through a Celite pad and concentrated under reduced pressure. The resulting brown oil was mixed with Et_2O (200 mL) and water (100 mL) and the mixture was acidified to pH=2 with HCl 6M. The Et_2O /water layers were decanted from solid residues, the Et_2O layer was separated and the water layer was extracted with Et_2O (3 x 100 mL). The combined organic extracts were washed with water and brine, dried over anhydrous Na_2SO_4 and concentrated under reduced pressure.

The crude product was purified by column chromatography (SiO₂, 40–60 μm, Hexanes/EtOAc 95:5 v/v) to afford bisallene **1a** (4.10 g, 61% yield) as a colourless solid.

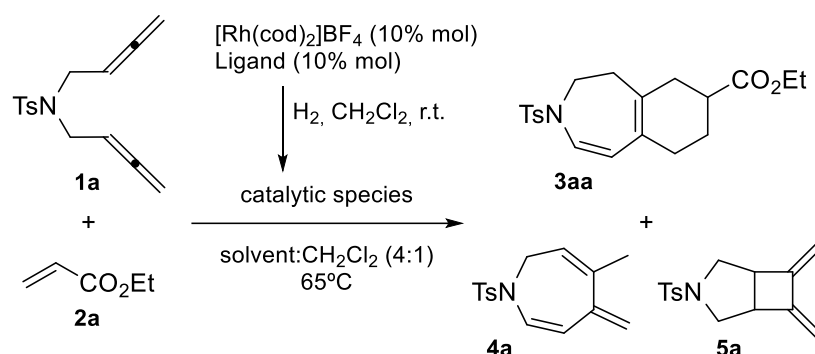
MW (C₁₅H₁₇NO₂S): 275.4 g/mol; **Rf**: 0.50 (hexanes/EtOAc 8:2); **¹H NMR (400 MHz, CDCl₃) δ (ppm)**: 2.41 (s, 3H), 3.89 (dt, *J* = 6.8, 2.4 Hz, 4H), 4.70 (dt, *J* = 6.8, 2.4 Hz, 4H), 4.93 (p, *J* = 6.8 Hz, 2H), 7.29 (d, *J* = 8.4, 2H), 7.69 (d, *J* = 8.4 Hz, 2H); **¹³C NMR (101 MHz, CDCl₃) δ (ppm)**: 21.61, 45.77, 76.27, 85.75, 127.27, 129.79, 137.66, 143.40, 209.78; **ESI-MS (m/z)**: [M+Na]⁺: 298.0. Spectral data in accordance with literature values.²



In a round-bottom flask equipped with a reflux condenser and a magnetic stirrer, a suspension of commercially available diyne **S2** (1.50 g, 15.96 mmol), paraformaldehyde (2.40 g, 80 mmol) and CuBr (2.30 g, 16.03 mmol) in 1,4-dioxane (60 mL) was stirred and heated at reflux. Diisopropylamine (9 mL, 6.48 g, 64 mmol) was then added and the resulting mixture was stirred for 16 h at reflux until completion (TLC monitoring). The reaction mixture was allowed to cool to room temperature, filtered through a Celite pad and concentrated under reduced pressure. The resulting brown oil was mixed with Et₂O (120 mL) and water (60 mL) and the mixture was acidified to pH=2 with HCl 6M. The Et₂O/water layers were decanted from any residues, the Et₂O layer was separated and the water layer was extracted with Et₂O (3 x 60 mL). The combined organic extracts were washed with water and brine, dried over anhydrous Na₂SO₄ and concentrated under reduced pressure. The crude product was purified by column chromatography (SiO₂, 40–60 μm, Hexanes/EtOAc 95:5 v/v) to provide bisallene **1b**¹ (394 mg, 20% yield) as a yellowish oil.

MW (C₈H₁₀O): 122.2 g/mol; **Rf**: 0.67 (hexanes/EtOAc 8:2); **IR (ATR) ν (cm⁻¹)**: 2920, 2854, 1953, 1450, 1357, 1318, 1251, 1077; **¹H NMR (400 MHz, CDCl₃) δ (ppm)**: 4.03 (dt, *J* = 6.8, 2.4 Hz, 4H), 4.78 (dt, *J* = 6.8, 2.4 Hz, 4H), 5.23 (quint, *J* = 6.8 Hz, 2H); **¹³C NMR (101 MHz, CDCl₃) δ (ppm)**: 67.68, 75.78, 87.67, 209.49.

Table S1. Optimization of the rhodium(I)-catalyzed cycloaddition of bisallene **1a with alkene **2a****



Entry	Ligand	Solvent	[1a] (mM)	Temperature (°C)	1a:2a ratio	Yield of 3aa / 4a / 5a (%)
1	(<i>R</i>)-BINAP	Toluene	18	65	1:10	30 / 29 / -
2	(<i>R</i>)-BINAP	DCE	18	65	1:10	- / - / -
3	(<i>R</i>)-BINAP	Acetonitrile	18	65	1:10	29 / 18 / -
4	(<i>R</i>)-BINAP	1,4-Dioxane	18	65	1:10	42 / 53 / -
5	(<i>R</i>)-BINAP	EtOH	18	65	1:10	18 / 24 / -
6	(<i>R</i>)-BINAP	THF	18	65	1:10	46 / 39 / -
7	(<i>R</i>)-BINAP	THF	18	65	1:50	45 / 45 / -
8	(<i>R</i>)-BINAP	THF	9	65	1:10	46 / 52 / -
9	(<i>R</i>)-BINAP	THF	9	65	1:50	49 / 45 / -
10	(<i>R</i>)-Tol-BINAP	THF	9	65	1:50	54 / 44 / -
11	(<i>R</i>)-H ₈ -BINAP	THF	9	65	1:50	54 / 38 / -
12	(<i>R</i>)-Monophos	THF	9	65	1:50	26 / 18 / -
13	BIPHEP	THF	9	65	1:50	- / 37 / -
14	(<i>R</i>)-DTBM-Segphos	THF	9	65	1:50	65 / 5 / 15
15	(<i>R</i>)-DTBM-Segphos	THF	9	40	1:50	60 / - / 15
16 ^b	(<i>R</i>)-DTBM-Segphos	THF	9	40	1:50	44 / - / 15
17 ^c	-	THF	9	40	1:50	- / - / -
18	-	THF	9	40	1:50	- / - / -

^a Reaction conditions: 0.09 mmol of **1a**, 10-50 equivalents of **2a**, 10% mol of Rh catalyst in 10-20 mL of solvent:CH₂Cl₂ (4:1) at 65°C for 4h or 40°C for 16h. The 10% mol mixture of [Rh(cod)₂]BF₄ and phosphine was treated with hydrogen in dichloromethane (CH₂Cl₂) solution for catalyst activation prior to substrate addition. ^b The reaction was run with 5% mol of [Rh(cod)₂]BF₄ and 5% mol of ligand.

^c The reaction was run without [Rh(cod)₂]BF₄.

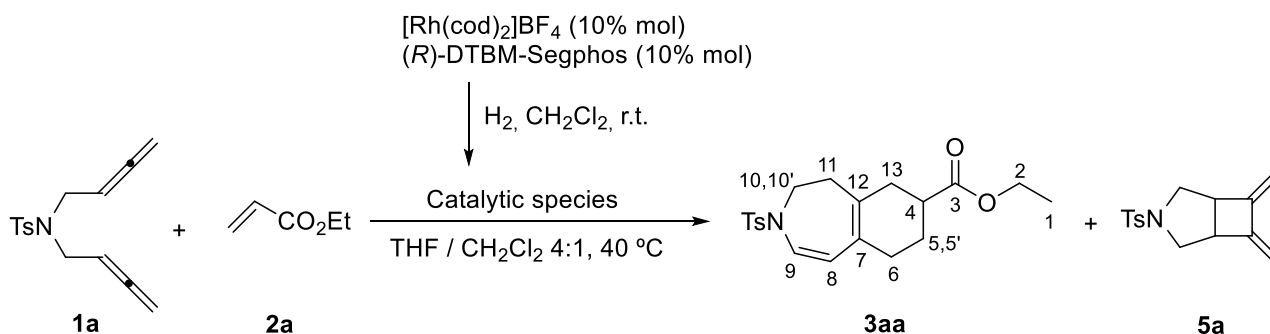
We started by studying the cycloaddition of *N*-tosyl-tethered bisallene **1a** and ethyl acrylate **2a** using 10% mol of cationic rhodium complex $[\text{Rh}(\text{cod})_2]\text{BF}_4$ with (*R*)-BINAP in mixtures of solvents with 4:1 ratio (varying solvents: CH_2Cl_2) at 65°C (entries 1-6). With a **1a:2a** ratio of 1:10 and a 18 mM concentration of bisallene (**1a**), two different compounds, **3aa** and **4a**, were obtained in varying quantities in all cases except when 1,2-dichloroethane (DCE) was used as co-solvent (entry 2). The best results were obtained with THF, which improved both the yield of **3aa** and its selectivity towards **4a** (entry 6). After a complete NMR analysis (see SI) of compound **3aa**, it was possible to determine the structure of the cycloadduct, confirming that a 4-aza-bicyclo[5.4.0]undeca-1(7),2-diene skeleton had been forged, purportedly originating from the oxidative coupling of the two external double bonds of **1a** and double bond isomerization. The seven-membered cross-conjugated triene **4a** was generated alongside **3aa** by cycloisomerization of the starting bisallene without participation of the alkene in an outcome that is complementary to the selectivity observed by Ma and Mukai.³⁻⁵

We next examined the effect of various reaction parameters on the efficiency of the process, focusing on improving the selectivity towards **3**. We varied two further parameters: first, the excess of the alkene was increased to 50 equiv. (entry 7) and, second, the concentration of the bisallene was reduced to 9 mM (entry 8). An additive effect was observed when the two factors were combined ($[\text{1a}] = 9 \text{ mM}$ and 50 equiv. of **2a**, entry 9). We then resorted to a combination of a cationic rhodium complex $[\text{Rh}(\text{cod})_2]\text{BF}_4$ with several phosphines as ligands: (*R*)-Tol-BINAP (entry 10), (*R*)-H₈-BINAP (entry 11), (*R*)-Monophos (entry 12), BIPHEP (entry 13) and (*R*)-DTBM-Segphos (entry 14). Intriguingly, only triene **4a** was obtained in 37% yield using BIPHEP as the phosphine and the desired product - **3aa** - was not observed. When the bulky phosphine DTBM-Segphos was used, the yield of **3aa** was improved to 65%, and the yield of triene **4a** was reduced to 5%. However, another by-product **5a**, originating also from the cycloisomerization of the bisallene, was obtained in 15% yield. Lowering the temperature to 40°C avoided the formation of **4a**, resulting in our optimized set of conditions (entry 15). An attempt to reduce the catalyst loading from 10% to 5% was detrimental for the yield of **3aa**, and we therefore decided to work with a 10% mol of rhodium throughout our study.

Two control experiments were run. First, in the absence of the Rh catalyst (entry 17) and, second, in the presence of $[\text{Rh}(\text{cod})_2]\text{BF}_4$ and without the bisphosphine (entry 18). Starting bisallene **1a** was recovered in both cases, revealing the essential role of the two components in this transformation.

Synthesis of compounds 3aa-3bj

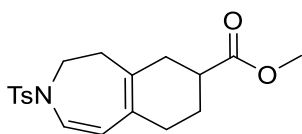
Scheme S3. General procedure for the synthesis of product 3aa



In a 10 mL capped vial, a mixture of $[\text{Rh(cod)}_2]\text{BF}_4$ (7.4 mg, 0.018 mmol) and $(R)\text{-DTBM-Segphos}$ (23.6 mg, 0.020 mmol) was purged with nitrogen and dissolved in anhydrous CH_2Cl_2 (4 mL). Hydrogen gas was bubbled into the catalyst solution and the mixture was stirred for 30 min. The resulting mixture was concentrated to dryness under a stream of nitrogen, dissolved again in anhydrous CH_2Cl_2 (4 mL) and transferred via syringe into a solution of bisallene **1a** (50 mg, 0.18 mmol, 1 equiv.) and ethyl acrylate **2a** (1.0 mL, 9.00 mmol, 50 equiv.) in anhydrous THF (16 mL) preheated to 40 °C and under inert atmosphere. The resulting mixture was stirred at 40 °C for 16h. The solvent was removed under reduced pressure and the crude reaction mixture was purified by column chromatography on silica gel using hexane/EtOAc mixtures as the eluent (98:2 to 95:5 v/v). Concentration under reduced pressure afforded compound **5a** (7.7 mg, 15% yield) as a colourless solid, and **3aa** (40.2 mg, 60% yield) as a pale yellow oil (in order of elution).

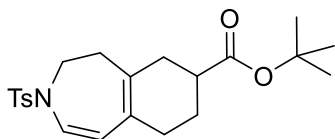
3aa: MW ($\text{C}_{20}\text{H}_{25}\text{NO}_4\text{S}$): 375.48 g/mol; Rf: 0.49 (Hexane/EtOAc 8:2); IR (ATR) ν (cm^{-1}): 2924, 1724, 1344, 1161; $^1\text{H NMR}$ (400 MHz, CDCl_3) δ (ppm): 1.22 (t, $J = 7.1$, 3H, H1), 1.51 - 1.62 (m, 1H, H5/5'), 1.90 - 1.97 (m, 1H, H5/H5'), 2.05 - 2.13 (m, 2H, H11), 2.10 - 2.17 (m, 2H, H6), 2.15 - 2.33 (m, 2H, H13), 2.38 - 2.47 (m, 1H, H4), 2.42 (s, 3H, $\text{CH}_3\text{-Ar}$), 3.47 (ddd, $J = 13.4, 6.1, 3.0$ Hz, 1H, H10/10'), 3.64 - 3.71 (m, 1H, H10/H10'), 4.11 (q, $J = 7.1$ Hz, 2H, H2), 4.86 (d, $J = 10.3$ Hz, 1H, H8), 6.66 (d, $J = 10.3$ Hz, 1H, H9), 7.30 (d, $J = 8.2$ Hz, 2H, CH-Ar), 7.66 (d, $J = 8.2$ Hz, 2H, CH-Ar); $^{13}\text{C NMR}$ (101 MHz, CDCl_3) δ (ppm): 14.35 (C1), 21.70 ($\text{CH}_3\text{-Ar}$), 25.41 (C5), 30.91 (C6), 34.59 (C13), 36.32 (C11), 39.52 (C4), 47.08 (C10), 60.49 (C2), 110.58 (C8), 124.74 (C9), 126.11 (C7), 127.18 (CH-Ar), 130.01 (CH-Ar), 133.54 (C12), 135.72 (C-Ar), 143.96 (C-Ar), 175.57 (C3); ESI-HRMS (m/z) calcd for $[\text{M}+\text{Na}]^+ = 398.1397$; found 398.1405.

5a: MW ($\text{C}_{15}\text{H}_{17}\text{NO}_2\text{S}$): 275.4 g/mol; Rf: 0.35 (Hexane/EtOAc 8:2); $^1\text{H NMR}$ (400 MHz, CDCl_3) δ (ppm): 2.43 (s, 3H), 2.75 (dd, $J = 9.6, 6.0$ Hz, 2H), 3.28 - 3.34 (m, 2H), 3.62 (d, $J = 9.6$ Hz, 2H), 4.80 (s, 2H), 5.22 (s, 2H), 7.31 (d, $J = 8.3$ Hz, 2H), 7.68 (d, $J = 8.3$ Hz, 2H); $^{13}\text{C NMR}$ (101 MHz, CDCl_3) δ (ppm): 21.68, 44.81, 53.49, 105.69, 128.24, 129.61, 132.28, 143.68, 149.15; ESI-MS (m/z) $[\text{M}+\text{H}]^+ = 275.1$. Spectral data in accordance with literature values.²



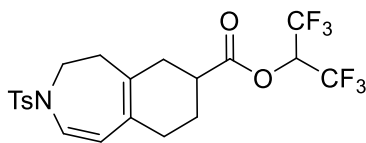
Compound 3ab was obtained from bisallene **1a** (52 mg, 0.19 mmol) and methyl acrylate (0.84 mL, 9.3 mmol), following the general procedure. Purification by column chromatography (silica gel, 40–63 μ m, Hexanes/EtOAc) provided **5a** (7.7 mg, 15% yield) as a colourless solid and **3ab** (36 mg, 53% yield) as a yellow oil.

MW ($C_{19}H_{23}NO_4S$): 361.46 g/mol **Rf**: 0.31 (Hexane/EtOAc 8:2); **IR (ATR) ν (cm^{-1})**: 2924, 1727, 1341, 1158; **1H NMR (400 MHz, $CDCl_3$) δ (ppm)**: 1.51 - 1.63 (m, 1H), 1.91 - 1.98 (m, 1H), 2.06 - 2.33 (m, 6H), 2.40 - 2.50 (m, 1H), 2.42 (s, 3H), 3.48 (ddd, J = 13.4, 6.2, 3.0 Hz, 1H), 3.66 (s, 3H), 3.63 - 3.71 (m, 1H), 4.86 (d, J = 10.3 Hz, 1H), 6.66 (d, J = 10.3 Hz, 1H), 7.31 (d, J = 8.3 Hz, 2H), 7.66 (d, J = 8.3 Hz, 2H); **^{13}C NMR (101 MHz, $CDCl_3$) δ (ppm)**: 21.70, 25.40, 30.90, 34.58, 36.33, 39.42, 47.08, 51.82, 110.52, 124.82, 126.15, 127.20, 130.02, 133.44, 135.76, 143.97, 176.00; **ESI-HRMS (m/z)** calcd for $[M+Na]^+$ = 384.1240; found 384.1236.



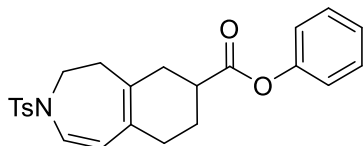
Compound 3ac was obtained from bisallene **1a** (49.6 mg, 0.18 mmol) and tert-butyl acrylate (1.36 mL, 98%, 9.1 mmol), following the general procedure. Purification by column chromatography (silica gel, 40–63 μ m, Hexanes/EtOAc) provided **5a** (7.1 mg, 14 %yield) as a colourless solid and **3ac** (36.6 mg, 50% yield) as a pale yellow oil.

MW ($C_{22}H_{29}NO_4S$): 403.54 g/mol; **Rf**: 0.36 (Hexane/EtOAc 9:1); **IR (ATR) ν (cm^{-1})**: 2924, 1719, 1343, 1149; **1H NMR (400 MHz, $CDCl_3$) δ (ppm)**: 1.41 (s, 9H), 1.48 - 1.59 (m, 1H), 1.85 - 1.94 (m, 1H), 2.08 - 2.27 (m, 6H), 2.29 - 2.38 (m, 1H), 2.42 (s, 3H), 3.48 (ddd, J = 13.4, 6.1, 2.9 Hz, 1H), 3.63 - 3.71 (m, 1H), 4.86 (d, J = 10.3 Hz, 1H), 6.66 (d, J = 10.3 Hz, 1H), 7.30 (d, J = 8.4, 2H), 7.66 (d, J = 8.4 Hz, 2H); **^{13}C NMR (101 MHz, $CDCl_3$) δ (ppm)**: 21.72, 25.48, 28.20, 30.95, 34.74, 36.35, 40.43, 47.12, 80.24, 110.73, 124.65, 126.09, 127.21, 130.02, 133.82, 135.78, 143.95, 174.99; **ESI-HRMS (m/z)** calcd for $[M+Na]^+$ = 426.1710; found 426.1712.



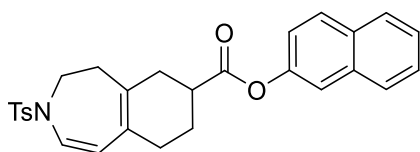
Compound 3ad was obtained from bisallene **1a** (51.8 mg, 0.19 mmol) and 1,1,1,3,3,3-hexafluoroisopropyl acrylate (1.55 mL, 99%, 9.2 mmol), following the general procedure. Purification by column chromatography (silica gel, 40–63 μ m, Hexanes/EtOAc) provided **3ad** (49.3 mg, 53% yield) as a yellowish oil and **5a** (4.3 mg, 8% yield) as a colourless solid.

MW ($C_{21}H_{21}F_6NO_4S$): 497.45 g/mol; **Rf**: 0.40 (Hexane/EtOAc 9:1); **IR (ATR) ν (cm^{-1})**: 2926, 1772, 1349, 1197, 1163; **1H NMR (400 MHz, $CDCl_3$) δ (ppm)**: 1.65 - 1.77 (m, 1H), 1.98 - 2.06 (m, 1H), 2.11 - 2.40 (m, 6H), 2.45 (s, 3H), 2.67 - 2.76 (m, 1H), 3.52 (ddd, J = 13.6, 6.4, 2.9 Hz, 1H), 3.66 - 3.74 (m, 1H), 4.88 (d, J = 10.3 Hz, 1H), 5.76 (hept, $^3J_{H-F}$ = 6.1 Hz, 1H), 6.72 (d, J = 10.3 Hz, 1H), 7.34 (d, J = 8.4 Hz, 2H), 7.69 (d, J = 8.4 Hz, 2H); **^{13}C NMR (101 MHz, $CDCl_3$) δ (ppm)**: 21.71, 24.92, 30.28, 33.89, 36.21, 38.89, 47.00, 66.51 (quint, $^2J_{C-F}$ = 34.7), 110.11, 120.53 (q, $^1J_{C-F}$ = 283.3), 125.27, 126.37, 127.22, 130.06, 132.29, 135.66, 144.08, 172.16; **ESI-HRMS (m/z)** calcd for $[M+Na]^+$ = 520.0988; found 520.1001.



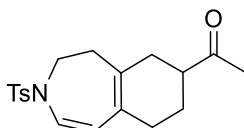
Compound 3ae was obtained from bis(allene) **1a** (50.2 mg, 0.18 mmol) and phenyl acrylate (1.25 mL, 9.1 mmol), following the general procedure. Purification by column chromatography (silica gel, 40–63 μ m, Hexanes/EtOAc 98:2 to 90:10) provided **3ae** (50.4 mg, 65% yield) as a pale yellow oil.

MW ($C_{24}H_{25}NO_4S$): 423.53 g/mol; **Rf**: 0.24 (Hexane/EtOAc 9:1); **IR (ATR) ν (cm^{-1})**: 2923, 1748, 1340, 1157; **1H NMR (400 MHz, $CDCl_3$) δ (ppm)**: 1.69 - 1.80 (m, 1H), 2.07 - 2.18 (m, 3H), 2.19 - 2.27 (m, 2H), 2.30 - 2.49 (m, 2H), 2.42 (s, 3H), 2.68 - 2.77 (m, 1H), 3.51 (ddd, J = 13.4, 6.2, 2.9 Hz, 1H), 3.67 - 3.74 (m, 1H), 4.90 (d, J = 10.3 Hz, 1H), 6.70 (d, J = 10.3 Hz, 1H), 7.04 (dd, J = 8.6, 1.2 Hz, 2H), 7.19 - 7.24 (m, 1H), 7.31 (d, J = 8.4 Hz, 2H), 7.32 - 7.41 (m, 2H), 7.67 (d, J = 8.4 Hz, 2H); **^{13}C NMR (101 MHz, $CDCl_3$) δ (ppm)**: 21.72, 25.39, 30.78, 34.45, 36.35, 39.61, 47.09, 110.45, 121.58, 124.97, 125.92, 126.26, 127.21, 129.55, 130.05, 133.21, 135.73, 144.02, 150.86, 174.04; **ESI-HRMS (m/z)** calcd for $[M+Na]^+$ = 446.1397; found 446.1397.



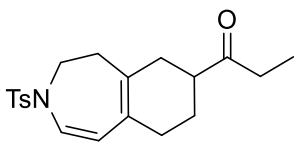
Compound 3af was obtained from bisallene **1a** (49.9 mg, 0.18 mmol) and naphthyl acrylate (909 mg, 4.6 mmol), following the general procedure. Purification by column chromatography (silica gel, 40–63 μ m, Hexanes/EtOAc 98:2 to 90:10) provided **3af** (58 mg, 68% yield) as a pale yellow solid.

MW ($C_{28}H_{27}NO_4S$): 473.59 g/mol; **Rf**: 0.34 (Hexane/EtOAc 8:2); **MP** ($^{\circ}C$): 144 - 146 (Hexane/EtOAc 9:1); **IR (ATR) ν (cm^{-1})**: 2921, 1745, 1345, 1161; **1H NMR (400 MHz, $CDCl_3$) δ (ppm)**: 1.73 - 1.86 (m, 1H), 2.12 - 2.30 (m, 5H), 2.34 - 2.54 (m, 2H), 2.42 (s, 3H), 2.74 - 2.82 (m, 1H), 3.53 (ddd, J = 13.4, 6.3, 2.9 Hz, 1H), 3.68 - 3.76 (m, 1H), 4.91 (d, J = 10.3 Hz, 1H), 6.71 (d, J = 10.3 Hz, 1H), 7.18 (dd, J = 8.9, 2.3 Hz, 1H), 7.32 (d, J = 8.3 Hz, 2H), 7.43 - 7.53 (m, 3H), 7.68 (d, J = 8.3 Hz, 2H), 7.79 (dd, J = 7.1, 2.1 Hz, 1H), 7.82 - 7.86 (m, 2H); **^{13}C NMR (101 MHz, $CDCl_3$) δ (ppm)**: 21.72, 25.45, 30.83, 34.50, 36.37, 39.70, 47.10, 110.44, 118.53, 121.15, 125.01, 125.83, 126.29, 126.72, 127.21, 127.72, 127.90, 129.53, 130.05, 131.55, 133.20, 133.87, 135.73, 144.02, 148.50, 174.21; **ESI-HRMS (m/z)** calcd for $[M+Na]^+$ = 496.1553; found 496.1547.



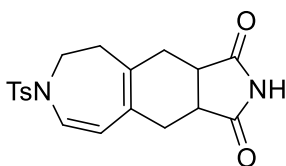
Compound 3ag was obtained from bisallene **1a** (49.5 mg, 0.18 mmol) and 3-buten-2-one (0.74 mL, 99%, 9.0 mmol), following the general procedure. Purification by column chromatography (silica gel, 40–63 μ m, Hexanes/EtOAc 98:2 to 90:10) provided **5a** (5.8 mg, 12% yield) as a colourless solid and **3ag** (45 mg, 72% yield) as a yellowish oil.

MW ($C_{19}H_{23}NO_3S$): 345.46 g/mol; **Rf**: 0.17 (Hexane/EtOAc 8:2); **IR (ATR) ν (cm^{-1})**: 2921, 1703, 1342, 1160; **1H NMR (400 MHz, $CDCl_3$) δ (ppm)**: 1.41 - 1.50 (m, 1H), 1.89 - 1.96 (m, 1H), 2.04 - 2.27 (m, 6H), 2.14 (s, 3H), 2.41 (s, 3H), 2.44 - 2.53 (m, 1H), 3.46 (ddd, J = 13.5, 6.8, 2.3 Hz, 1H), 3.64 - 3.72 (m, 1H), 4.85 (d, J = 10.3 Hz, 1H), 6.66 (d, J = 10.3 Hz, 1H), 7.30 (d, J = 8.3 Hz, 2H), 7.65 (d, J = 8.3 Hz, 2H); **^{13}C NMR (101 MHz, $CDCl_3$) δ (ppm)**: 21.69, 25.04, 28.16, 31.20, 33.77, 36.40, 47.05, 47.39, 110.46, 124.78, 126.10, 127.17, 130.01, 133.61, 135.70, 143.98, 211.19; **ESI-HRMS (m/z)** calcd for $[M+Na]^+$ = 368.1291; found 368.1294.



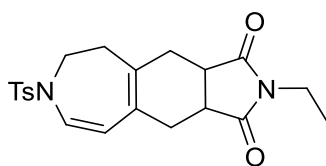
Compound 3ah was obtained from bisallene **1a** (50 mg, 0.18 mmol) and 1-penten-3-one (0.93 mL, 97%, 9.1 mmol), following the general procedure. Purification by column chromatography (silica gel, 40–63 μ m, Hexanes/EtOAc 98:2 to 90:10) provided **3ah** (48.8 mg, 75% yield) as a yellowish oil.

MW ($C_{20}H_{25}NO_3S$): 359.48 g/mol; **Rf**: 0.29 (Hexane/EtOAc 8:2); **IR (ATR) ν (cm^{-1})**: 2924, 1704, 1342, 1160; **1H NMR (400 MHz, $CDCl_3$) δ (ppm)**: 1.03 (t, J = 7.3 Hz, 3H), 1.40 - 1.52 (m, 1H), 1.83 - 1.93 (m, 1H), 2.01 - 2.30 (m, 6H), 2.37 - 2.56 (m, 3H), 2.42 (s, 3H), 3.47 (ddd, J = 13.4, 7.1, 2.2 Hz, 1H), 3.65 – 3.74 (m, 1H), 4.86 (d, J = 10.3 Hz, 1H), 6.66 (d, J = 10.3 Hz, 1H), 7.31 (d, J = 8.4 Hz, 2H), 7.66 (d, J = 8.4 Hz, 2H); **^{13}C NMR (101 MHz, $CDCl_3$) δ (ppm)**: 7.91, 21.72, 25.30, 31.30, 34.08, 34.10, 36.45, 46.47, 47.08, 110.53, 124.78, 126.08, 127.21, 130.03, 133.82, 135.76, 143.99, 213.86; **ESI-HRMS (m/z)** calcd for $[M+Na]^+$ = 382.1447; found 382.1447.



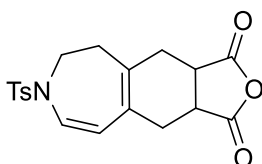
Compound 3ai was obtained from bisallene **1a** (50 mg, 0.18 mmol) and maleimide (88 mg, 0.91 mmol), following the general procedure. Purification by column chromatography (silica gel, 40–63 μ m, hexanes/EtOAc 8:2 to 1:1) provided **3ai** (51 mg, 76% yield) as a pale yellow solid.

MW ($C_{19}H_{20}N_2O_4S$): 372.44 g/mol; **Rf**: 0.24 (Hexane/EtOAc 1:1); **MP ($^{\circ}C$)**: 221 - 223 (Hexane/EtOAc 1:1); **IR (ATR) ν (cm^{-1})**: 3220, 2924, 1775, 1699, 1331, 1157; **1H NMR (400 MHz, $CDCl_3$) δ (ppm)**: 2.25 - 2.35 (m, 4H), 2.42 (s, 3H), 2.44 - 2.56 (m, 2H), 3.02 - 3.12 (m, 2H), 3.41 - 3.57 (m, 2H), 4.97 (d, J = 9.9 Hz, 1H), 6.65 (d, J = 9.9 Hz, 1H), 7.31 (d, J = 8.3 Hz, 2H), 7.64 (d, J = 8.3 Hz, 2H), 8.06 (s, 1H); **^{13}C NMR (101 MHz, $CDCl_3$) δ (ppm)**: 21.72, 31.95, 32.17, 38.10, 40.89, 41.00, 46.51, 110.13, 126.84, 127.18, 127.42, 130.10, 135.16, 135.66, 144.22, 179.60, 179.78; **ESI-HRMS (m/z)** calcd for $[M+Na]^+$ = 395.1036; found 395.1043.



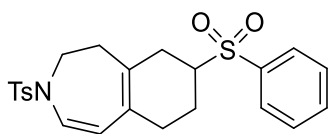
Compound 3aj was obtained from bisallene **1a** (49.8 mg, 0.18 mmol) and N-ethylmaleimide (603 mg, 4.8 mmol), following the general procedure. Purification by column chromatography (silica gel, 40–63 μ m, Hexanes/EtOAc 8:2 to 1:1) provided **3aj** (46.5 mg, 64% yield) as a pale yellow solid.

MW ($C_{21}H_{24}N_2O_4S$): 400.49 g/mol; **Rf**: 0.37 (Hexane/EtOAc 1:1); **MP** ($^{\circ}C$): 140 - 141 (Hexane/EtOAc 1:1); **IR (ATR) ν (cm^{-1})**: 2913, 1764, 1687, 1334, 1160; **1H NMR (400 MHz, $CDCl_3$) δ (ppm)**: 0.90 (t, J = 7.2 Hz, 3H), 2.14 - 2.36 (m, 4H), 2.41 (s, 3H), 2.47 - 2.58 (m, 2H), 2.94 - 3.04 (m, 2H), 3.39 (d, J = 7.2 Hz, 2H), 3.38 - 3.45 (m, 1H), 3.51 (ddd, J = 13.7, 6.9, 1.7 Hz, 1H), 4.96 (d, J = 10.0 Hz, 1H), 6.63 (d, J = 10.0 Hz, 1H), 7.28 (d, J = 8.3 Hz, 2H), 7.61 (d, J = 8.3 Hz, 2H); **^{13}C NMR (101 MHz, $CDCl_3$) δ (ppm)**: 13.24, 21.69, 32.30, 32.55, 33.81, 37.94, 39.63, 39.71, 46.39, 110.14, 126.55, 127.14, 127.44, 130.04, 135.18, 135.59, 144.11, 179.43, 179.74; **ESI-HRMS (m/z)** calcd for $[M+Na]^+$ = 423.1349; found 423.1348.



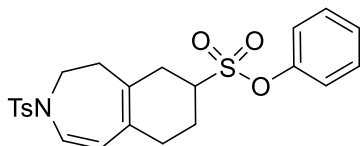
Compound 3ak was obtained from bisallene **1a** (49.6 mg, 0.18 mmol) and maleic anhydride (446 mg, 4.5 mmol), following the general procedure. Purification by column chromatography (silica gel, 40–63 μ m, Hexanes/EtOAc 8:2 to 1:1) provided **3ak** (54.8 mg, 81% yield) as a yellow solid.

MW ($C_{19}H_{19}NO_5S$): 373.42 g/mol; **Rf**: 0.46 (Hexane/EtOAc 1:1); **MP** ($^{\circ}C$): 156 - 157 (Hexane/EtOAc 1:1); **IR (ATR) ν (cm^{-1})**: 2919, 1841, 1769, 1348, 1159; **1H NMR (400 MHz, $CDCl_3$) δ (ppm)**: 2.17 - 2.26 (m, 1H), 2.31 - 2.41 (m, 3H), 2.44 (s, 3H), 2.50 - 2.62 (m, 2H), 3.27 - 3.38 (m, 2H), 3.49 - 3.55 (m, 2H), 4.98 (d, J = 10 Hz, 1H), 6.71 (d, J = 10 Hz, 1H), 7.32 (d, J = 8.4 Hz, 2H), 7.63 (d, J = 8.4 Hz, 2H); **^{13}C NMR (101 MHz, $CDCl_3$) δ (ppm)**: 21.73, 32.07, 32.20, 37.97, 40.26, 40.33, 46.30, 109.70, 127.09, 127.67, 127.76, 130.22, 134.93, 135.51, 144.49, 173.80, 174.09; **ESI-HRMS (m/z)** calcd for $[M+Na]^+$ = 396.0876; found 396.0876.



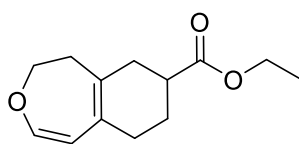
Compound 3al was obtained from bisallene **1a** (50.1 mg, 0.18 mmol) and phenyl vinyl sulfone (828 mg, 4.9 mmol), following the general procedure. Purification by column chromatography (silica gel, 40–63 μ m, Hexanes/EtOAc 98:2 to 90:10) provided **3al** (24.7 mg, 31% yield) as a pale yellow solid.

MW ($C_{23}H_{25}NO_4S_2$): 443.58 g/mol; **Rf**: 0.29 (Hexane/EtOAc 7:3); **MP** ($^{\circ}C$): 104 - 109 (dec.), (Hexane/EtOAc 9:1); **IR (ATR) ν (cm^{-1})**: 2923, 1343, 1302, 1160, 1143; **1H NMR (400 MHz, $CDCl_3$) δ (ppm)**: 1.37 - 1.50 (m, 1H), 1.92 - 2.15 (m, 6H), 2.20 - 2.28 (m, 1H), 2.32 (s, 3H), 2.91 - 3.01 (m, 1H), 3.34 (ddd, J = 13.6, 7.0, 2.3 Hz, 1H), 3.50 - 3.57 (m, 1H), 4.71 (d, J = 10.3 Hz, 1H), 6.57 (d, J = 10.3 Hz, 1H), 7.20 (d, J = 8.4 Hz, 2H), 7.43 - 7.50 (m, 2H), 7.51 - 7.59 (m, 3H), 7.72 - 7.81 (m, 2H); **^{13}C NMR (101 MHz, $CDCl_3$) δ (ppm)**: 21.73, 22.19, 30.83, 31.29, 36.21, 46.87, 60.18, 109.54, 125.61, 126.45, 127.20, 129.08, 129.32, 130.09, 131.46, 133.93, 135.56, 137.27, 144.16; **ESI-HRMS (m/z)** calcd for $[M+Na]^+$ = 466.1117; found 466.1117.



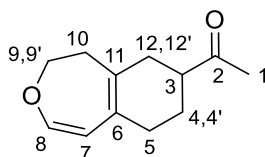
Compound 3am was obtained from bisallene **1a** (50.3 mg, 0.18 mmol) and phenyl vinyl sulfonate (1.0 g 5.4 mmol), following the general procedure. Purification by column chromatography (silica gel, 40–63 μ m, Hexanes/EtOAc 98:2 to 90:10) provided **3am** (50.2 mg, 60% yield) as a colourless solid.

MW ($C_{23}H_{25}NO_5S_2$): 459.57 g/mol; **Rf**: 0.48 (Hexane/EtOAc 7:3); **MP** ($^{\circ}C$): 125 - 126 (Hexane/EtOAc 9:1); **IR (ATR) ν (cm^{-1})**: 2919, 1364, 1341, 1159, 1143; **1H NMR (400 MHz, $CDCl_3$) δ (ppm)**: 1.78 - 1.92 (m, 1H), 2.08 - 2.24 (m, 2H), 2.30 (d, J = 7.6 Hz, 2H), 2.34 - 2.41 (m, 1H), 2.43 (s, 3H), 2.47 - 2.55 (m, 1H), 2.58 - 2.69 (m, 1H), 3.29 - 3.40 (m, 1H), 3.49 (ddd, J = 13.6, 7.0, 2.3 Hz, 1H), 3.67 - 3.75 (m, 1H), 4.87 (d, J = 10.3 Hz, 1H), 6.73 (d, J = 10.3 Hz, 1H), 7.21 - 7.25 (m, 2H), 7.27 - 7.30 (m, 1H), 7.32 (d, J = 8.3 Hz, 2H), 7.36 - 7.42 (m, 2H), 7.66 (d, J = 8.3 Hz, 2H); **^{13}C NMR (101 MHz, $CDCl_3$) δ (ppm)**: 21.74, 23.21, 30.59, 32.10, 36.18, 46.89, 56.81, 109.39, 122.09, 125.88, 126.55, 127.22, 127.25, 130.09, 130.12, 131.06, 135.56, 144.21, 149.05; **ESI-HRMS (m/z)** calcd for $[M+Na]^+$ = 482.1066; found 482.1078.



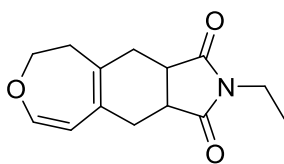
Compound 3ba was obtained from bisallene **1b** (23.4 mg, 0.19 mmol) and ethyl acrylate (1.0 mL, 99%, 9.1 mmol), following the general procedure. Purification by column chromatography (silica gel, 40–63 μ m, Hexanes/EtOAc 99:1) provided **3ba** (7.2 mg, 17% yield) as a pale yellow oil.

MW ($C_{13}H_{18}O_3$): 222.28 g/mol; **Rf**: 0.61(Hexane/EtOAc 9:1); **IR (ATR) ν (cm^{-1})**: 2924, 1729; **1H NMR (400 MHz, $CDCl_3$) δ (ppm)**: 1.26 (t, J = 7.1 Hz, 3H), 1.57 - 1.69 (m, 1H), 1.95 - 2.02 (m, 1H), 2.08 - 2.20 (m, 2H), 2.22 - 2.44 (m, 3H), 2.45 - 2.54 (m, 2H), 4.07 - 4.22 (m, 2H), 4.14 (q, J = 7.1 Hz, 2H), 4.57 (d, J = 7.9 Hz, 1H), 6.26 (d, J = 7.9 Hz, 1H); **^{13}C NMR (101 MHz, $CDCl_3$) δ (ppm)**: 14.40, 25.54, 30.72, 34.27, 38.90, 39.77, 60.49, 70.09, 105.83, 126.20, 131.98, 145.02, 175.86; **ESI-HRMS (m/z)** calcd for $[M+Na]^+$ = 245.1148; found 245.1146.



Compound 3bg was obtained from bisallene **1b** (23.4 mg, 0.19 mmol) and 3-buten-2-one (0.74, 99%, mL, 9.0 mmol), following the general procedure. Purification by column chromatography (silica gel, 40–63 μ m, Hexanes/EtOAc 98:2) provided **3bg** (10.0 mg, 27% yield) as a pale yellow oil.

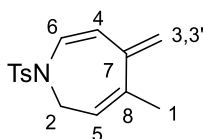
MW ($C_{12}H_{16}O_2$): 192.26 g/mol; **Rf**: 0.49 (Hexane/EtOAc 8:2); **IR (ATR) ν (cm^{-1})**: 2923, 1704; **1H NMR (400 MHz, $CDCl_3$) δ (ppm)**: 1.44 - 1.57 (m, 1H, H4/H4'), 1.92 - 2.01 (m, 1H, H4/H4'), 2.09 - 2.22 (m, 3H, H5, H12/H12'), 2.18 (s, 3H, H1), 2.23 - 2.34 (m, 1H, H12/H12'), 2.36 - 2.50 (m, 2H, H10), 2.50 - 2.60 (m, 1H, H3), 4.11 (ddd, J = 10.9, 6.8, 1.6 Hz, 1H, H9/H9'), 4.18 (ddd, J = 10.9, 5.9, 2.0 Hz, 1H, H9/H9'), 4.57 (d, J = 7.8 Hz, 1H, H7), 6.26 (d, J = 7.8 Hz, 1H, H8); **^{13}C NMR (101 MHz, $CDCl_3$) δ (ppm)**: 25.13 (C4), 28.21 (C1), 31.00 (C5), 33.51 (C12), 38.96 (C10), 47.70 (C3), 70.05 (C9), 105.73 (C7), 126.23 (C6), 132.01 (C11), 145.08 (C8), 211.52 (C2); **ESI-HRMS (m/z)** calcd for $[M+Na]^+$ = 215.1043; found 215.1037.



Compound 3bj was obtained from bisallene **1b** (23.4 mg, 0.19 mmol) and N-ethylmaleimide (580 mg, 4.6 mmol), following the general procedure. Purification by column chromatography (silica gel, 40–63 μ m, Hexanes/EtOAc 95:5 to 80:20) provided **3bj** (15.0 mg, 32% yield) as a pale yellow oil.

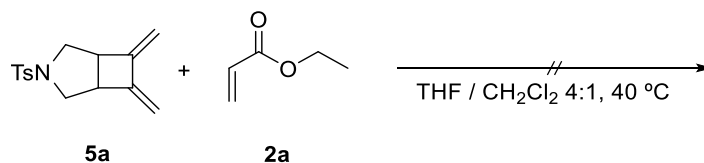
MW ($C_{14}H_{17}NO_3$): 247.29 g/mol; **Rf**: 0.21(Hexane/EtOAc 8:2); **IR (ATR) ν (cm^{-1})**: 2922, 1763, 1684; **1H NMR (400 MHz, $CDCl_3$) δ (ppm)**: 1.07 (t, J = 7.2 Hz, 3H), 2.27 - 2.38 (m, 2H), 2.47 - 2.63 (m, 4H), 2.99 - 3.06 (m, 2H), 3.48 (q, J = 7.2 Hz, 2H), 4.00 (ddd, J = 11.2, 6.2, 2.1 Hz, 1H), 4.09 (ddd, J = 11.2, 6.1, 2.2 Hz, 1H), 4.68 (d, J = 7.6 Hz, 1H), 6.25 (d, J = 7.6 Hz, 1H); **^{13}C NMR (101 MHz, $CDCl_3$) δ (ppm)**: 13.34, 31.83, 31.89, 33.90, 39.76, 39.79, 40.00, 69.63, 105.85, 127.48, 133.53, 147.04, 179.71, 180.02; **ESI-HRMS (m/z)** calcd for $[M+Na]^+$ = 270.1101; found 270.1107.

Compound 4a



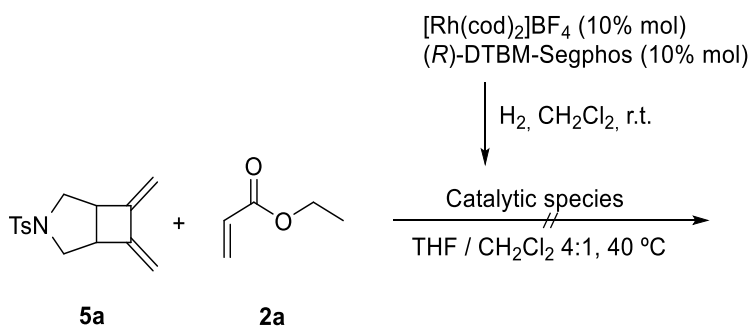
MW ($C_{15}H_{17}NO_2S$): 275.4 g/mol; **Rf**: 0.50 (Hexanes/EtOAc 8:2); **IR (ATR) ν (cm^{-1})**: 2921, 2852, 1456, 1337, 1158, 1090; **1H NMR (400 MHz, $CDCl_3$) δ (ppm)**: 1.76 (s, 3H, H1), 2.41 (s, 3H, CH_3 -Ar), 3.95 (d, J = 7.2 Hz, 2H, H2), 5.02 (s, 1H, H3/H3'), 5.09 (s, 1H, H3/H3'), 5.37 (d, J = 10.4 Hz, 1H, H4), 5.55 (t, J = 7.2 Hz, 1H, H5), 6.52 (d, J = 10.4, 1H, H6), 7.28 (d, J = 8.4 Hz, 2H, H-Ar), 7.66 (d, J = 8.4, 2H, H-Ar); **^{13}C NMR (101 MHz, $CDCl_3$) δ (ppm)**: 21.64 (CH_3 -Ar), 23.01 (C1), 45.60 (C2), 113.72 (C4), 117.68 (C3), 120.91 (C5), 127.01 (C6), 127.13 (CH-Ar), 129.83 (CH-Ar), 136.24 (C-Ar), 142.06 (C7), 143.46 (C8), 143.90 (C-Ar); **ESI-HRMS (m/z)** calcd for $[M+Na]^+$ = 298.0872; found: 298.0875.

Scheme S4. Mechanistic experiments using compound **5a** and ethyl acrylate **2a**



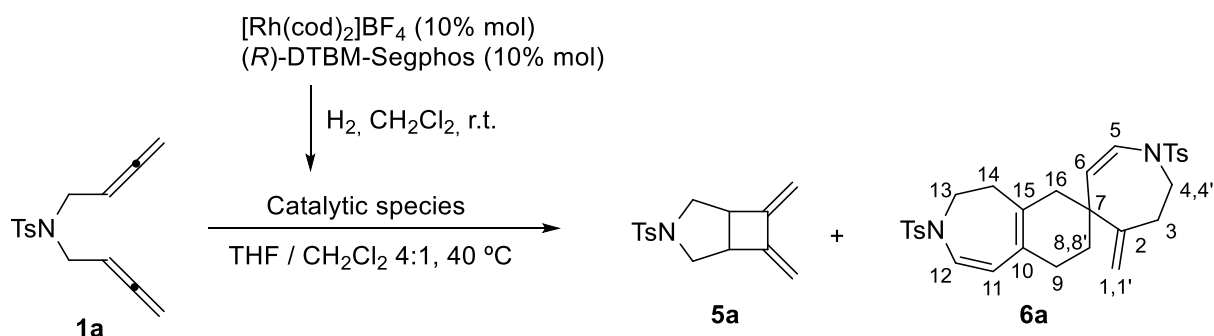
In a 25 mL round-bottom flask equipped with a magnetic stirrer and an inert atmosphere, a solution of **5a** (15 mg, 0.055 mmol) and ethyl acrylate **2a** (0.3 mL, 275 mg, 2.75 mmol) in a 4:1 mixture of THF/CH₂Cl₂ (6 mL) was stirred at 40 °C for 16h. The solvent and ethyl acrylate **2a** were removed under reduced pressure. ¹H NMR analysis of the crude product revealed the presence of unaltered starting material **5a**.

Scheme S5. Mechanistic experiments using compound **5a**, ethyl acrylate **2a** and Rh(I) catalyst



In a 10 mL capped vial, a mixture of [Rh(cod)₂]BF₄ (4.26 mg, 0.010 mmol) and (*R*)-DTBM-Segphos (12.4 mg, 0.011 mmol) was purged with nitrogen and dissolved in anhydrous CH₂Cl₂ (4 mL). Hydrogen gas was bubbled into the catalyst solution for 30 min. The resulting mixture was concentrated to dryness, dissolved again in anhydrous CH₂Cl₂ (2 mL) and transferred via syringe into a 40 °C preheated solution of **5a** (29 mg, 0.11 mmol) and ethyl acrylate **2a** (0.6 mL, 550 mg, 5.33 mmol) in anhydrous THF (10 mL) and under inert atmosphere. The resulting mixture was stirred at 40 °C for 16h. The solvent and ethyl acrylate **2a** were removed under reduced pressure and the crude reaction mixture was filtered through a short silica gel pad (Hexanes/EtOAc 8:2 v/v). ¹H NMR analysis of the crude product revealed the presence of unaltered starting material **5a**.

Scheme S6. Mechanistic experiments using compound **1a** and Rh(I) catalyst

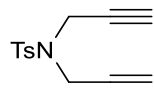


In a 10 mL capped vial, a mixture of $[\text{Rh}(\text{cod})_2]\text{BF}_4$ (7.4 mg, 0.018 mmol) and $(R)\text{-DTBM-Segphos}$ (23.6 mg, 0.020 mmol) was purged with nitrogen and dissolved in anhydrous CH_2Cl_2 (4 mL). Hydrogen gas was bubbled into the catalyst solution and the mixture was stirred for 30 min. The resulting mixture was concentrated to dryness, dissolved again in anhydrous CH_2Cl_2 (4 mL) and transferred via syringe into a preheated solution to 40°C of bisallene **1a** (48.4 mg, 0.18 mmol) in anhydrous THF (16 mL) and under inert atmosphere. The resulting mixture was stirred at 40°C for 16 h. The solvent was removed under reduced pressure and the crude reaction mixture was purified by column chromatography on silica gel using hexane/EtOAc mixtures as the eluent (95:5 to 90:10 v/v), affording first, compound **5a** (5.5 mg, 12% yield) as a colourless solid, and second, **6a** (28.3 mg, 58% yield) as a pale yellow solid.

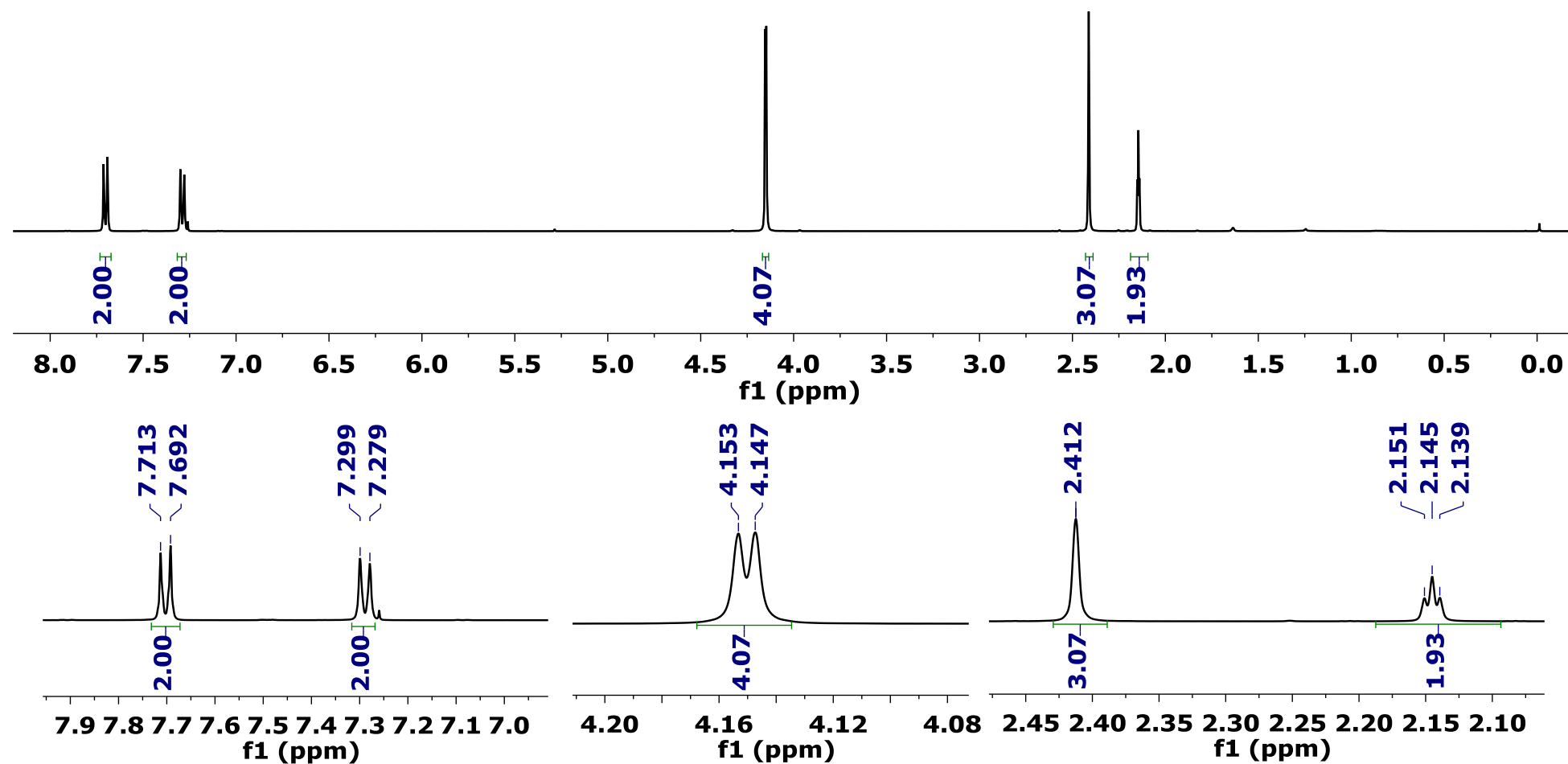
6a: **MW** ($\text{C}_{30}\text{H}_{34}\text{N}_2\text{O}_4\text{S}_2$): 550.73 g/mol; **Rf**: 0.26 (Hexane/EtOAc 8:2); **MP** ($^\circ\text{C}$): 87-92 (dec); **IR** (ATR) $\nu(\text{cm}^{-1})$: 2921, 1336, 1156; ^1H NMR (400 MHz, CDCl_3) δ (ppm): 1.46 - 1.55 (m, 1H, H8/H8'), 1.56 - 1.66 (m, 1H, H8/H8'), 1.93 - 2.20 (m, 6H, H9, H14, H16), 2.42 (s, 3H, $\text{CH}_3\text{-Ar}$), 2.42 (s, 3H, $\text{CH}_3\text{-Ar}$), 2.43 - 2.55 (m, 2H, H3), 3.38 - 3.48 (m, 1H, H4/H4'), 3.49 - 3.66 (m, 3H, H4/H4', H13), 4.52 (s, 1H, H1/H1'), 4.63 (s, 1H, H1/H1'), 4.71 (d, $J = 9.5$ Hz, 1H, H6), 4.84 (d, $J = 10.3$ Hz, 1H, H11), 6.27 (d, $J = 9.5$ Hz, 1H, H5), 6.64 (d, $J = 10.3$ Hz, 1H, H12), 7.28 (d, $J = 8.2$ Hz, 2H, CH-Ar), 7.31 (d, $J = 8.2$ Hz, 2H, CH-Ar), 7.66 (m, 4H, CH-Ar); ^{13}C NMR (101 MHz, CDCl_3) δ (ppm): 21.67 ($\text{CH}_3\text{-Ar}$), 21.71 ($\text{CH}_3\text{-Ar}$), 29.10 (C9), 32.71 (C8), 34.74 (C3), 36.69 (C14), 42.46 (C7), 44.58 (C16), 47.03 (C13), 50.10 (C4), 110.59 (C11), 111.82 (C1), 122.64 (C6), 124.72 (C12), 125.67 (C5), 125.83 (C10), 127.18 (CH-Ar), 127.19 (CH-Ar), 129.78 (CH-Ar), 130.01 (CH-Ar), 132.95 (C15), 135.83 (C-Ar), 136.25 (C-Ar), 143.72 (C-Ar), 143.97 (C-Ar), 149.30 (C2); **ESI-MS** (m/z) calcd for $[\text{M}+\text{Na}]^+ = 573.1852$; found 573.1836.

¹H and ¹³C NMR spectra

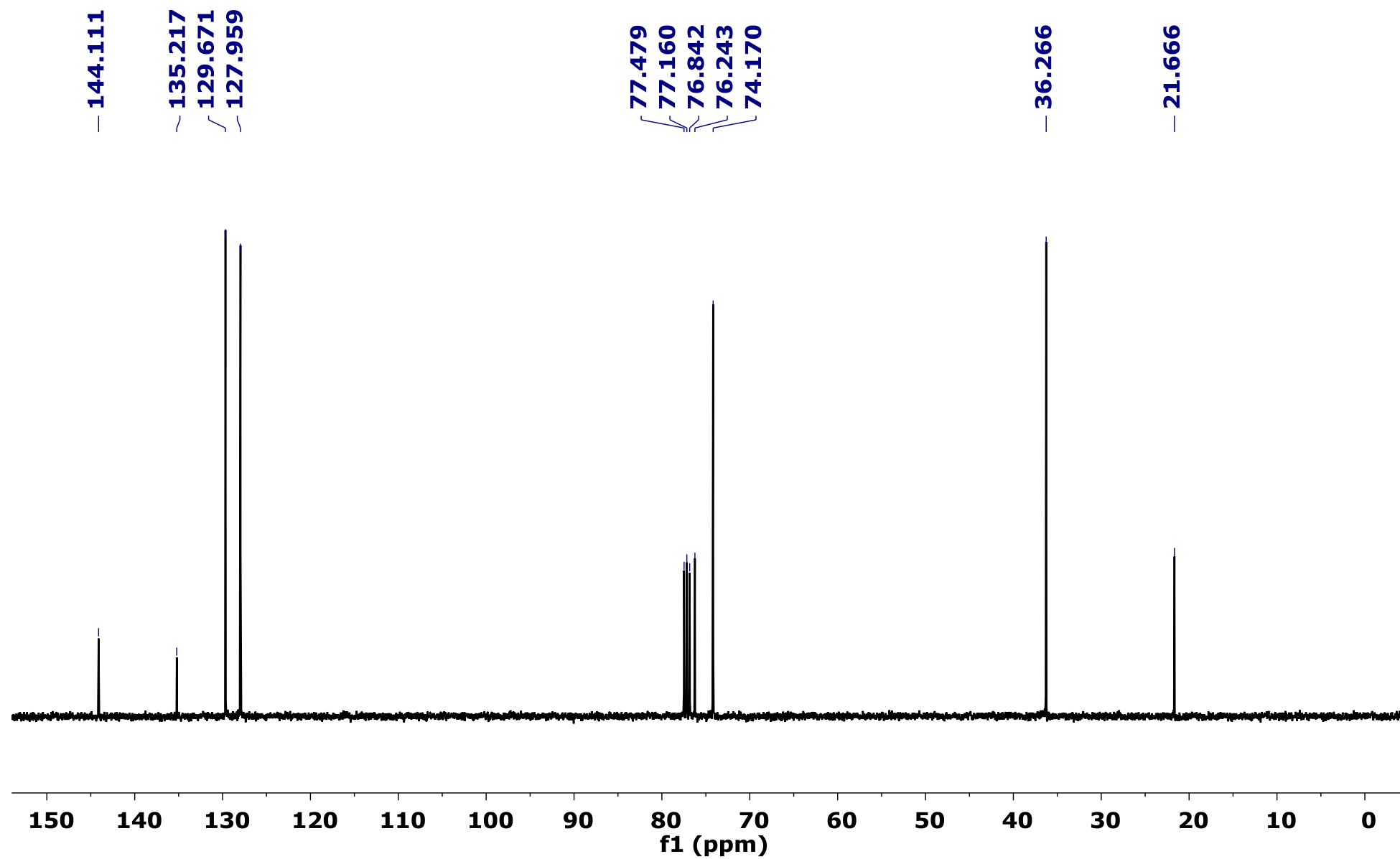
Diyne S1



¹H NMR (400 MHz, CDCl₃)

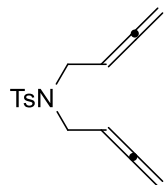


¹³C NMR (101 MHz, CDCl₃)

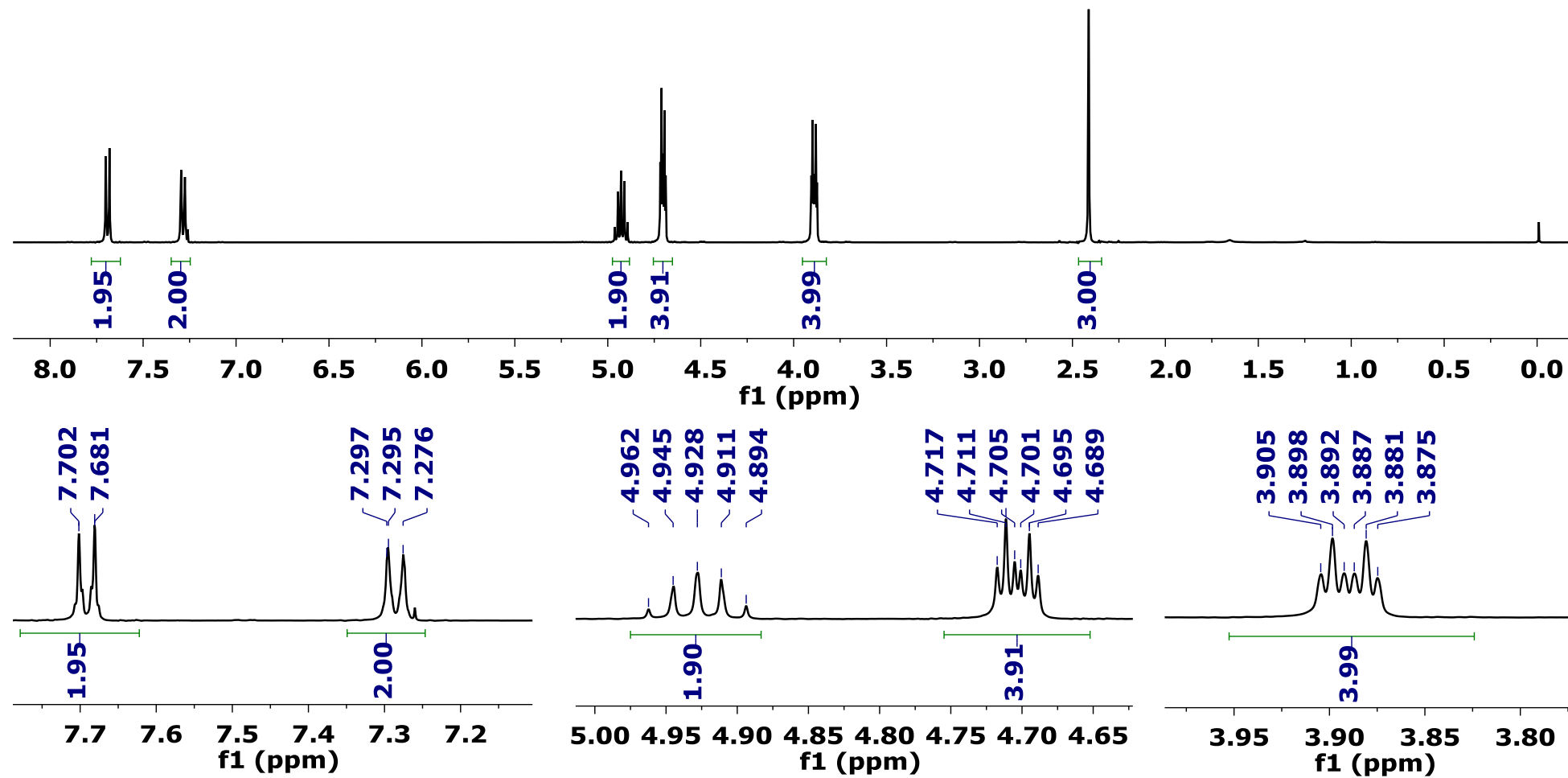


S21

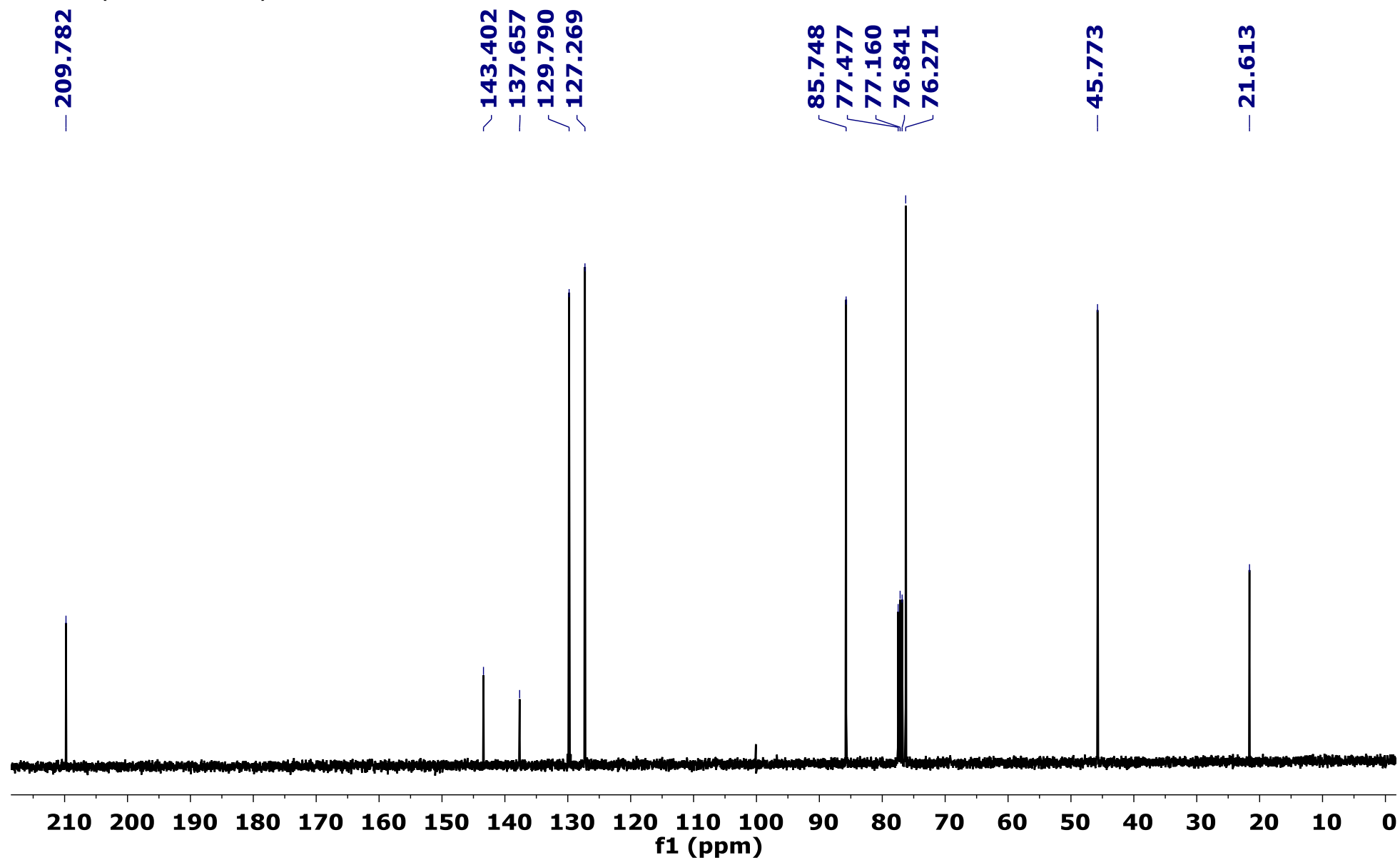
Bisallene 1a



^1H NMR (400 MHz, CDCl_3)

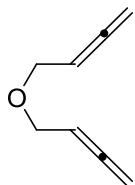


¹³C NMR (101 MHz, CDCl₃)

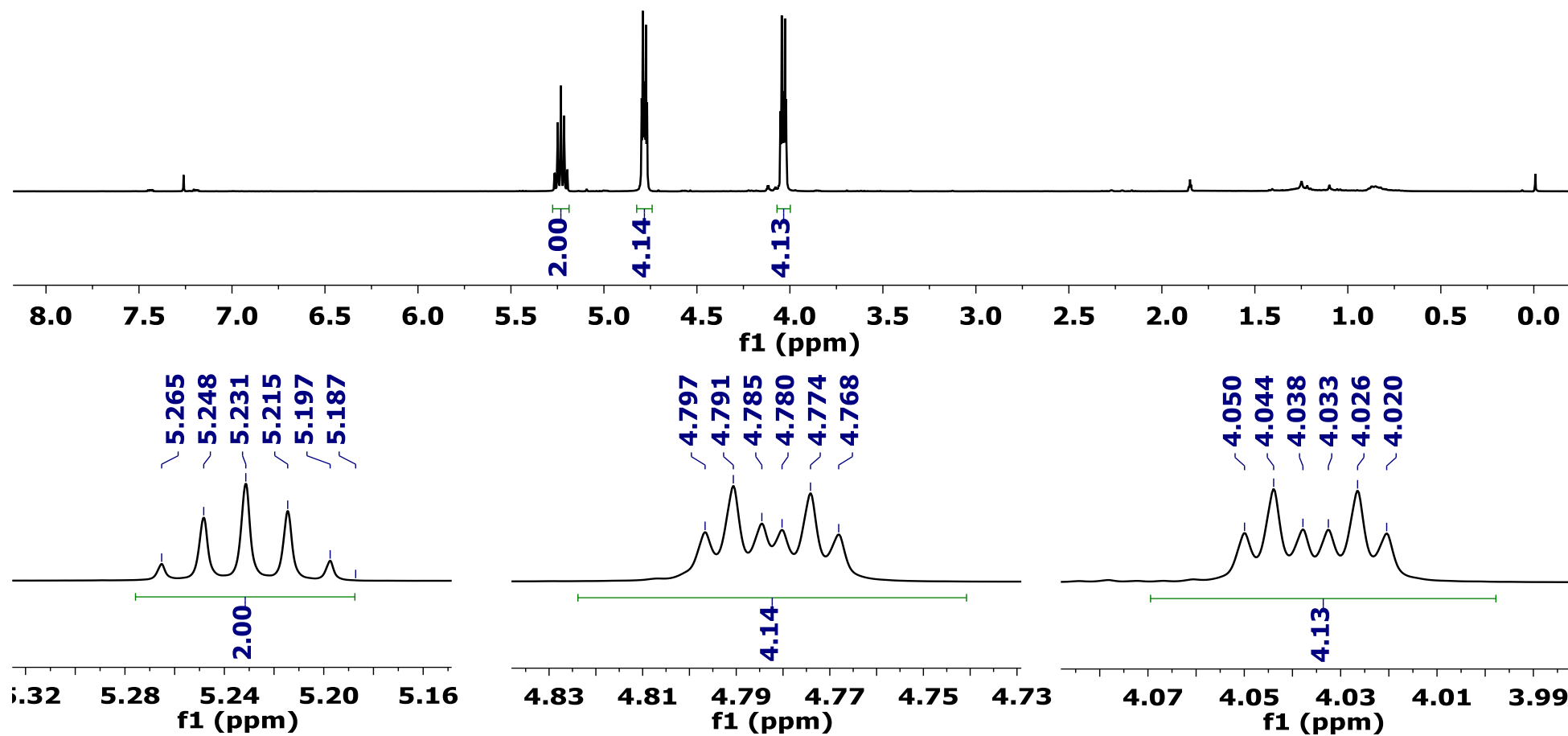


S23

Bisallene 1b

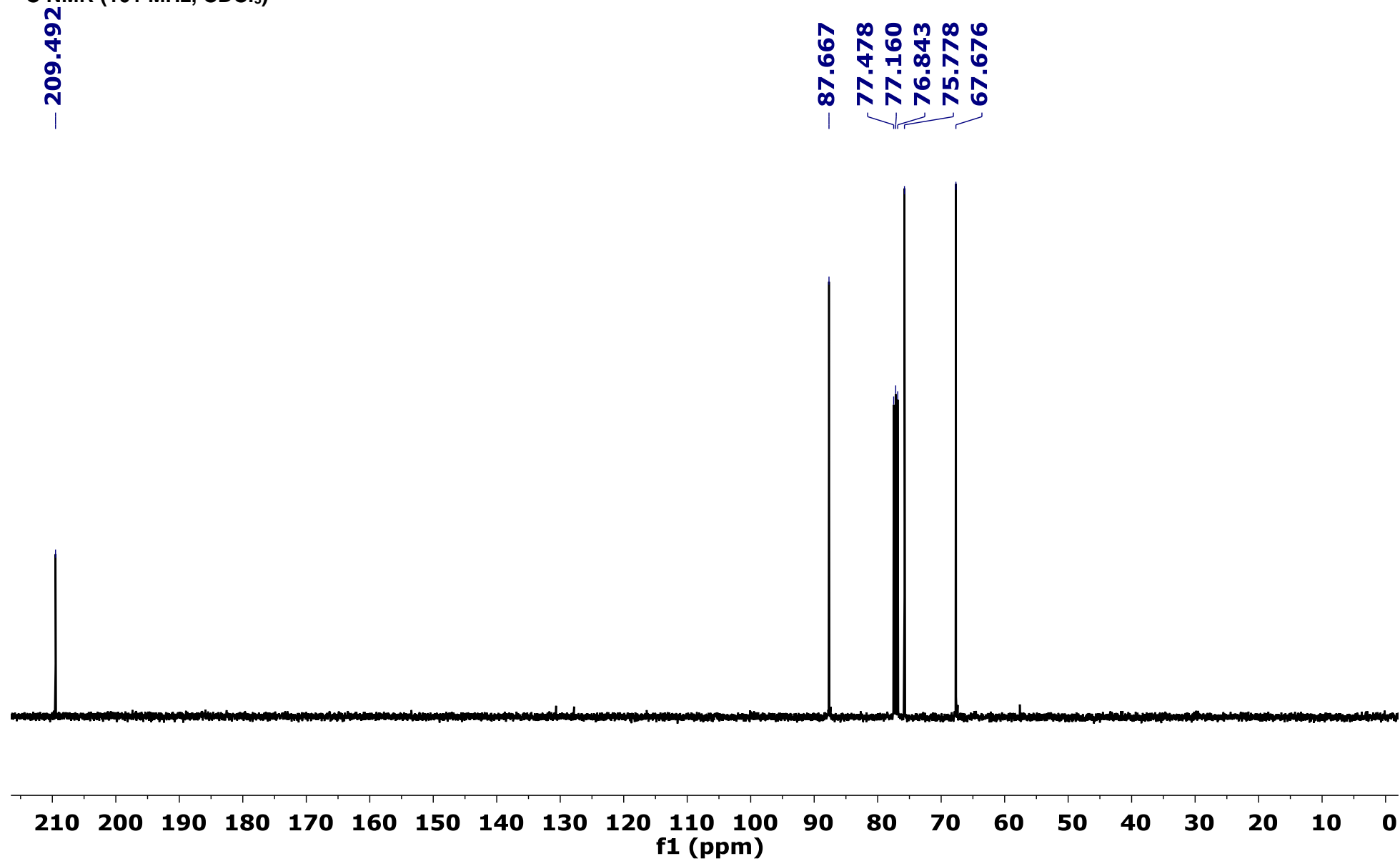


^1H NMR (400 MHz, CDCl_3)

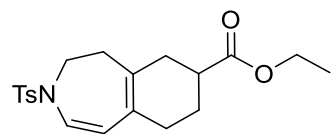


S24

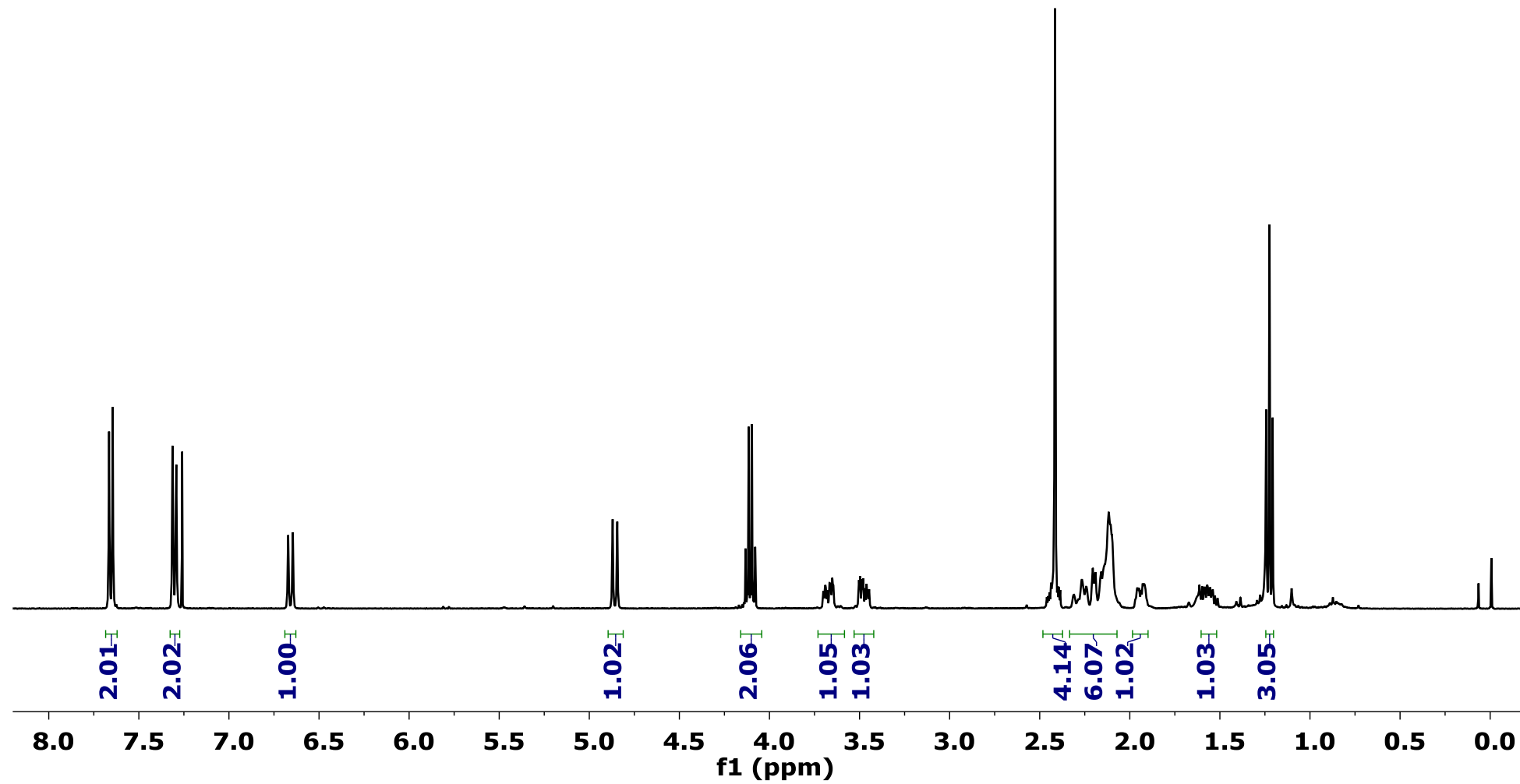
¹³C NMR (101 MHz, CDCl₃)

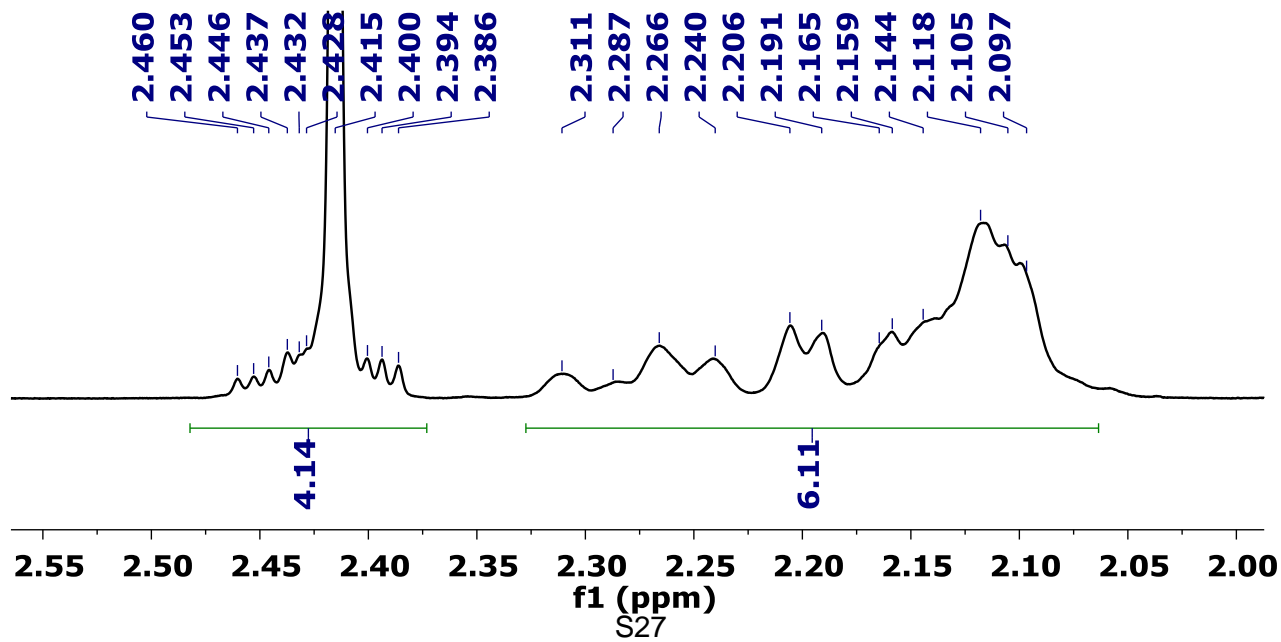
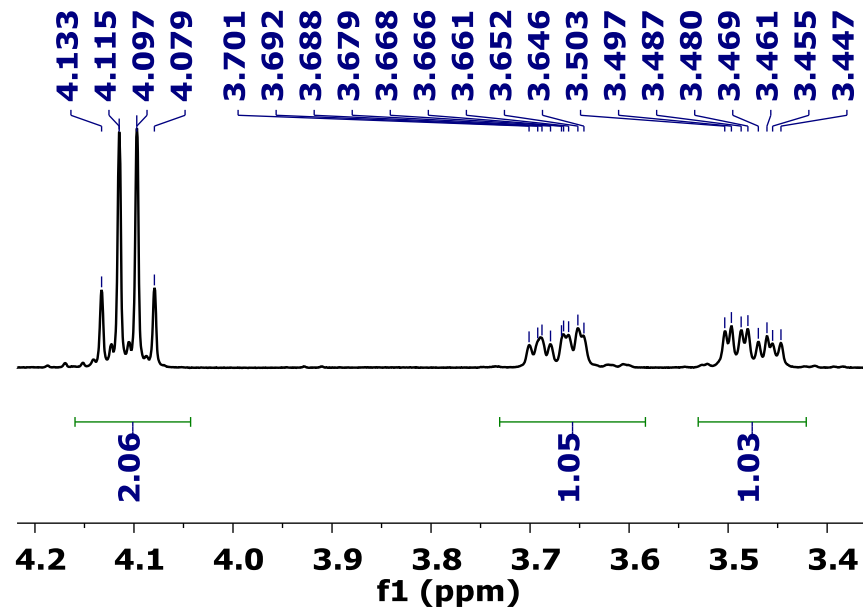
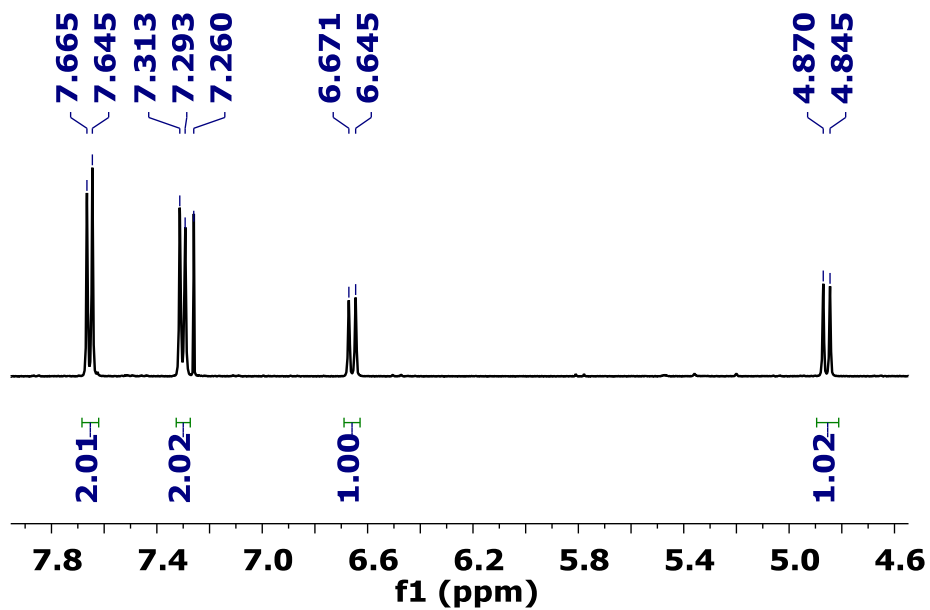


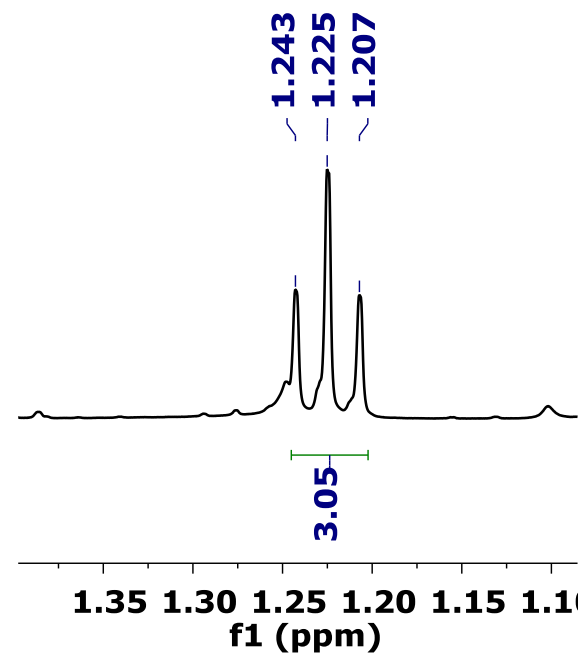
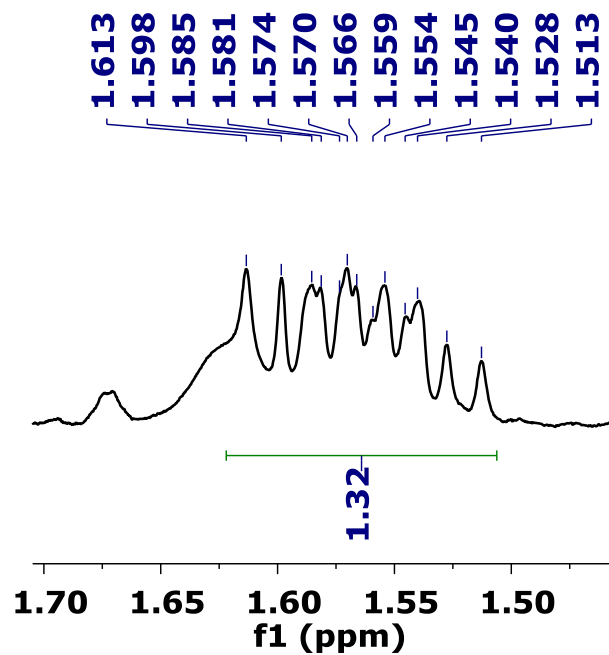
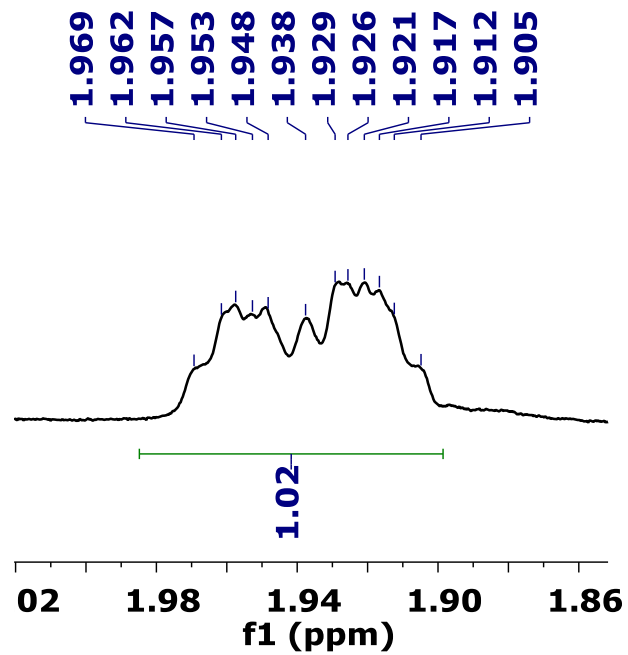
Product 3aa



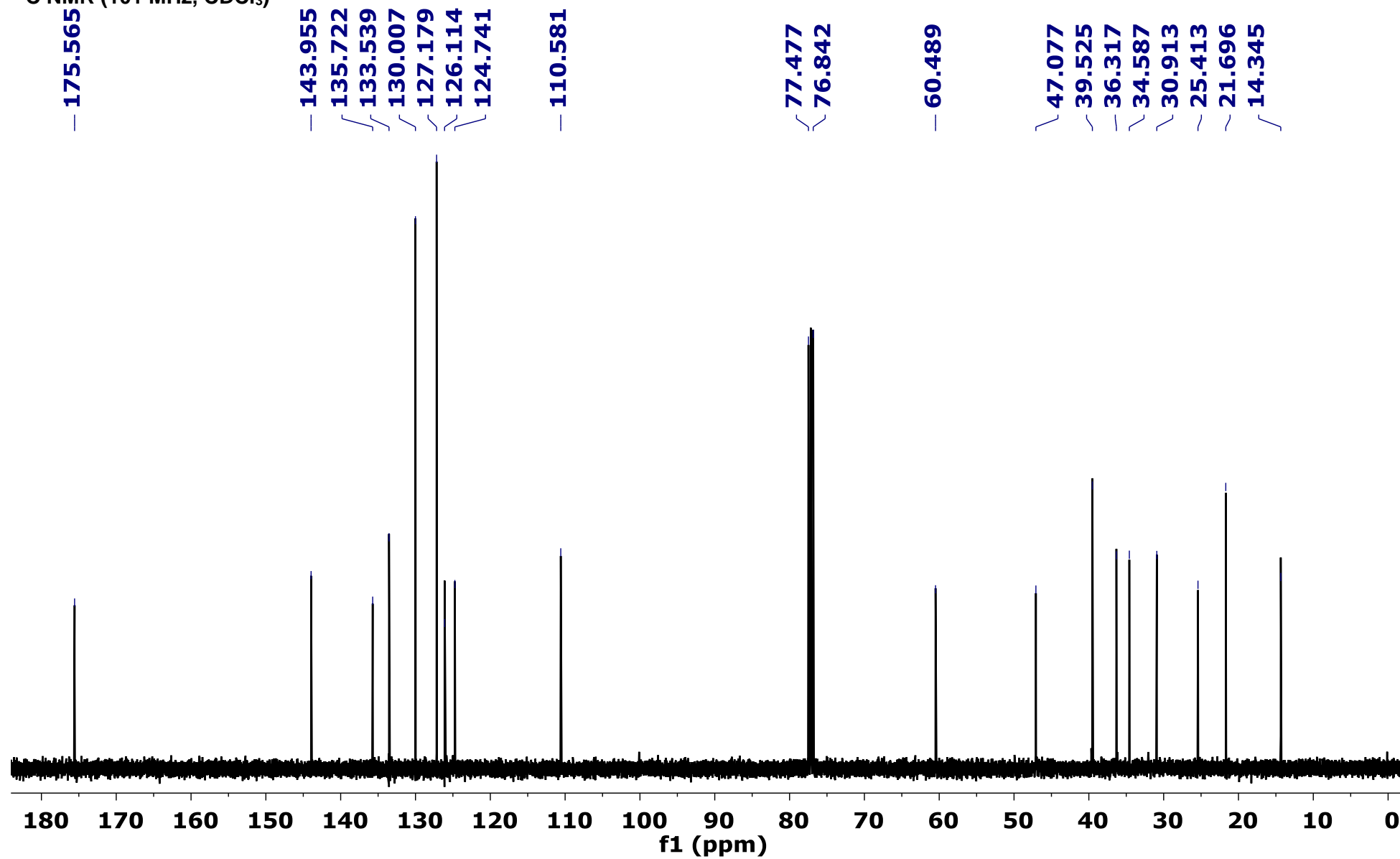
^1H NMR (400 MHz, CDCl_3)



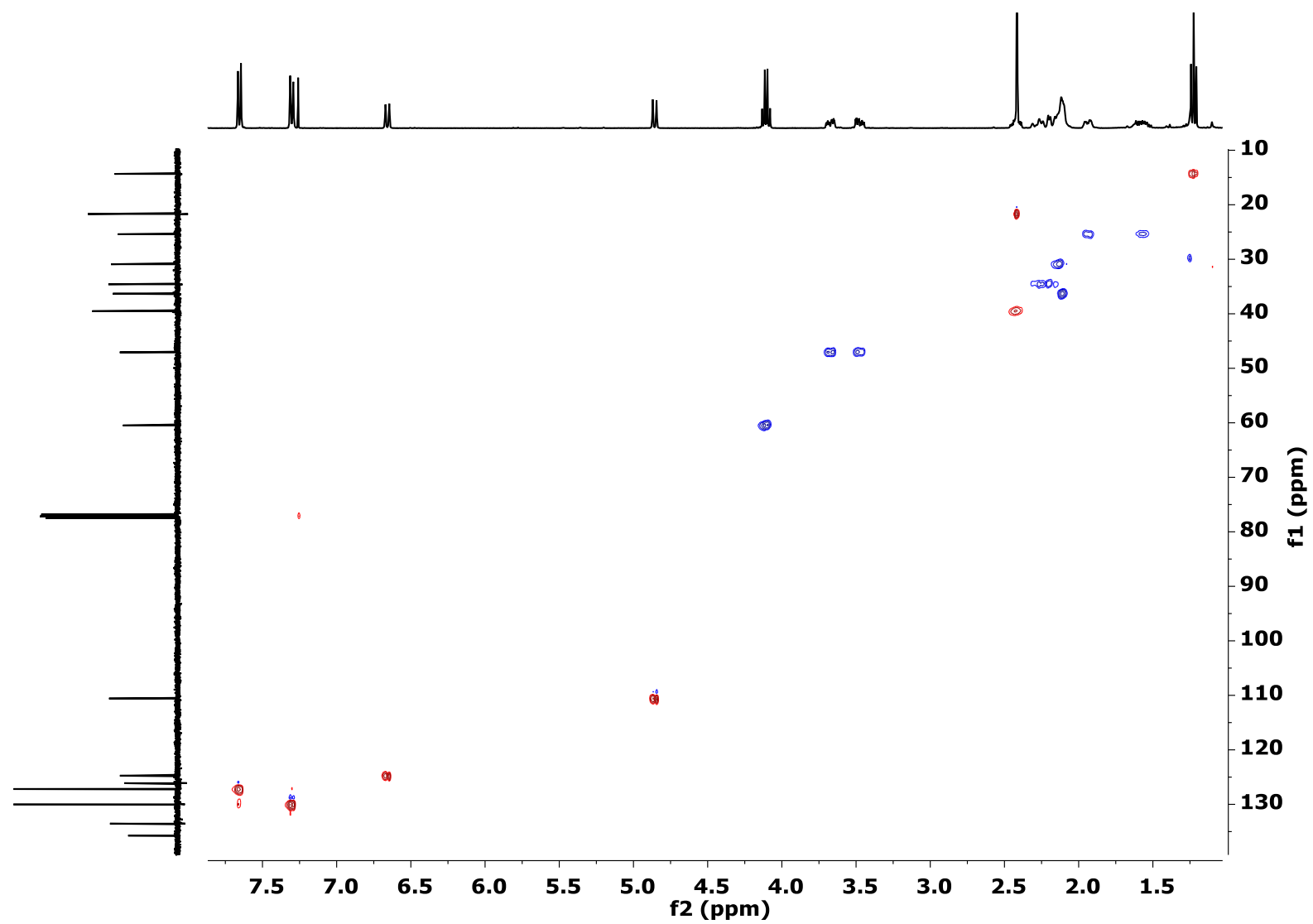




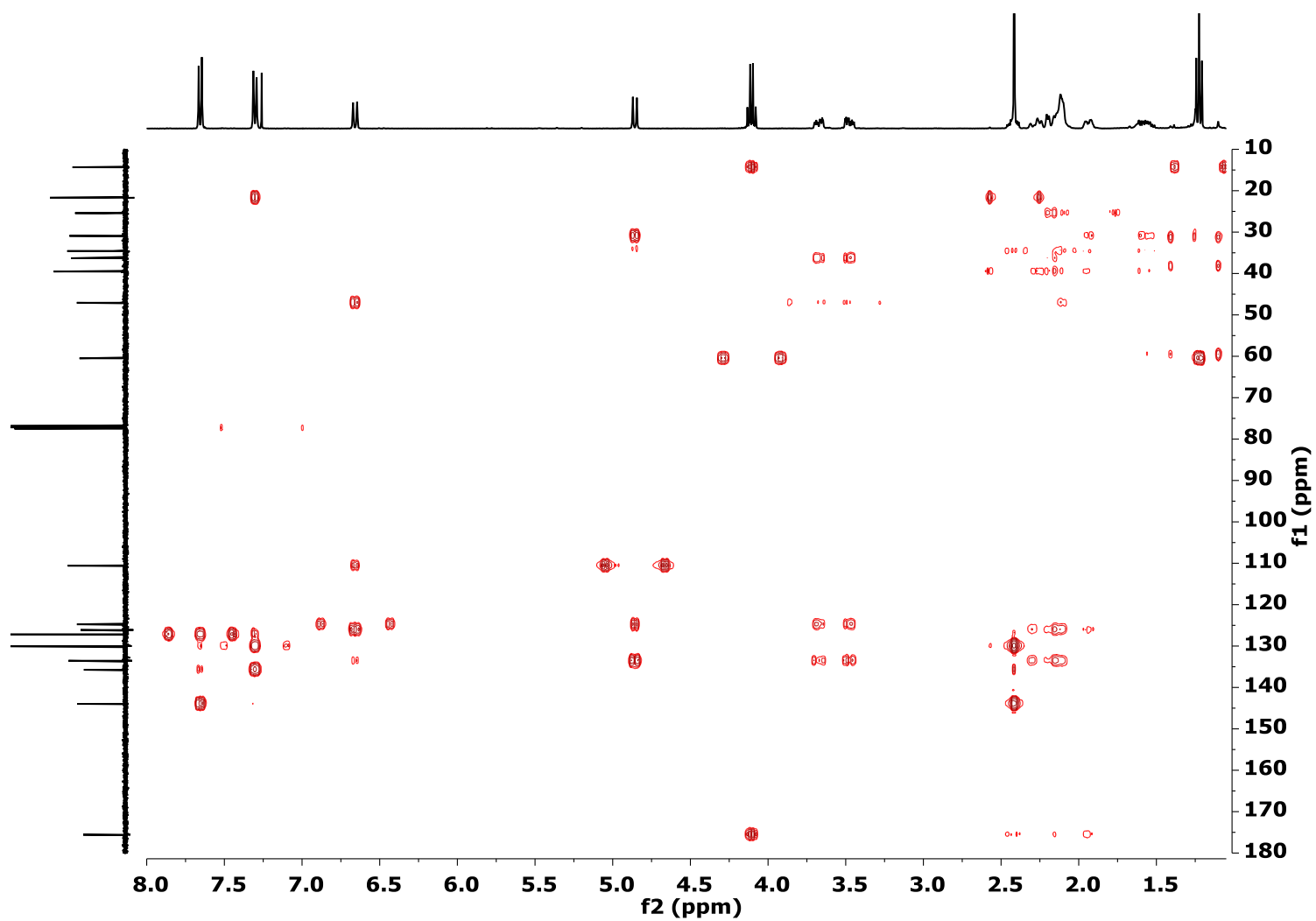
¹³C NMR (101 MHz, CDCl₃)



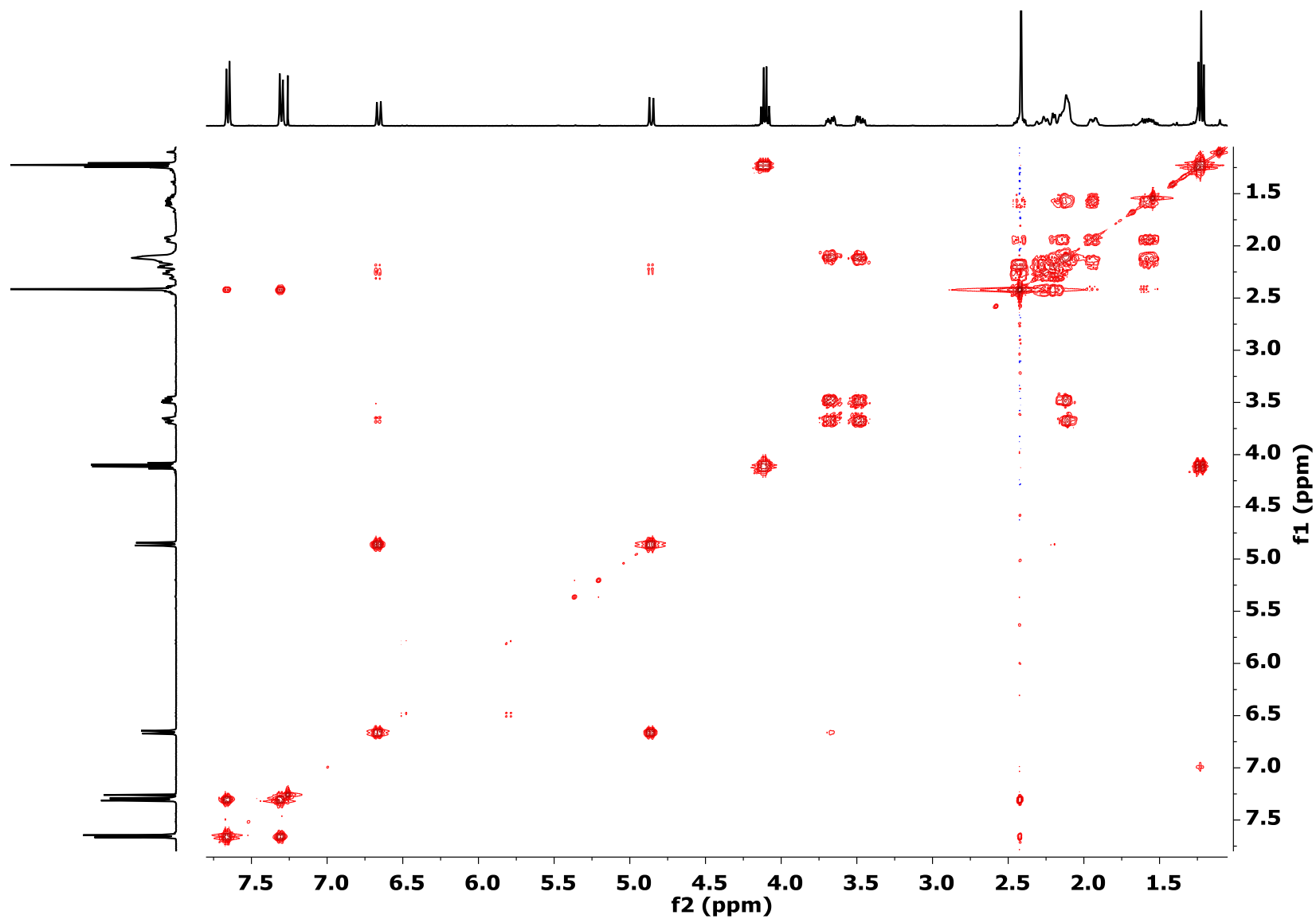
2D NMR HSQC

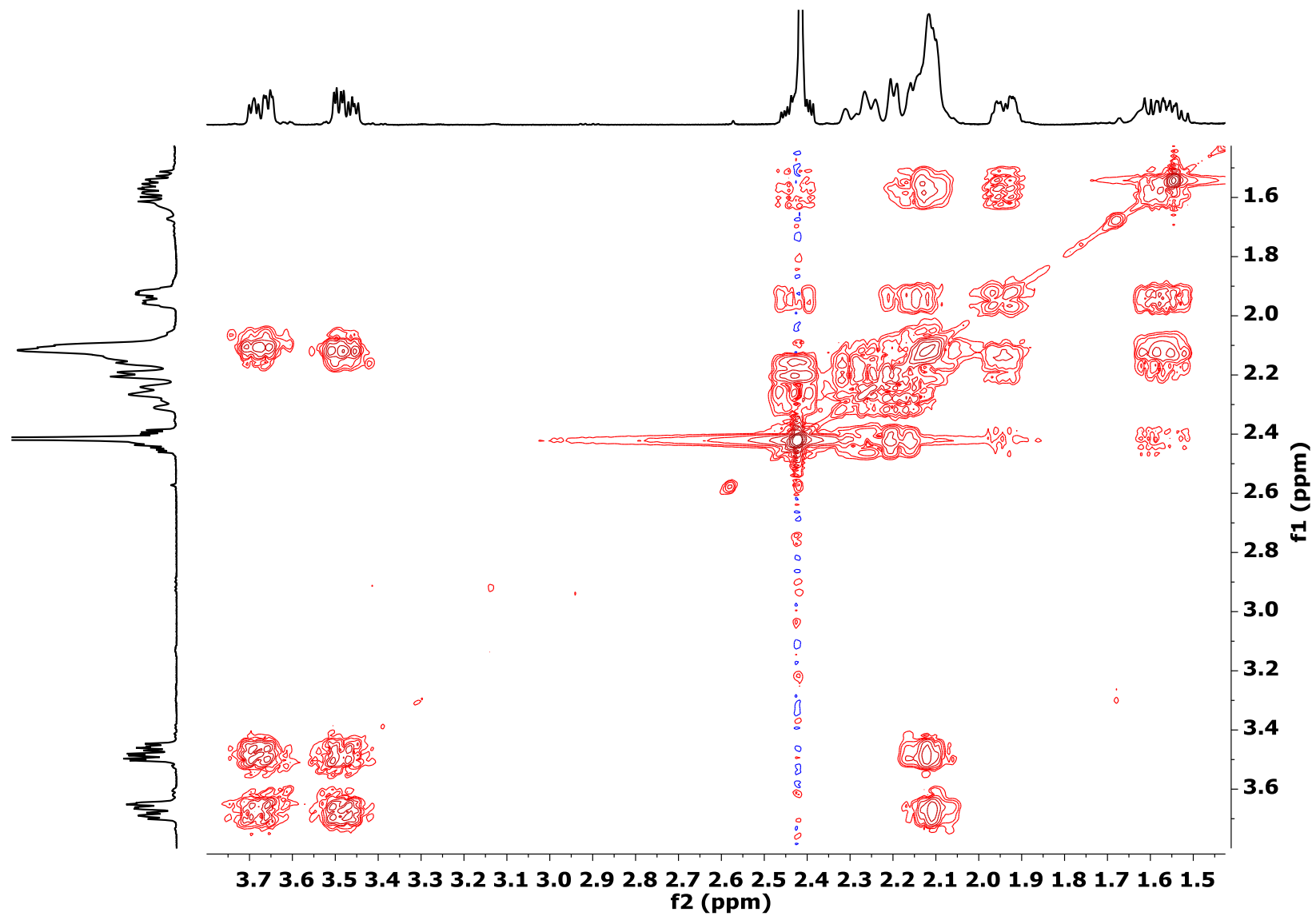


2D NMR HMBC

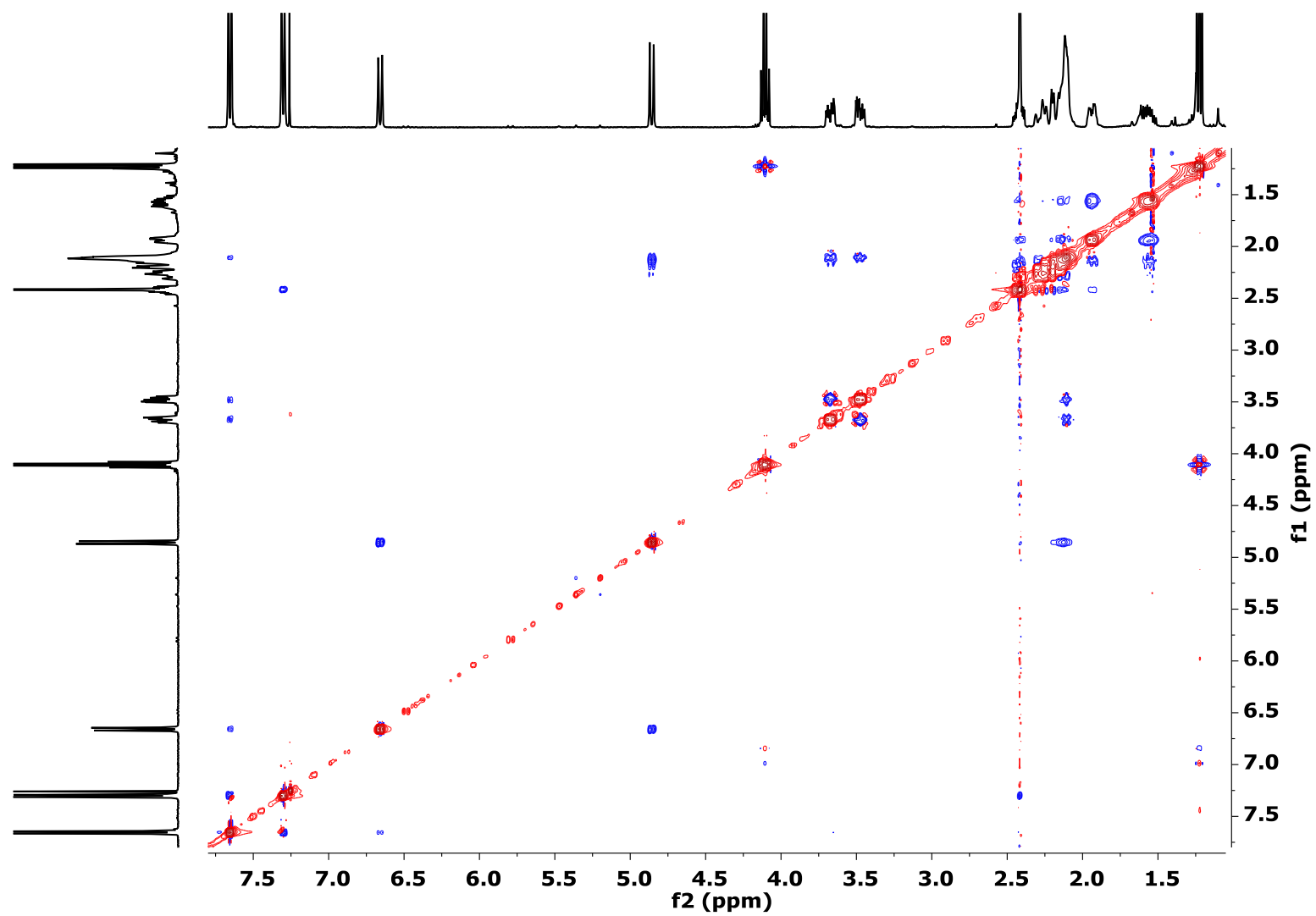


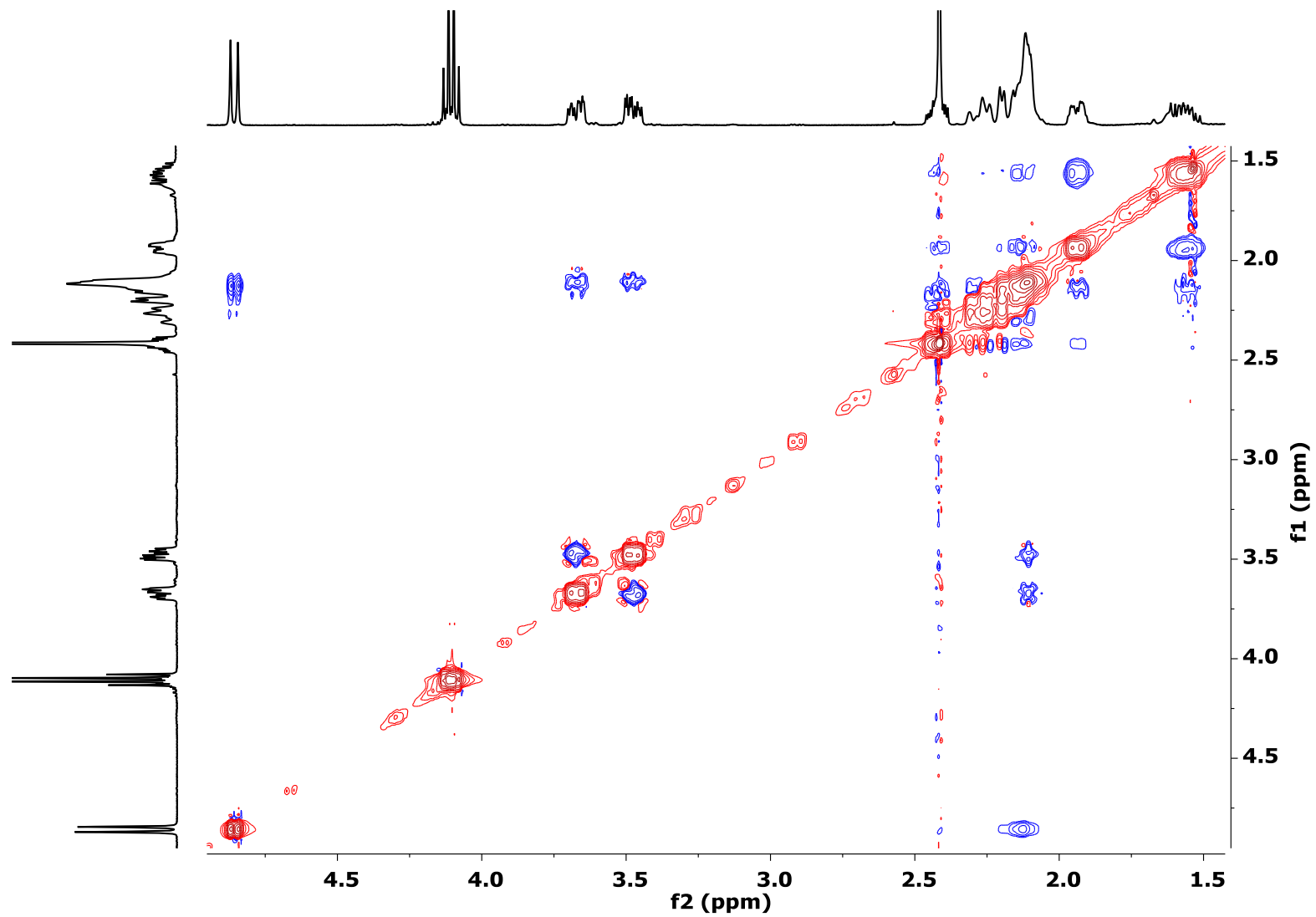
2D NMR COSY



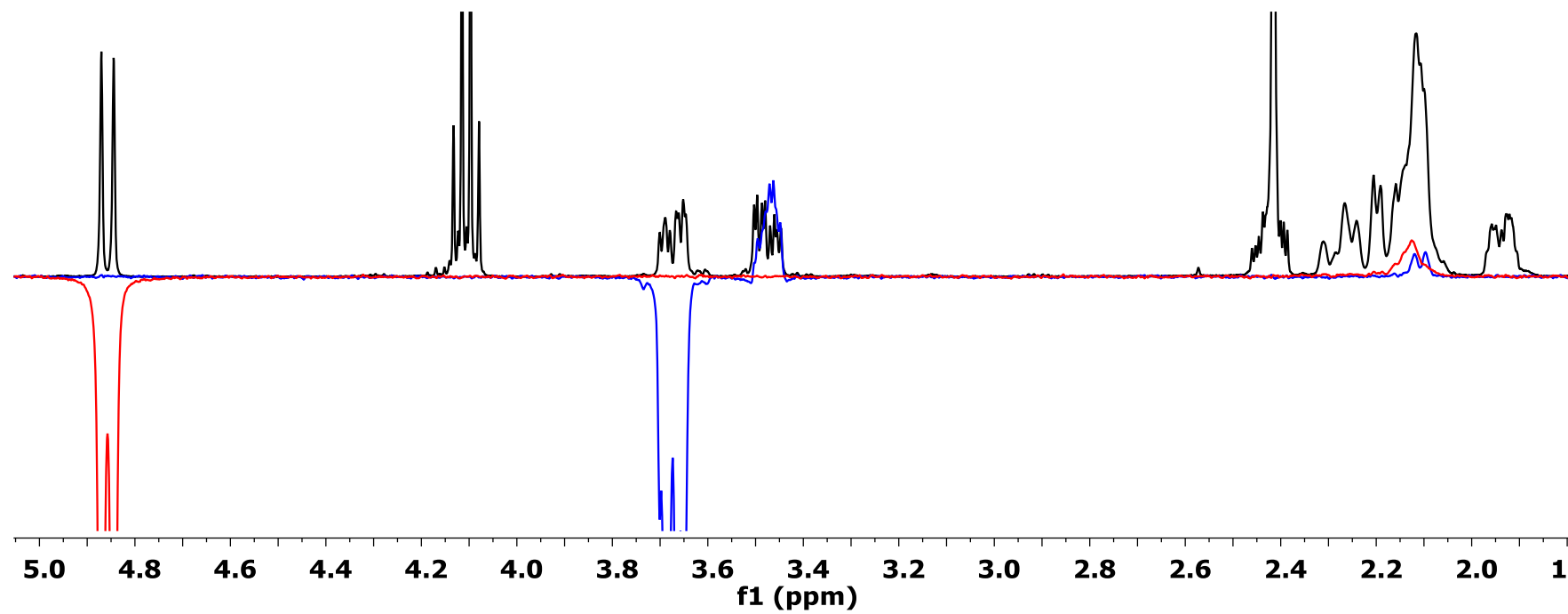


2D NMR NOESY

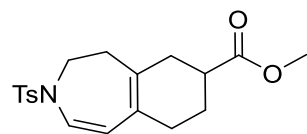




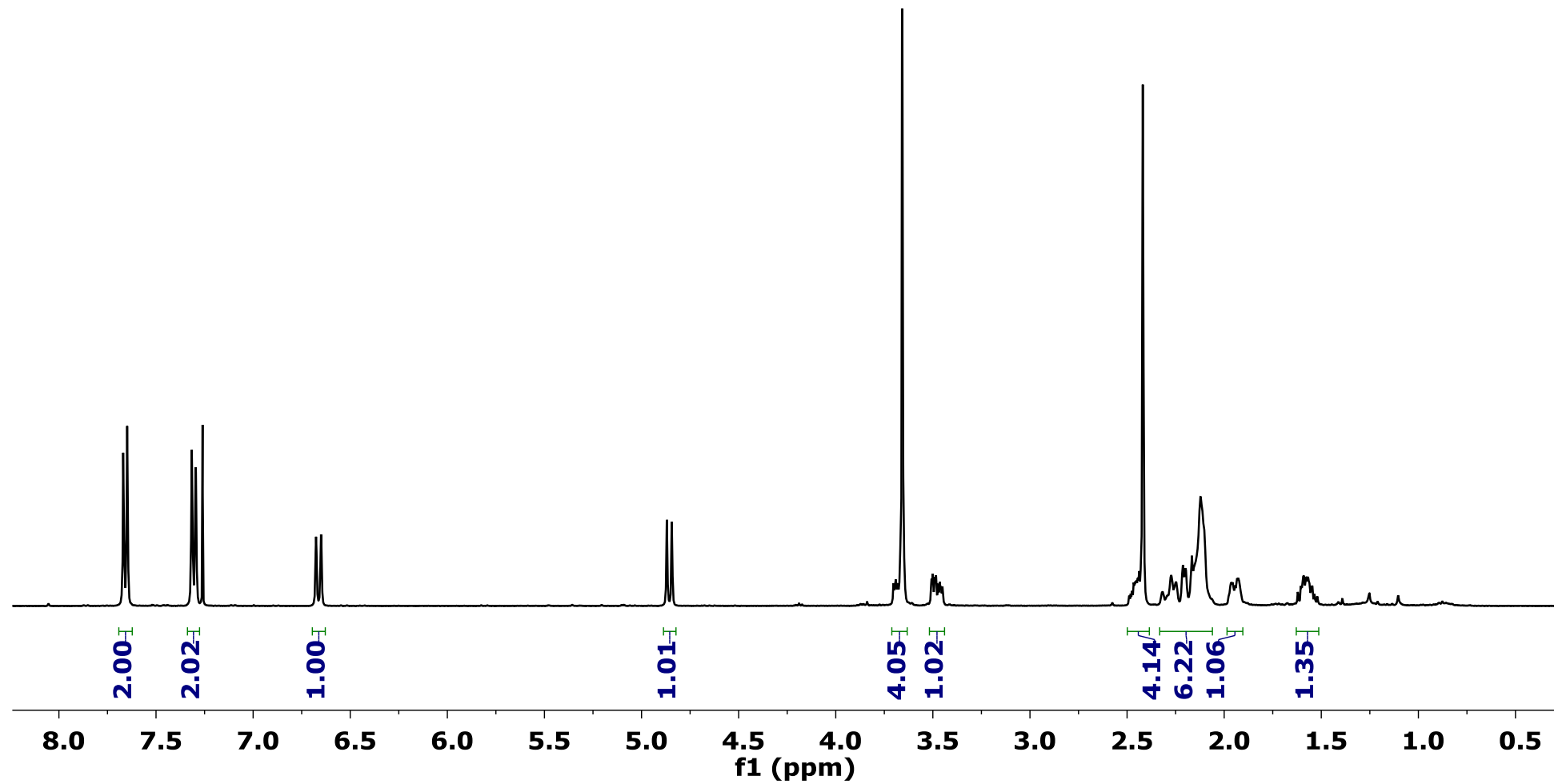
1D NMR SELECTIVE NOESY

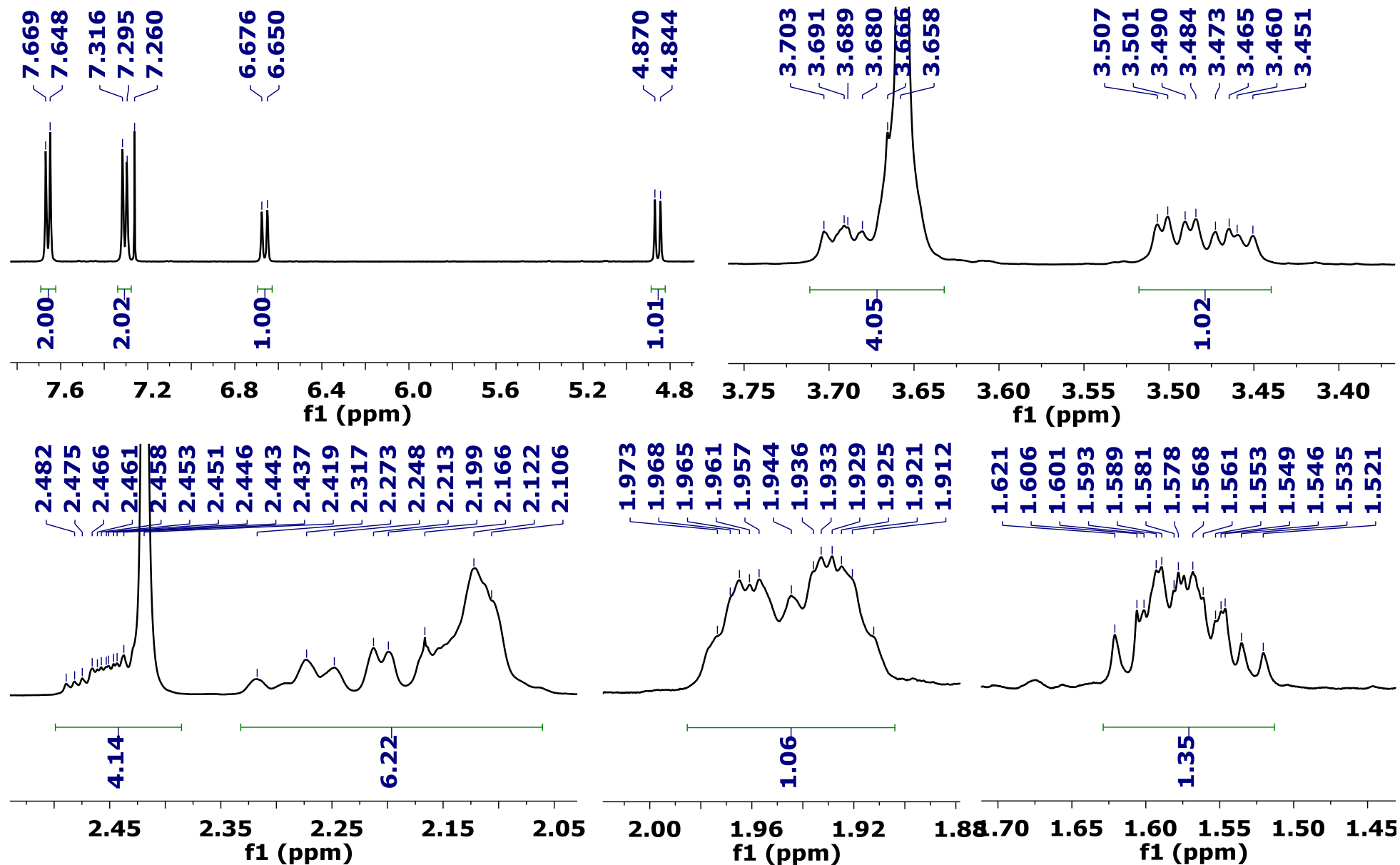


Product 3ab

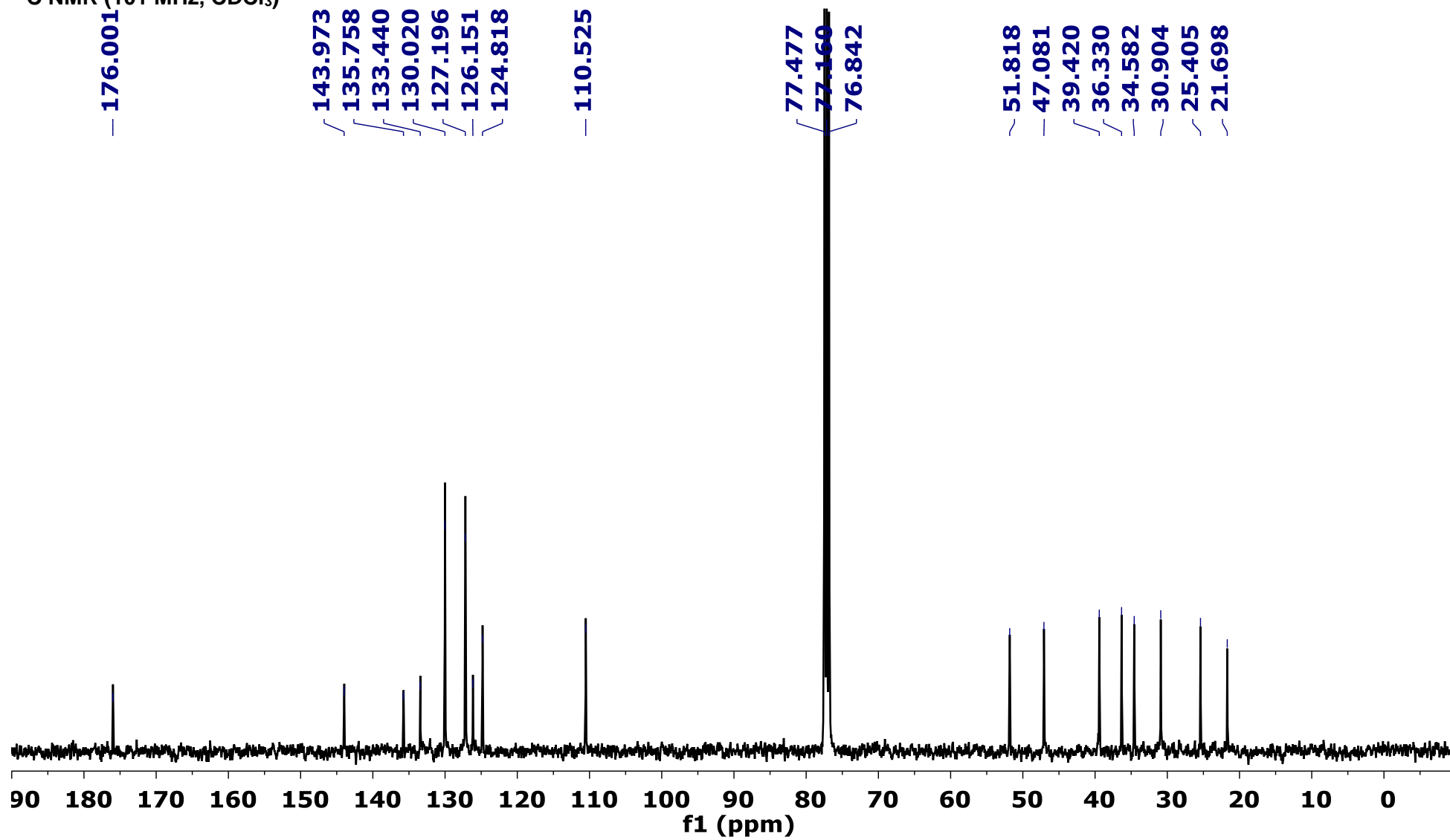


^1H NMR (400 MHz, CDCl_3)

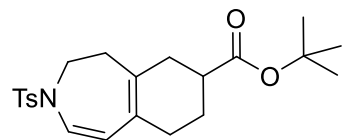




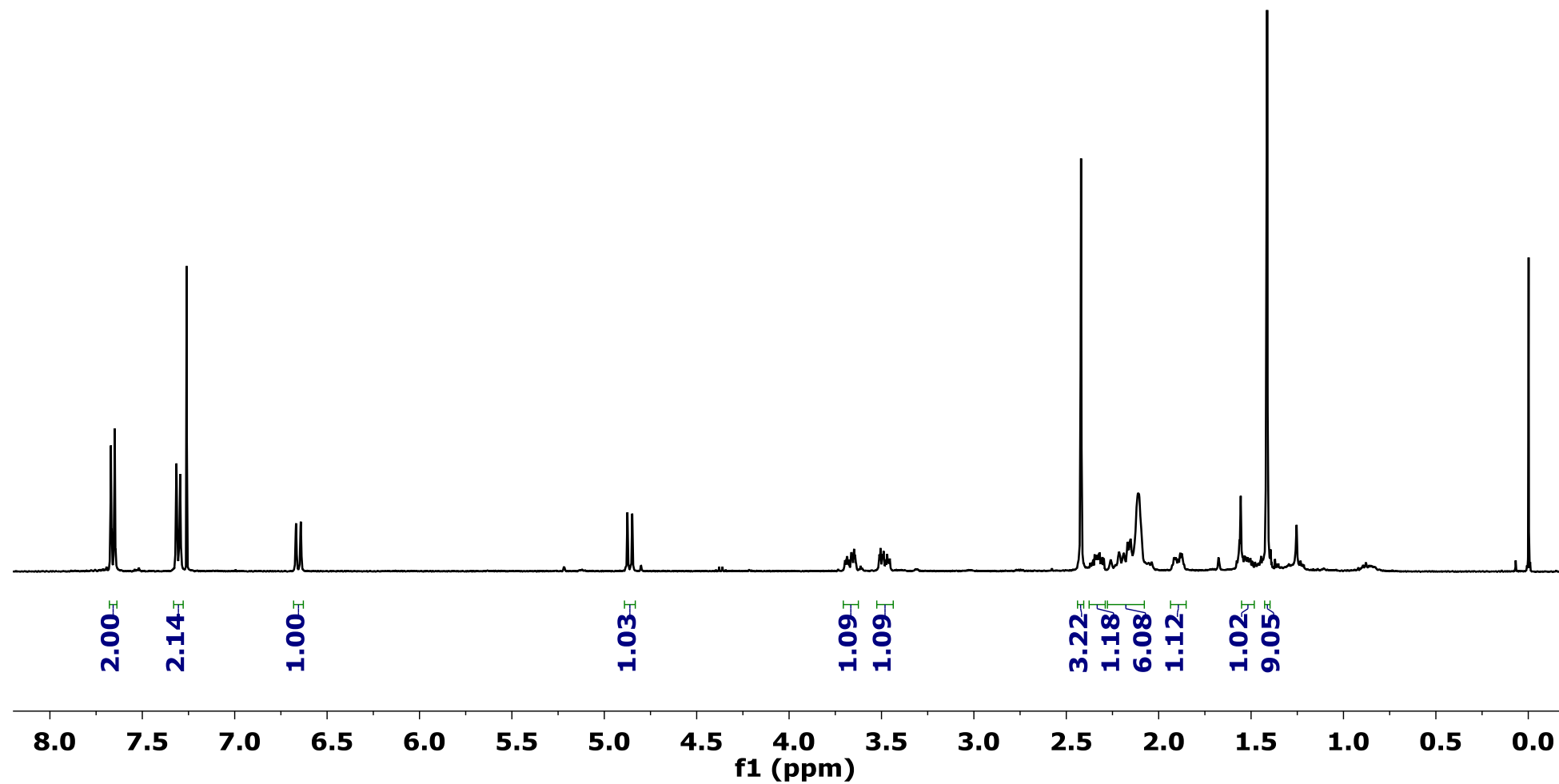
¹³C NMR (101 MHz, CDCl₃)

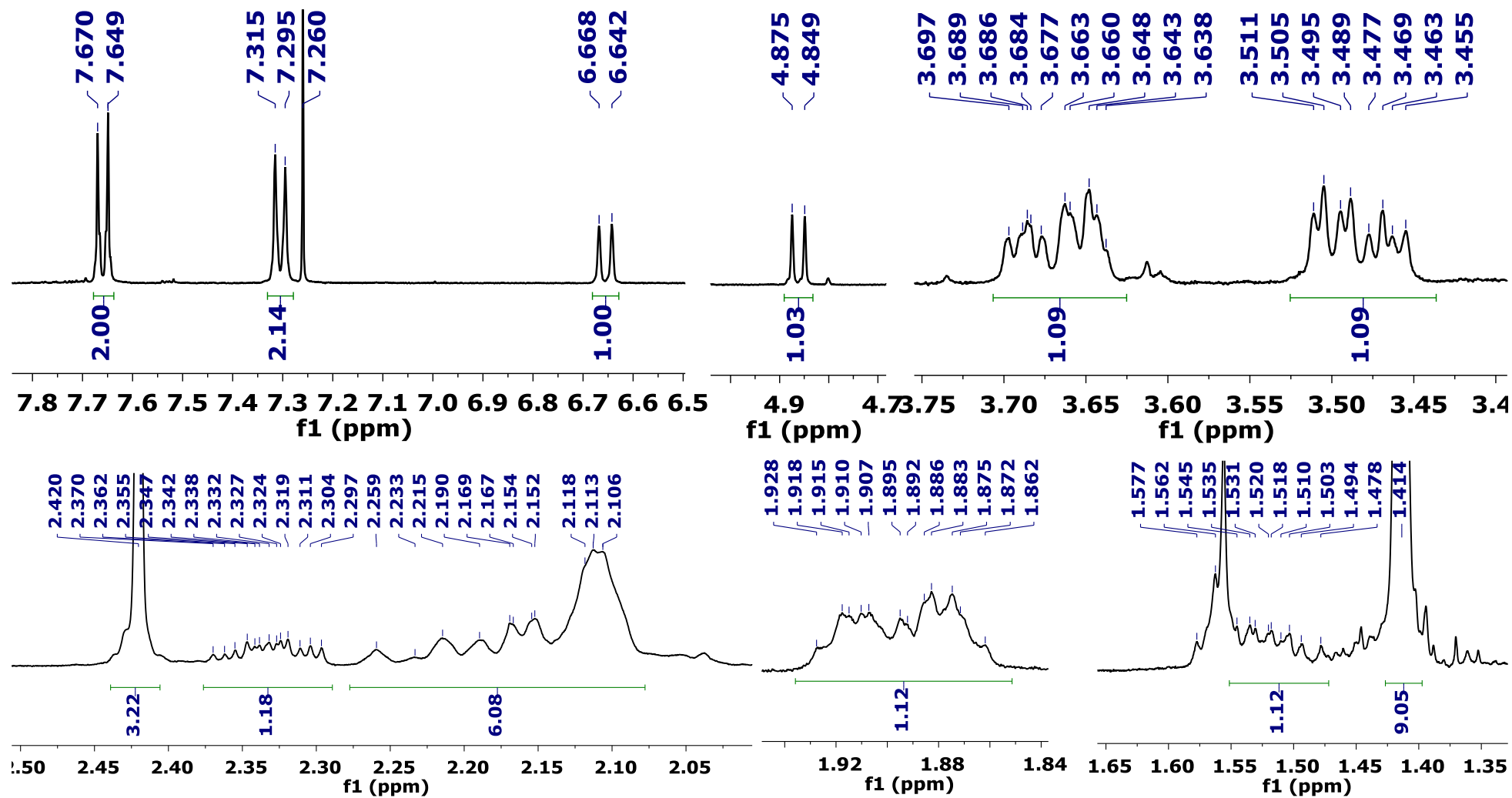


Product 3ac

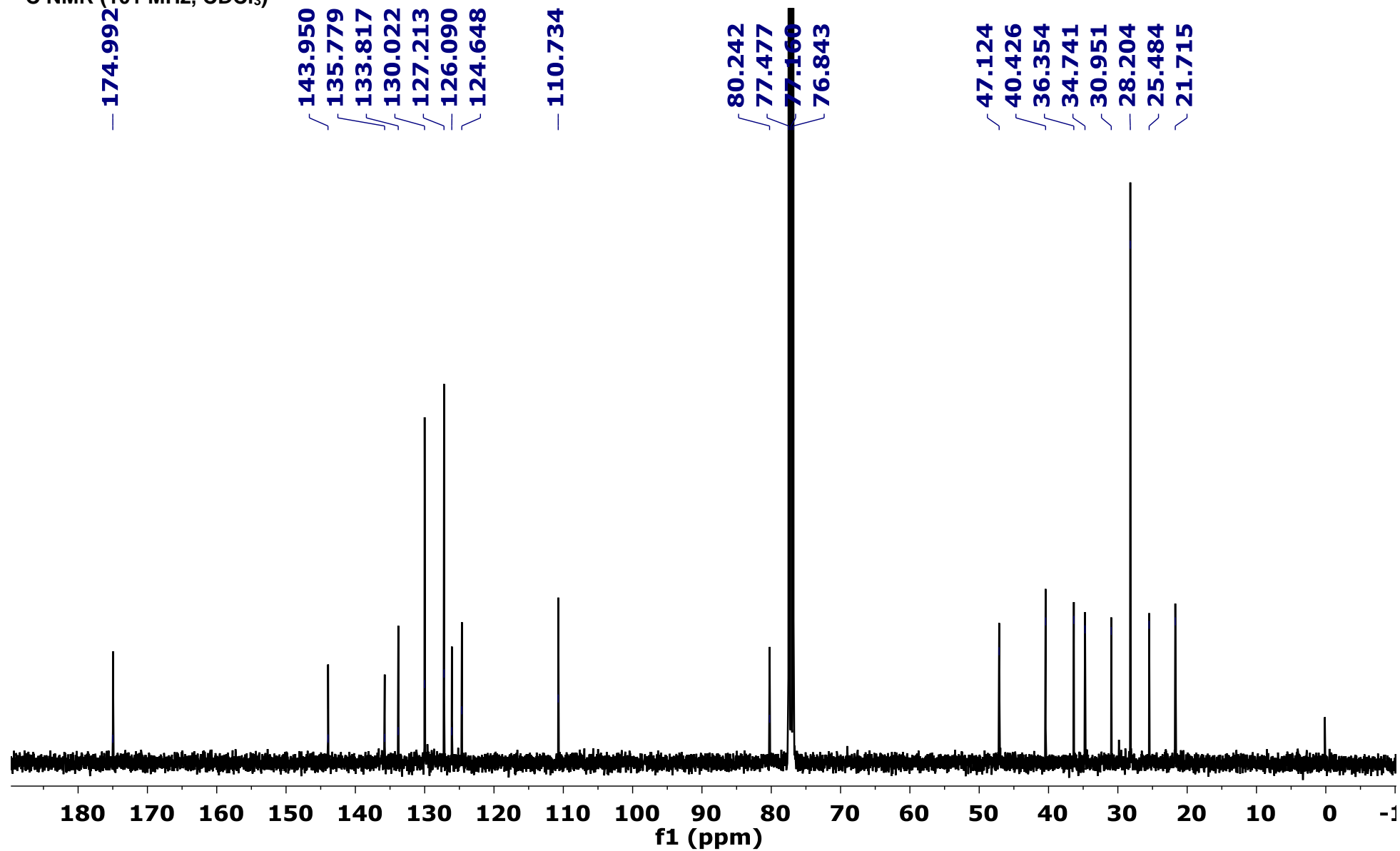


^1H NMR (400 MHz, CDCl_3)

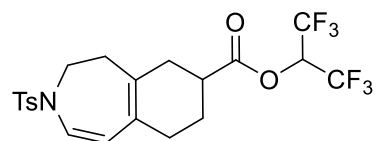




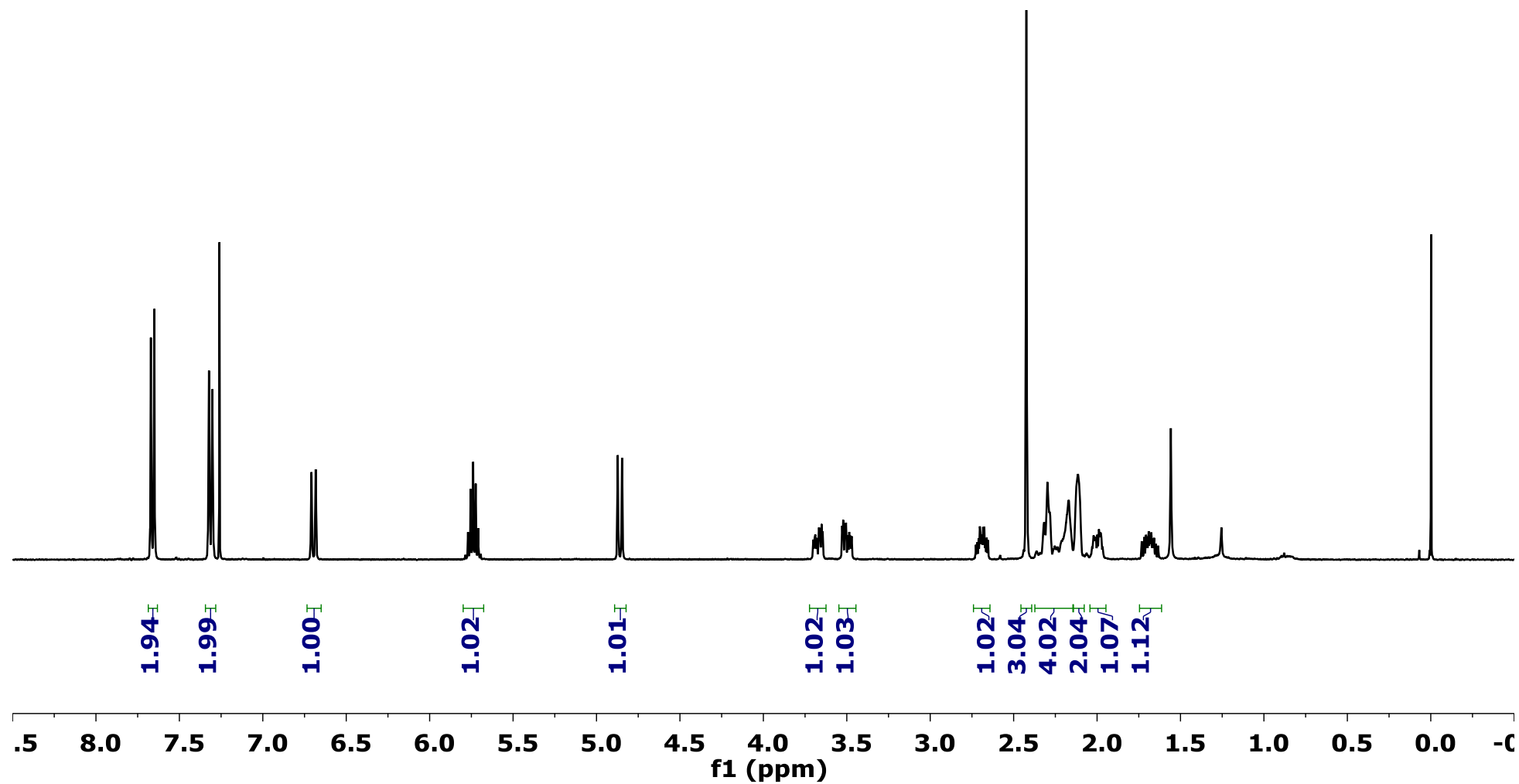
¹³C NMR (101 MHz, CDCl₃)



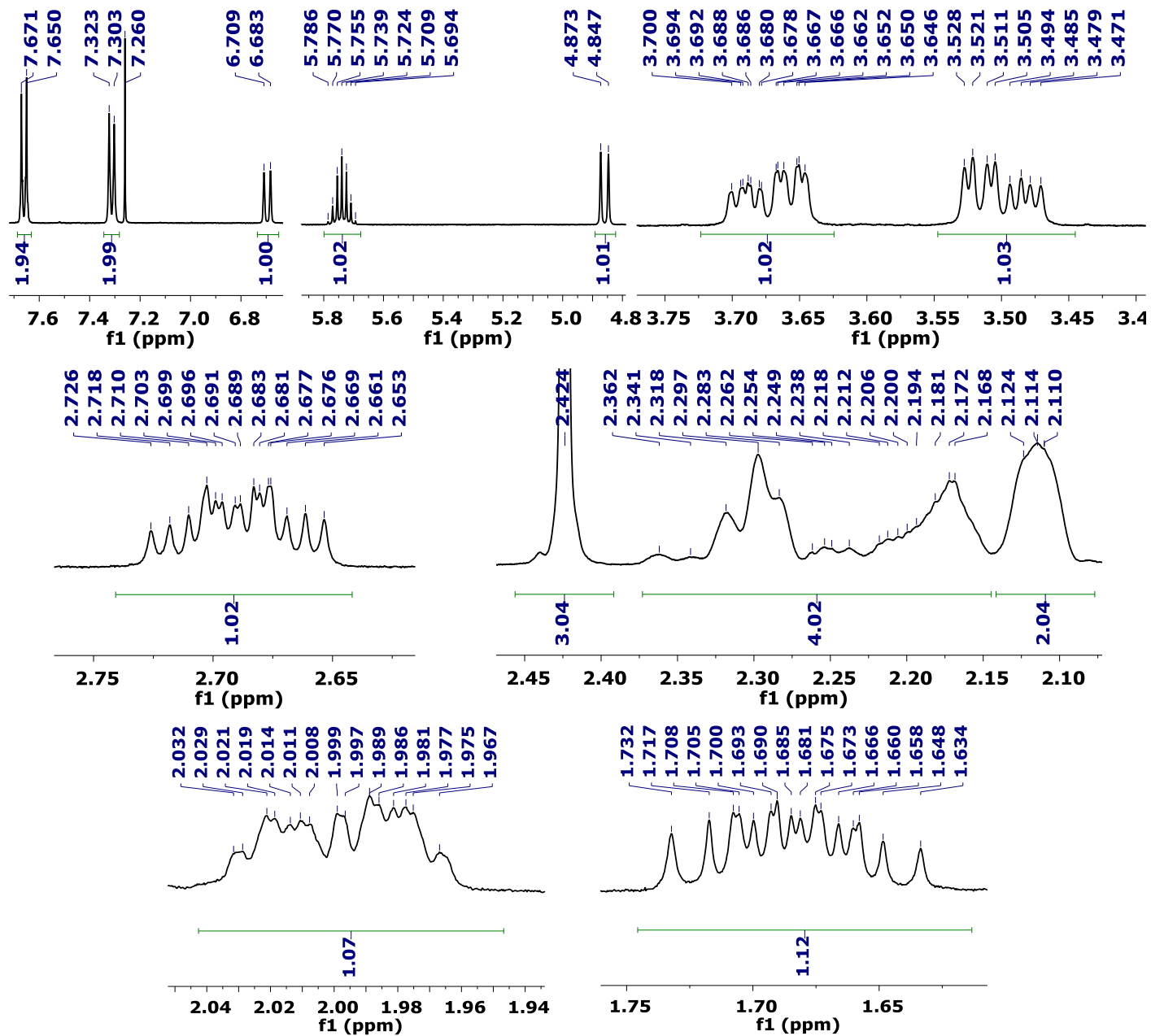
Product 3ad



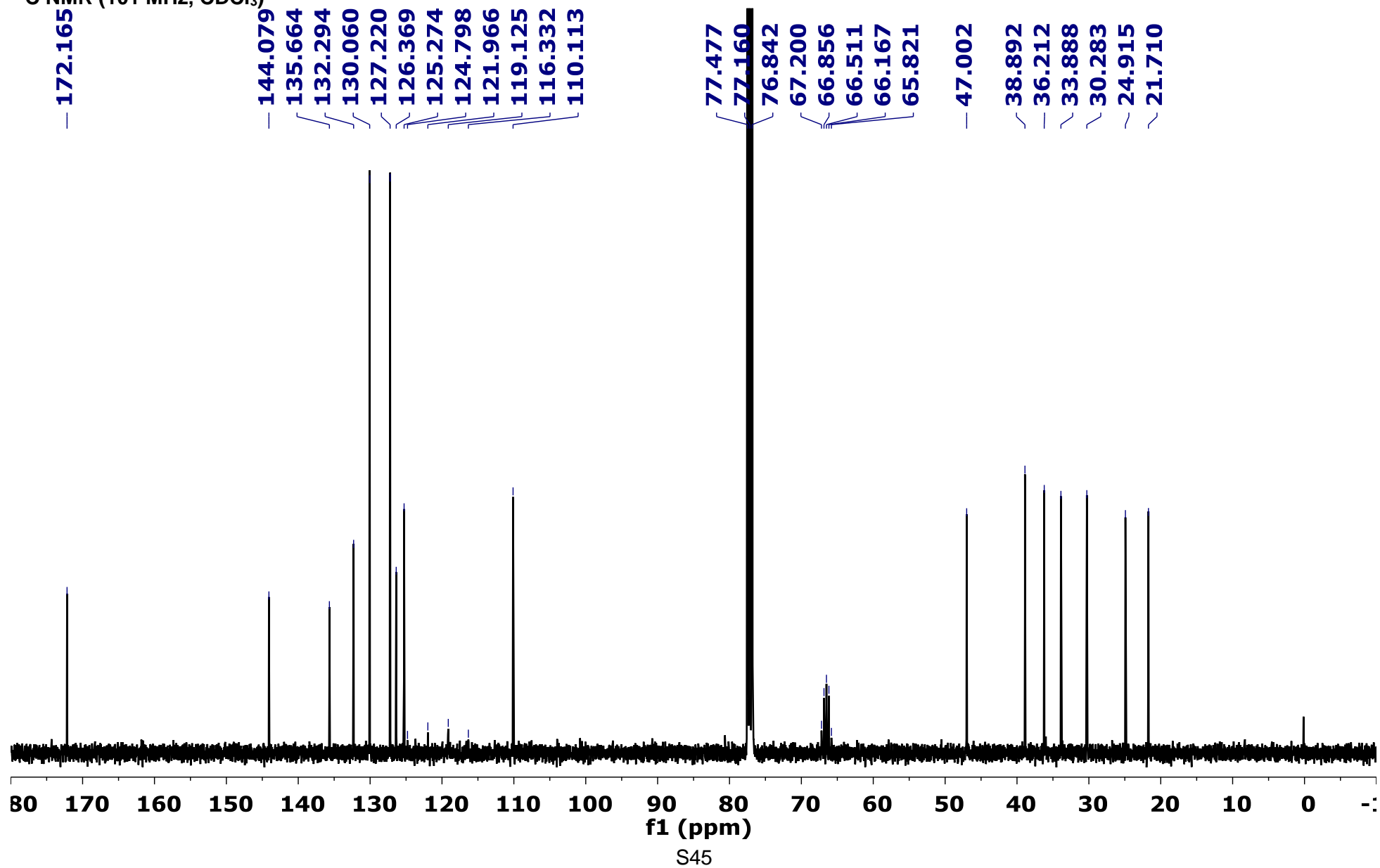
^1H NMR (400 MHz, CDCl_3)

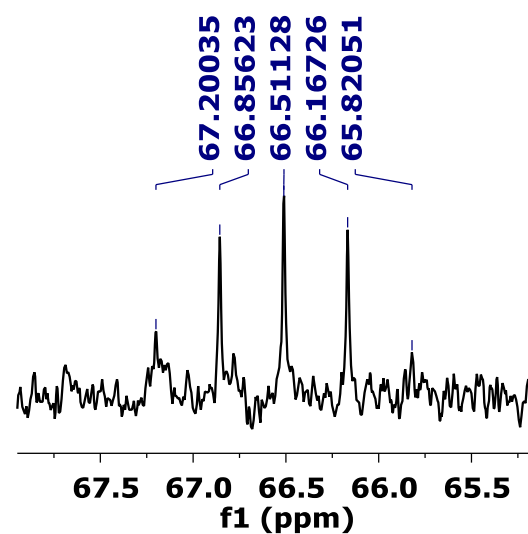
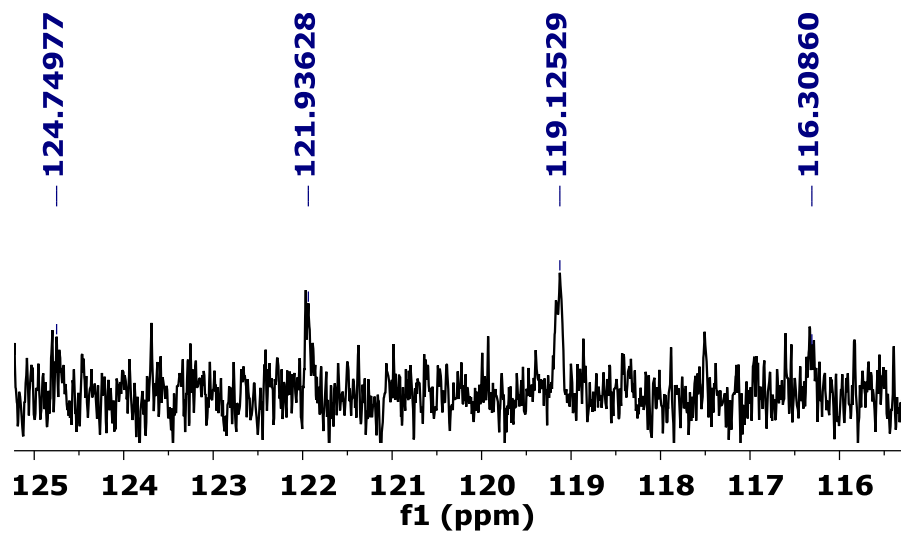


S43

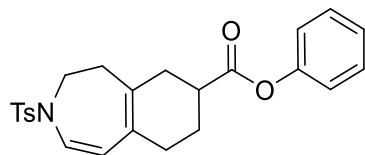


¹³C NMR (101 MHz, CDCl₃)

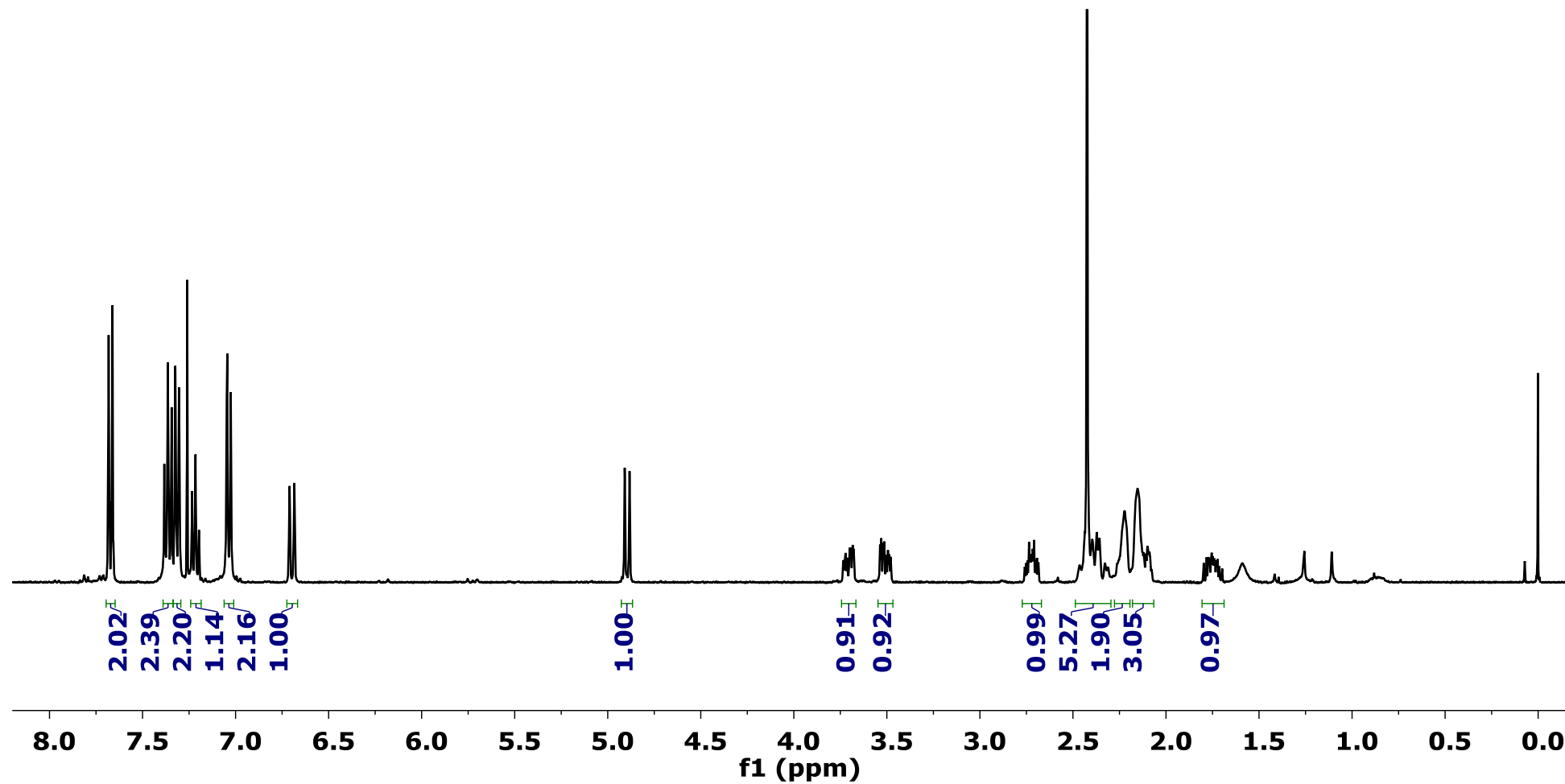


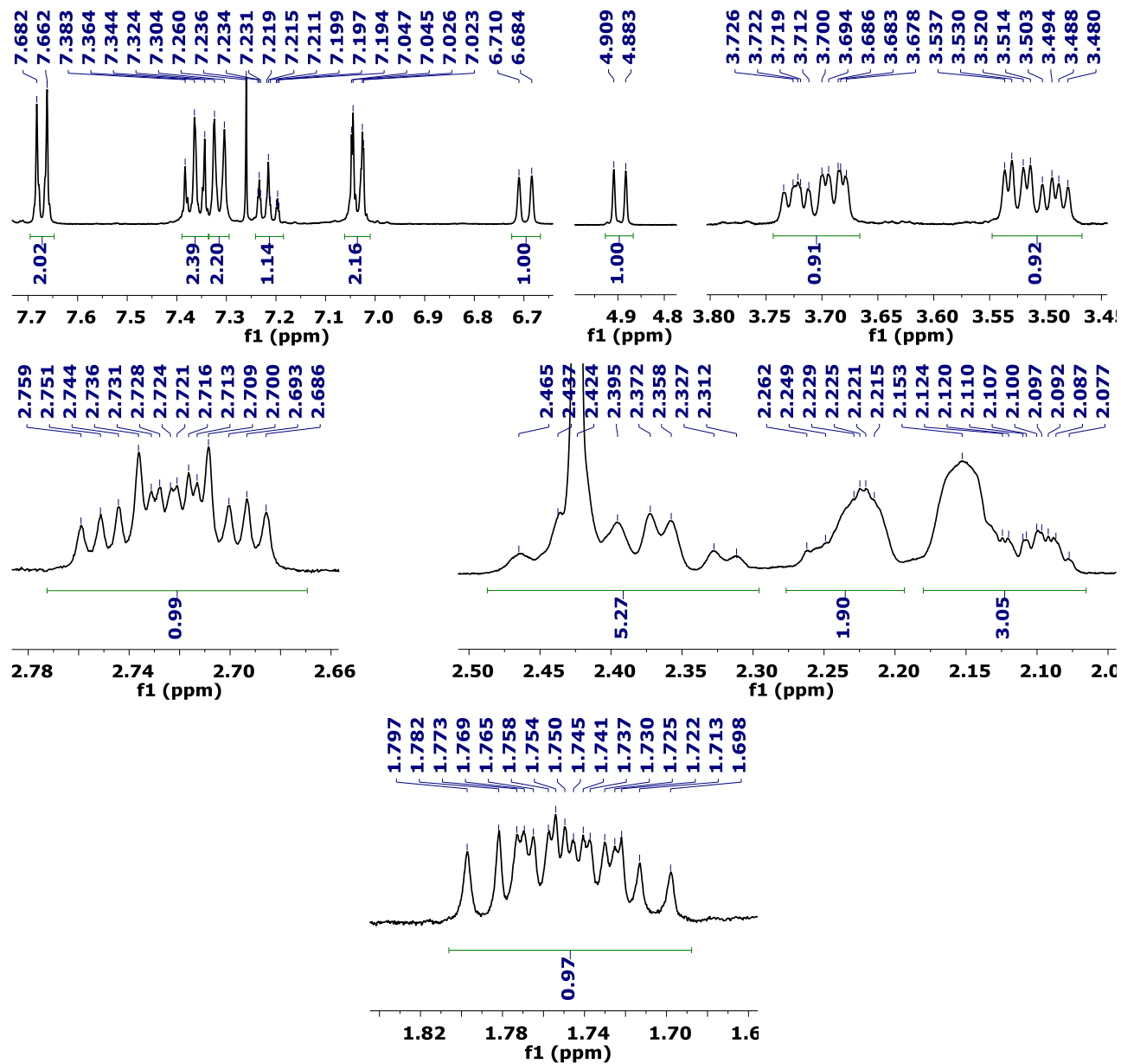


Product 3ae

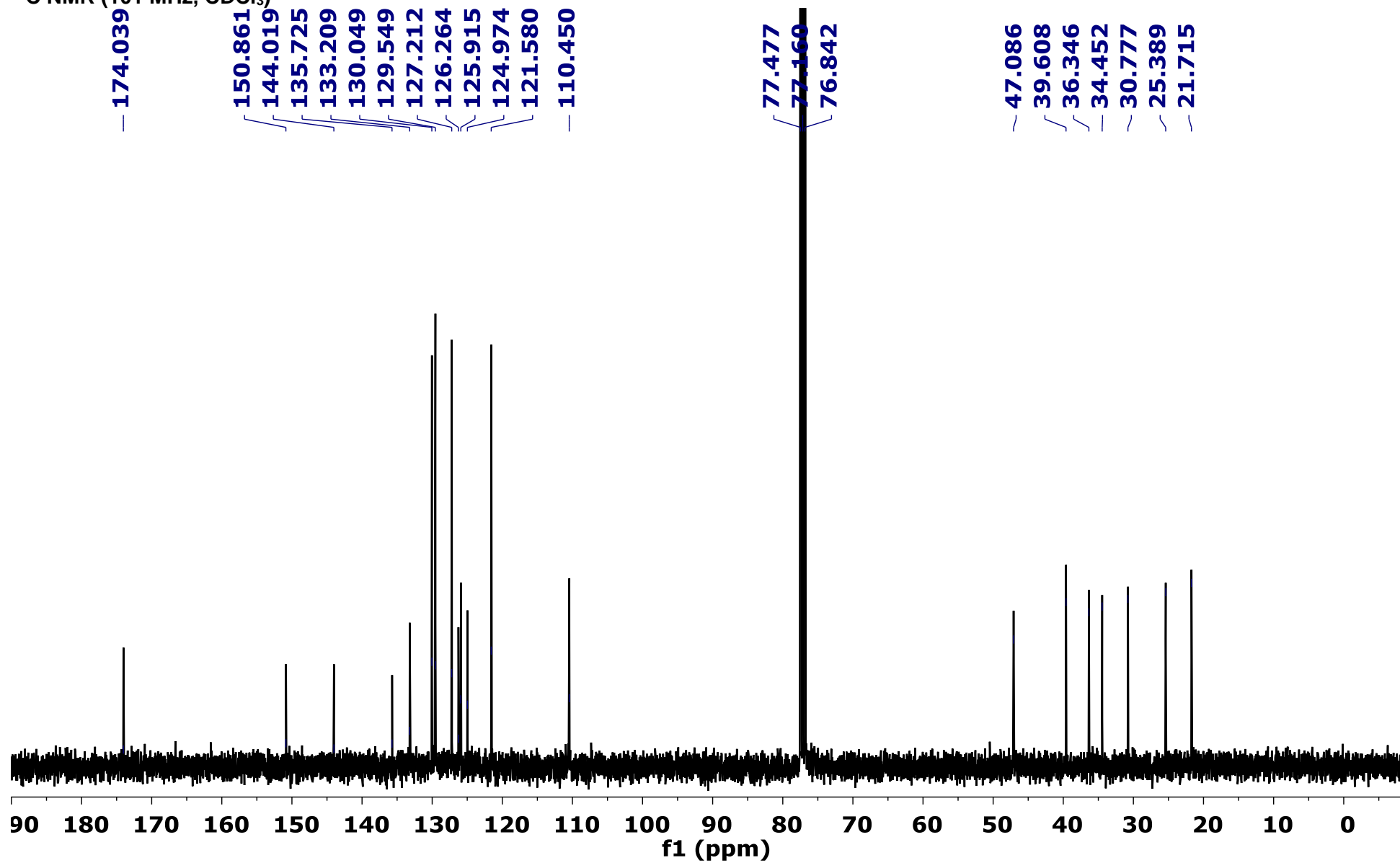


¹H NMR (400 MHz, CDCl₃)

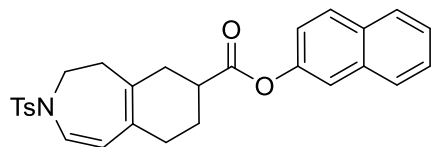




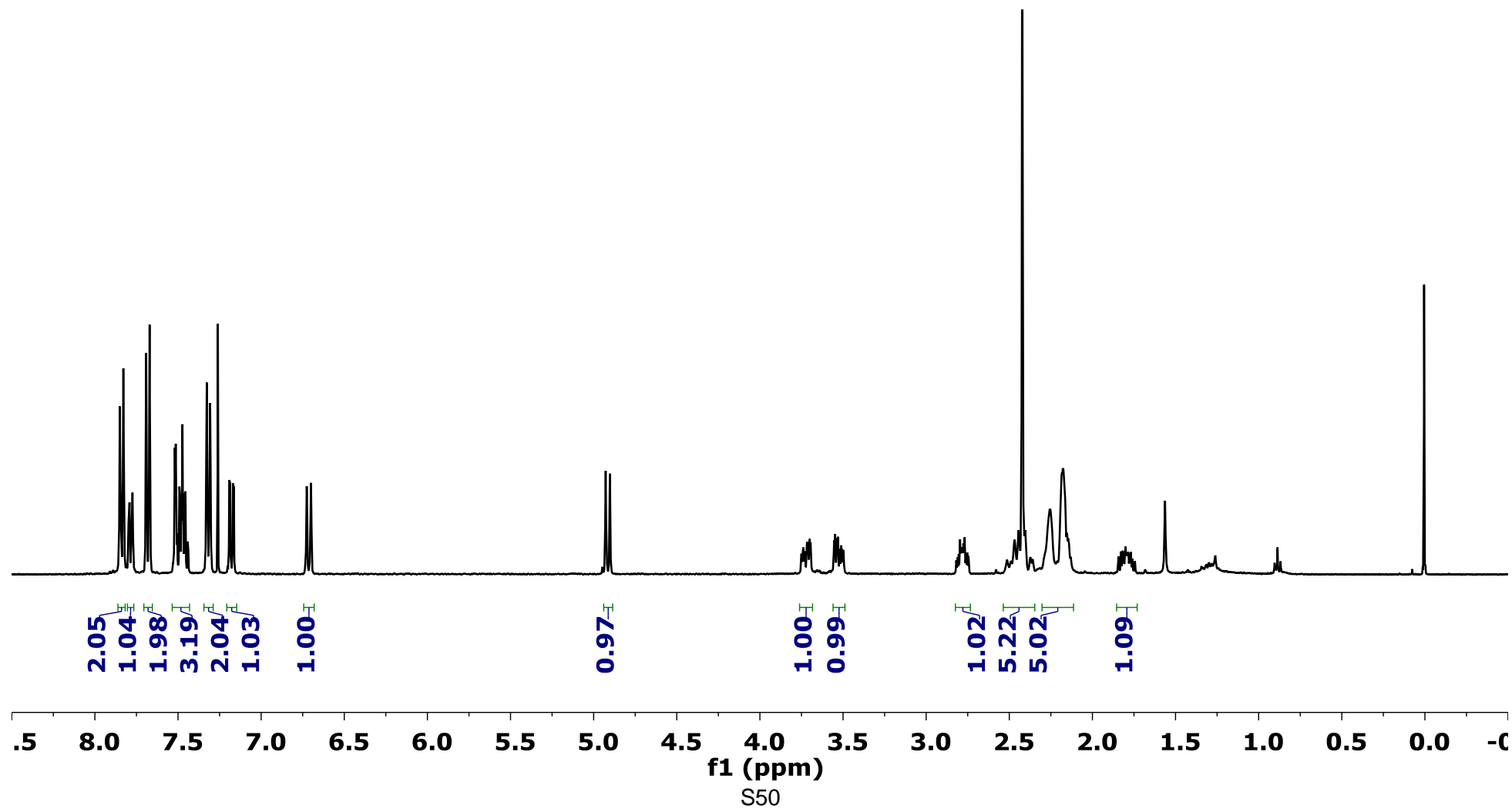
¹³C NMR (101 MHz, CDCl₃)

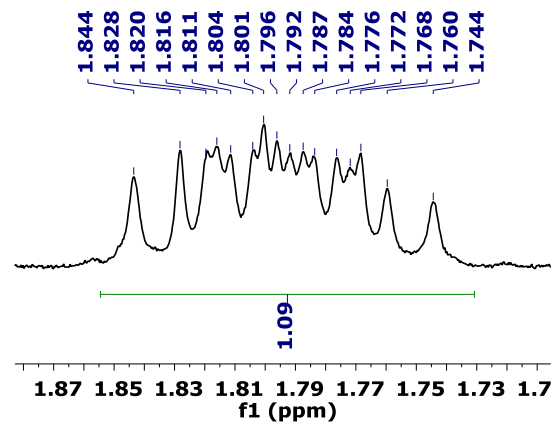
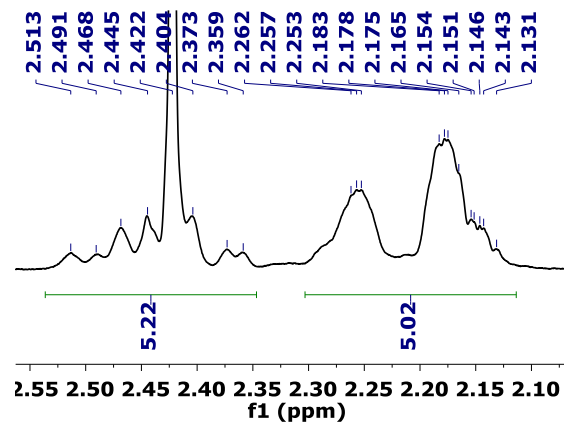
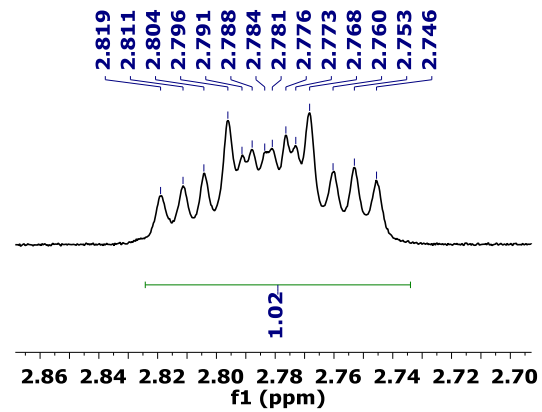
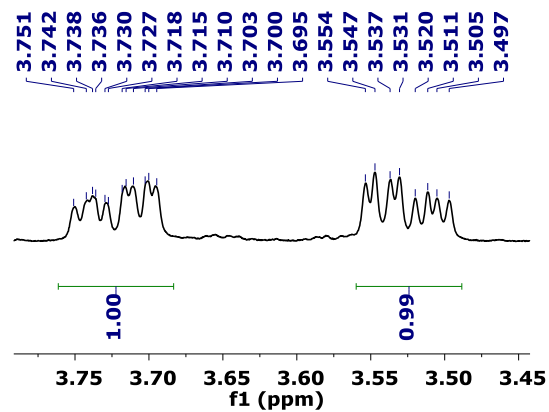
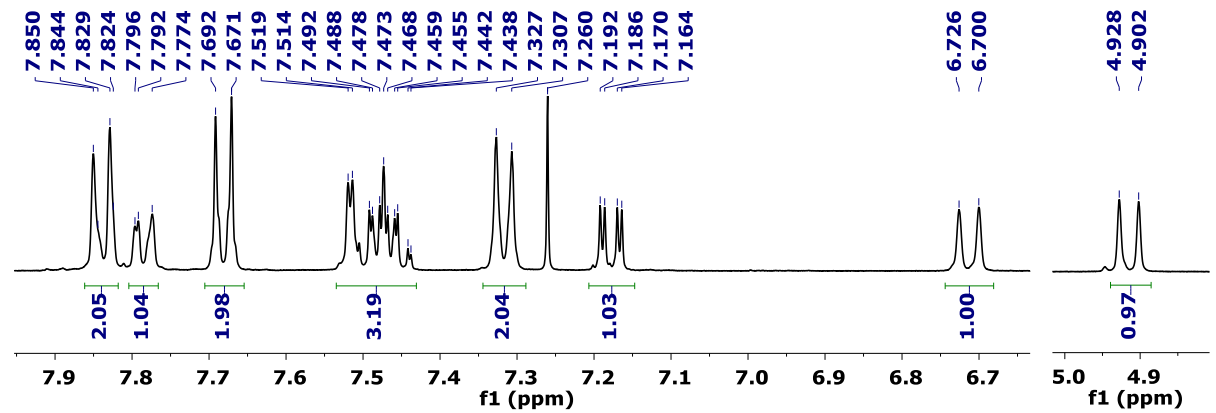


Product 3af

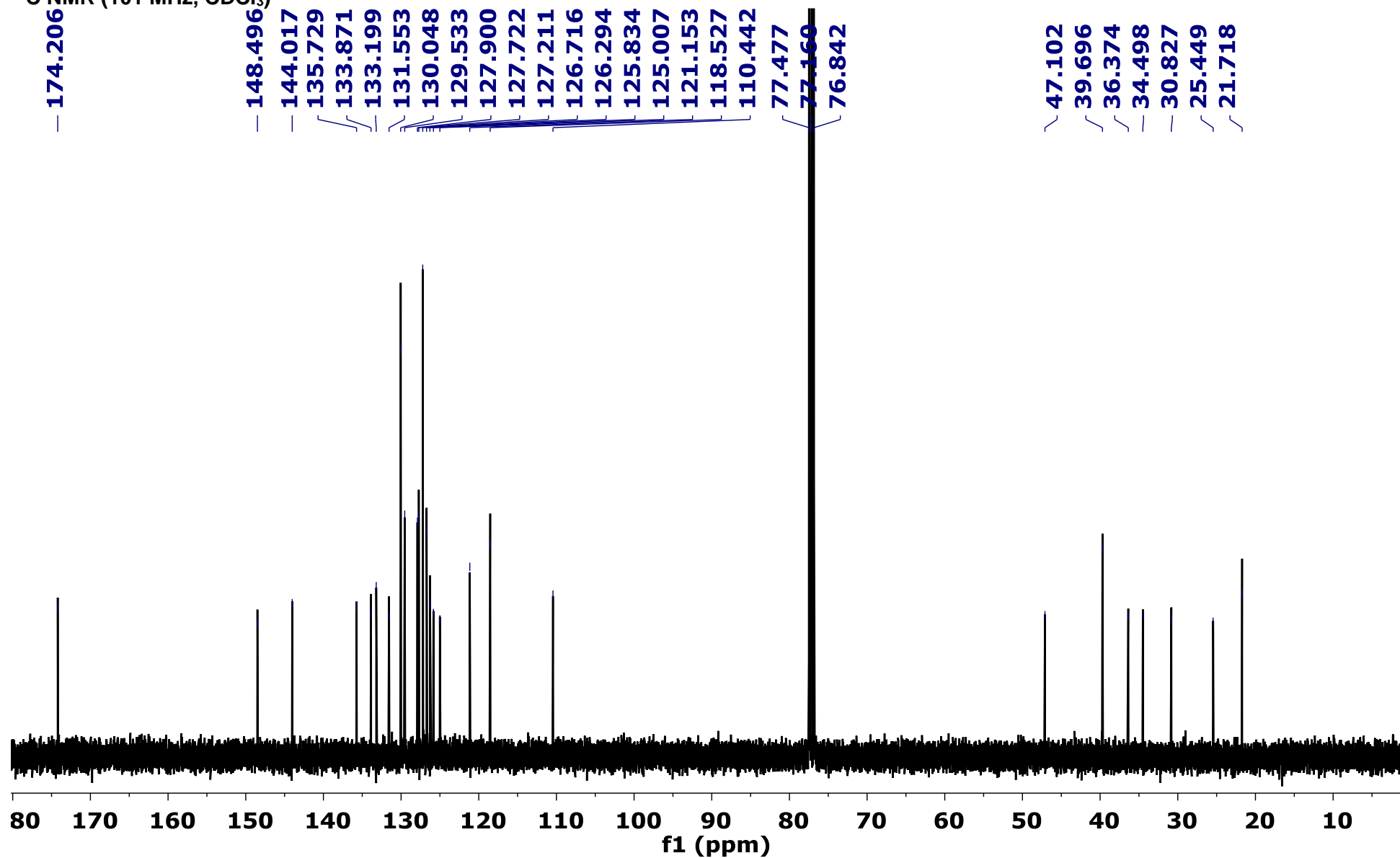


^1H NMR (400 MHz, CDCl_3)

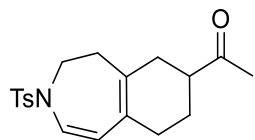




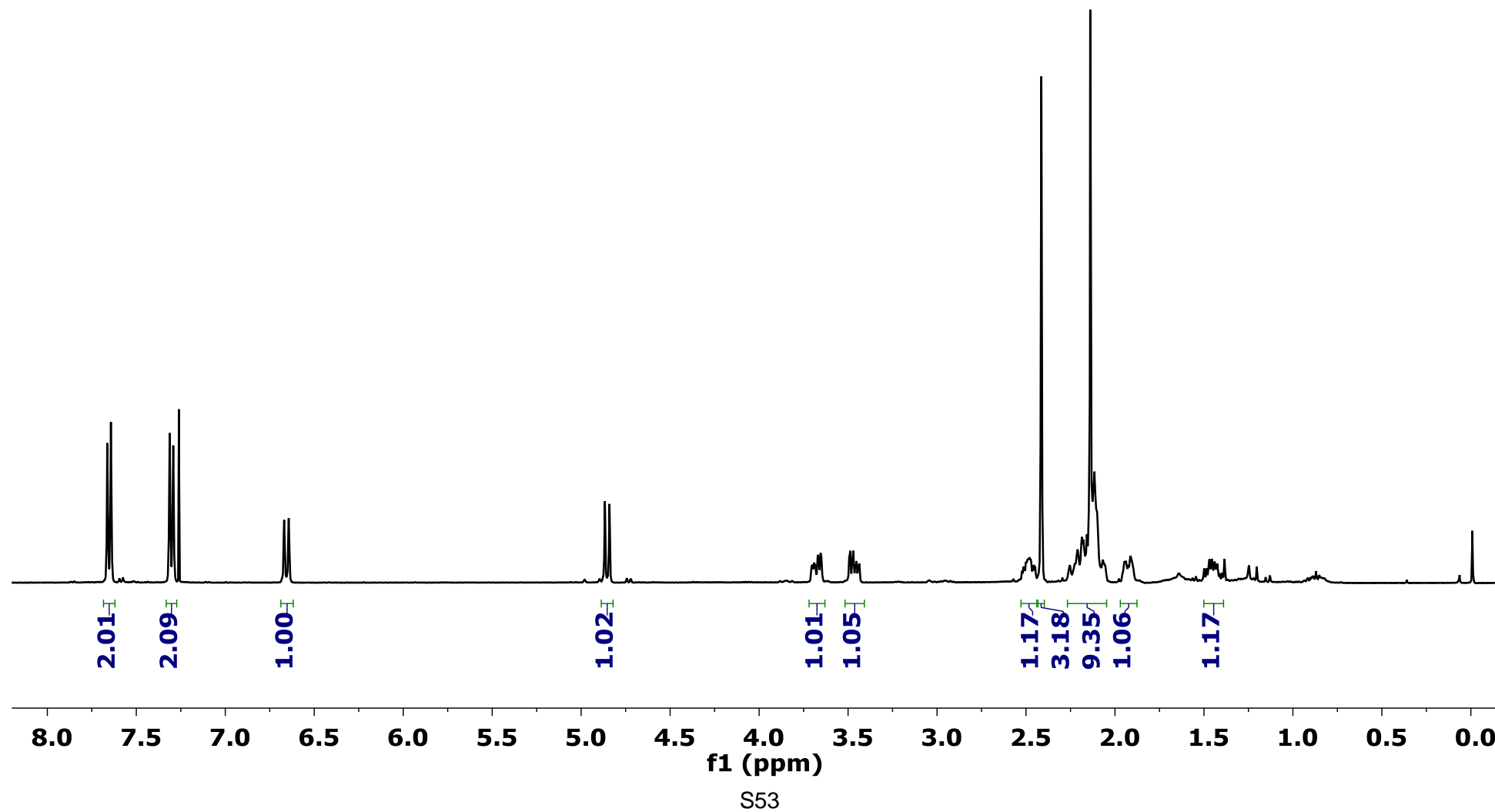
¹³C NMR (101 MHz, CDCl₃)

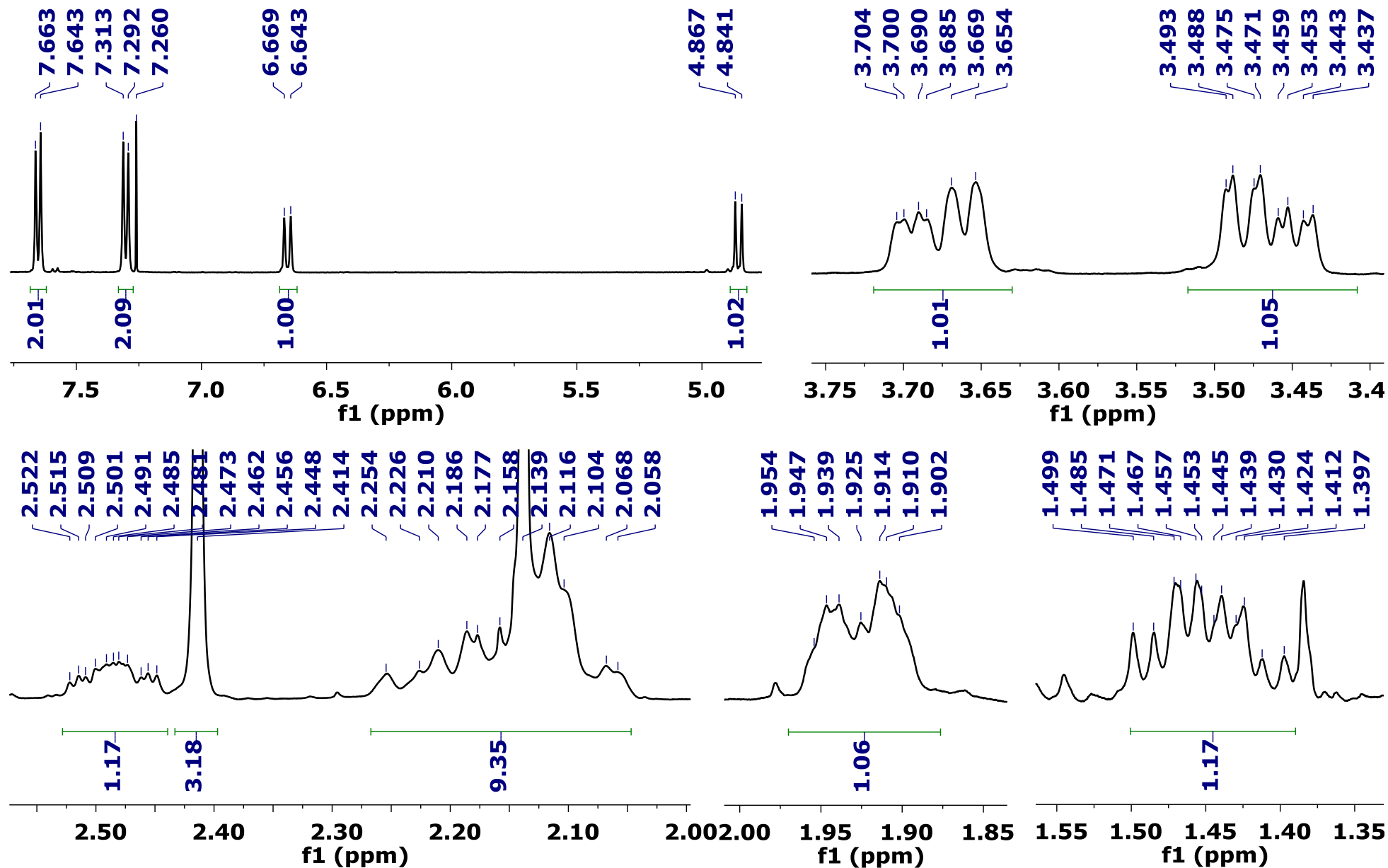


Product 3ag

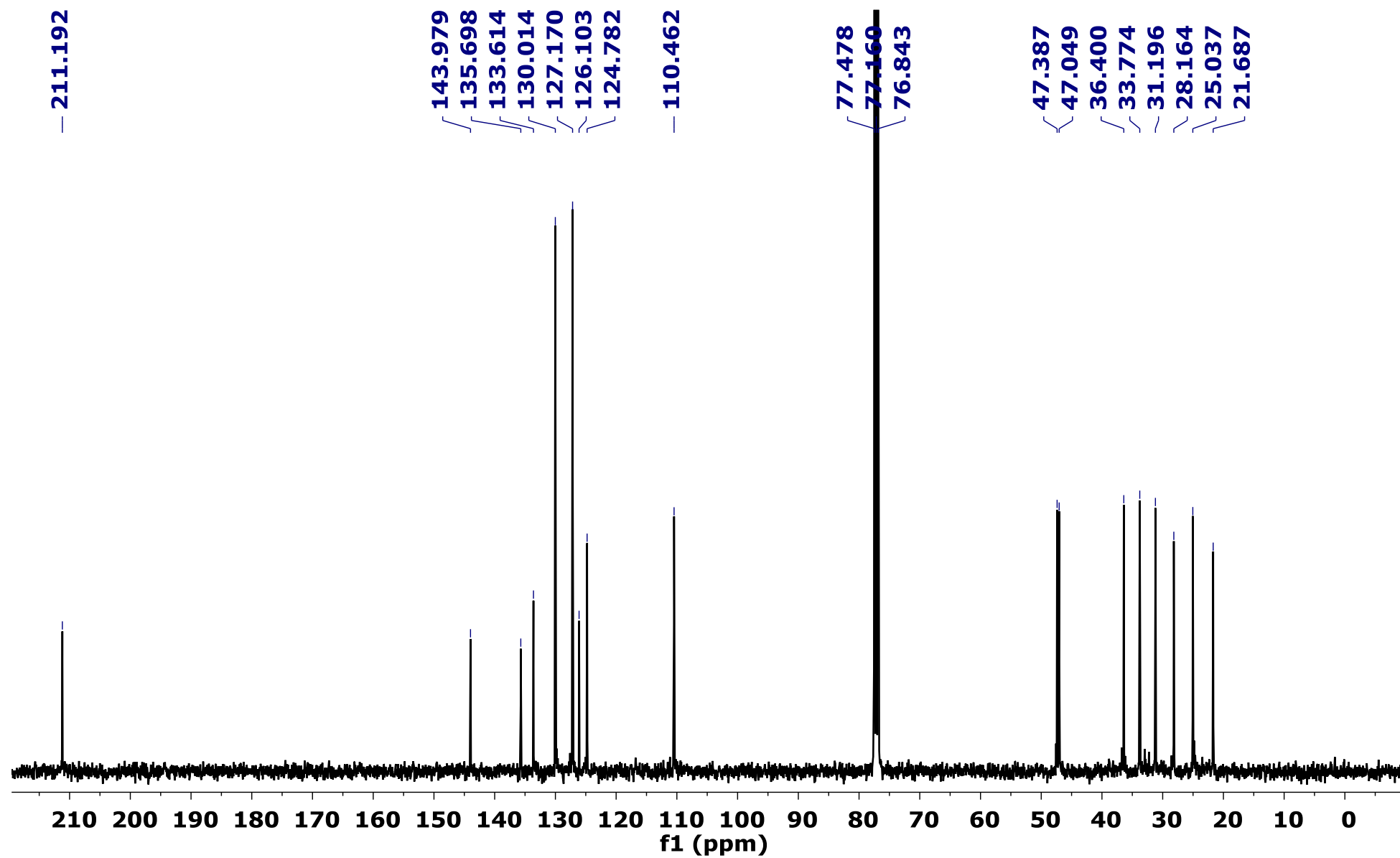


^1H NMR (400 MHz, CDCl_3)



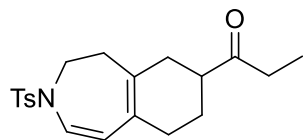


^{13}C NMR (101 MHz, CDCl_3)

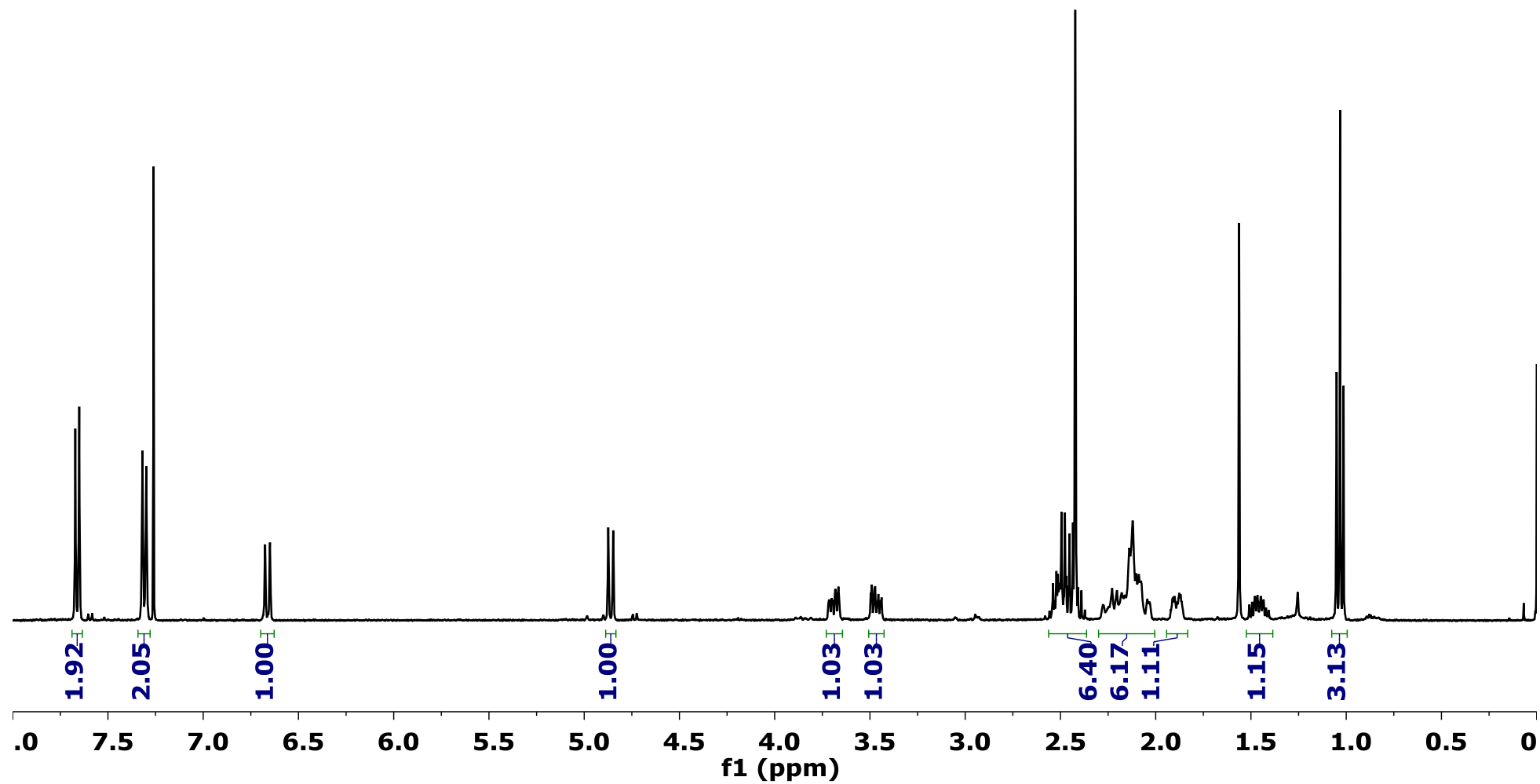


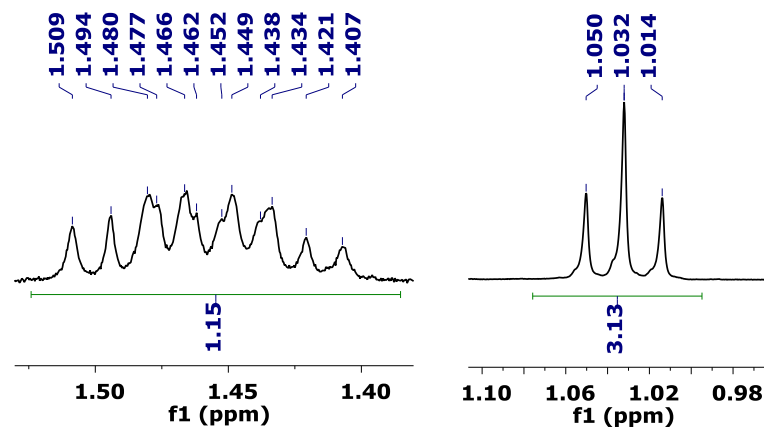
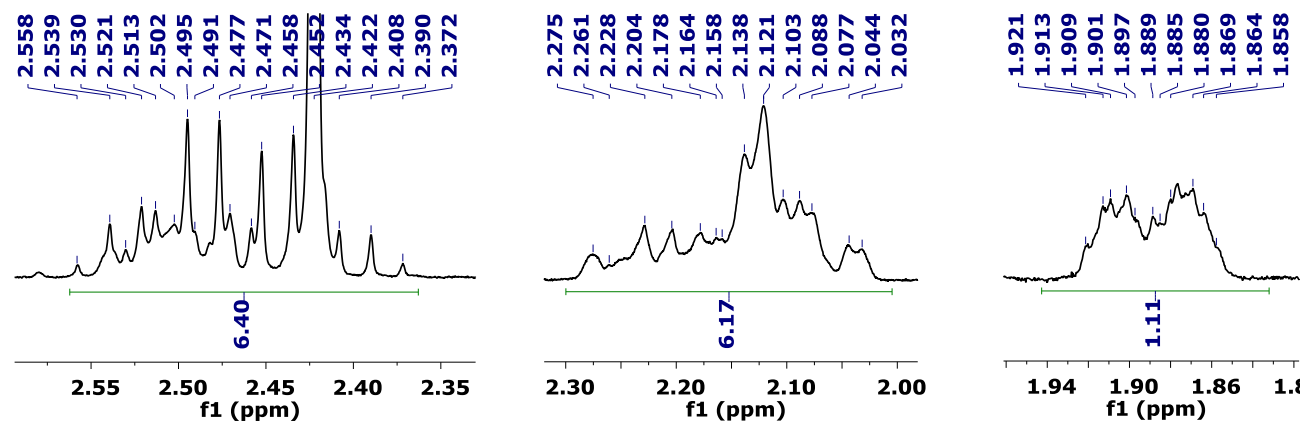
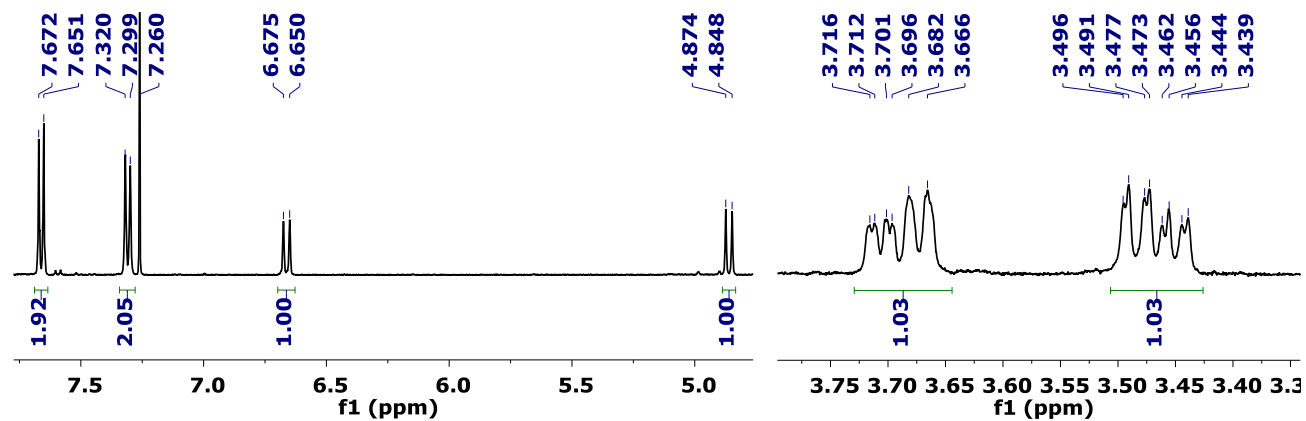
S55

Product 3ah

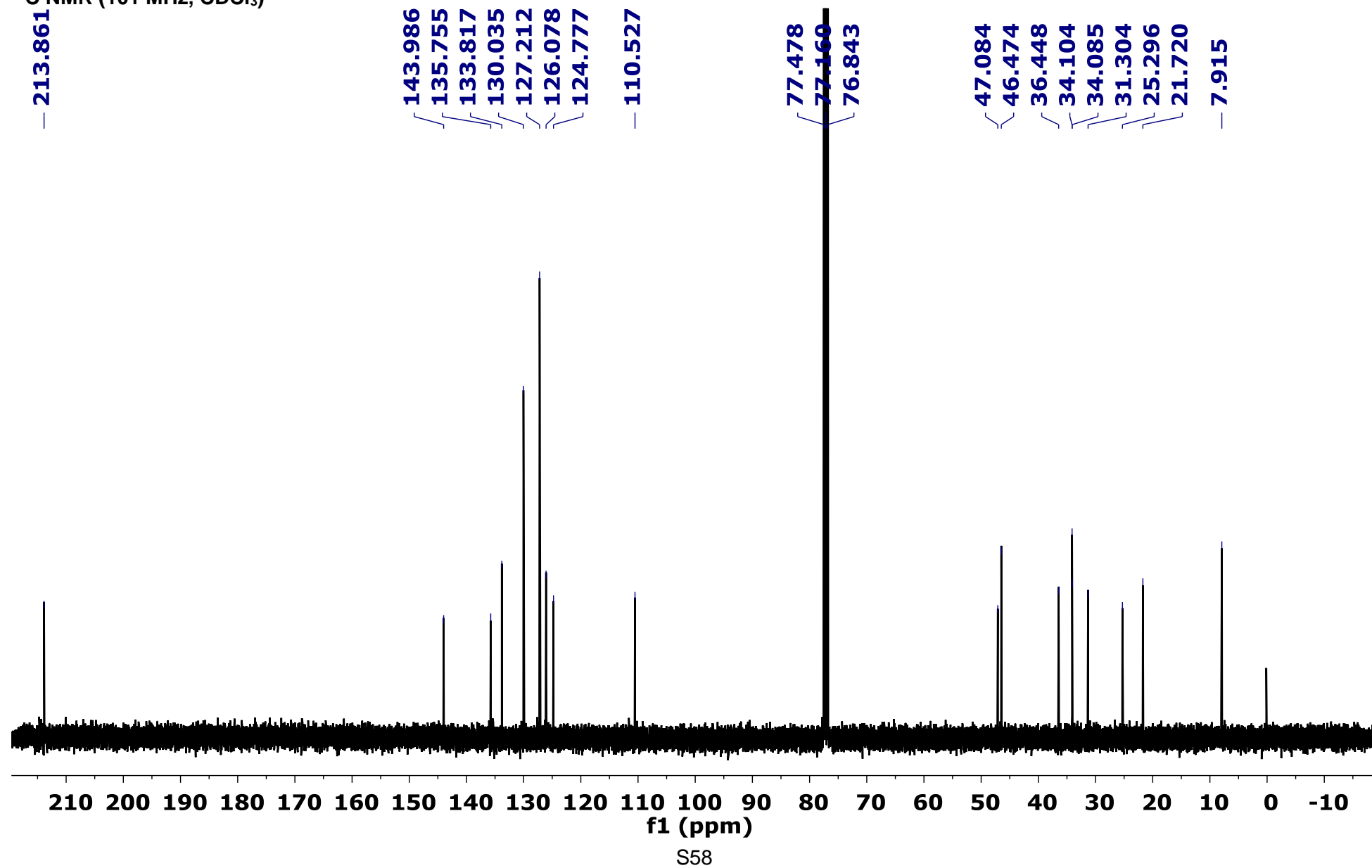


^1H NMR (400 MHz, CDCl_3)

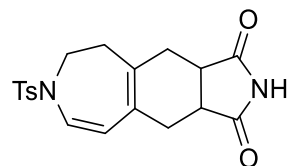




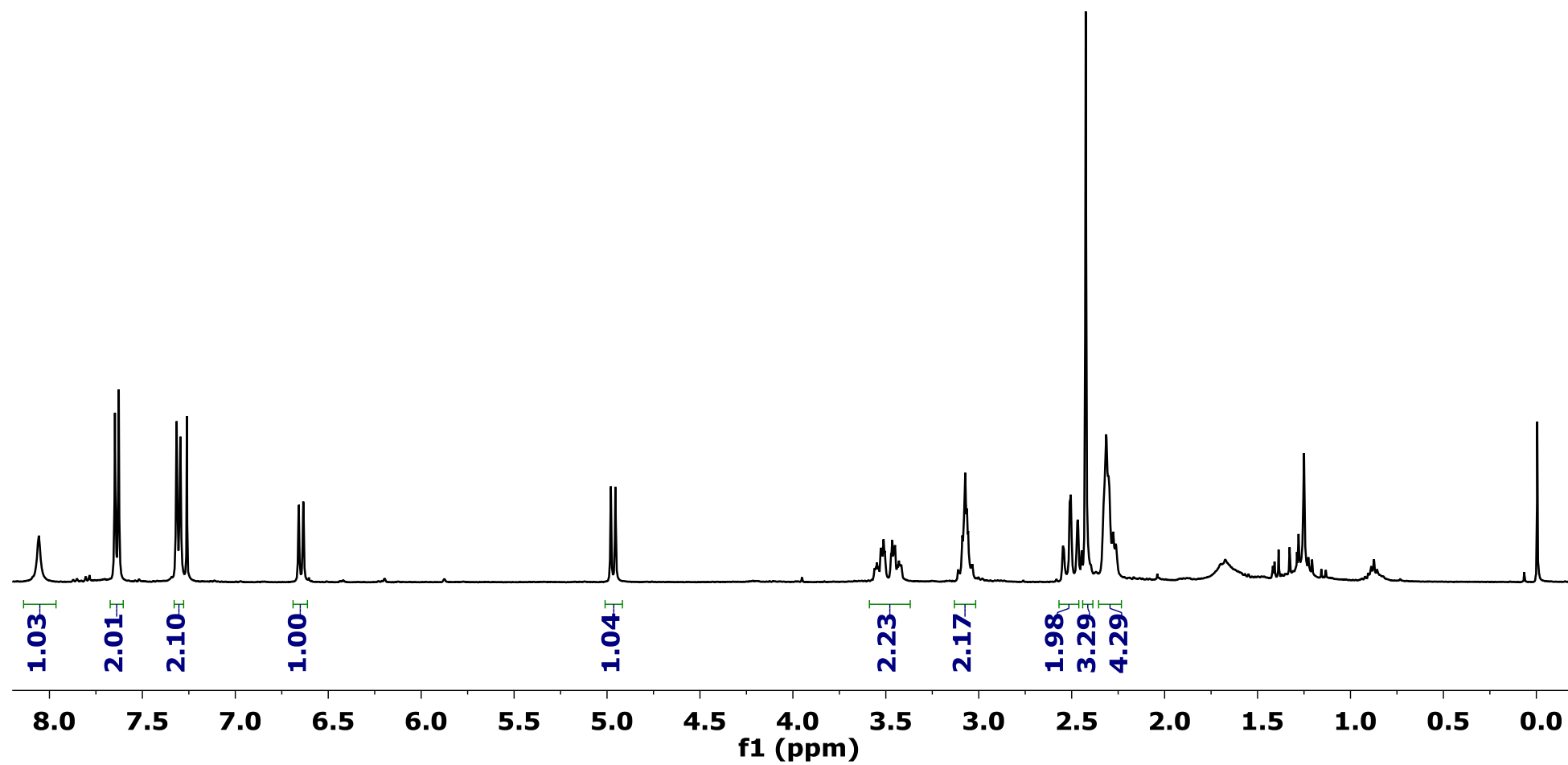
¹³C NMR (101 MHz, CDCl₃)

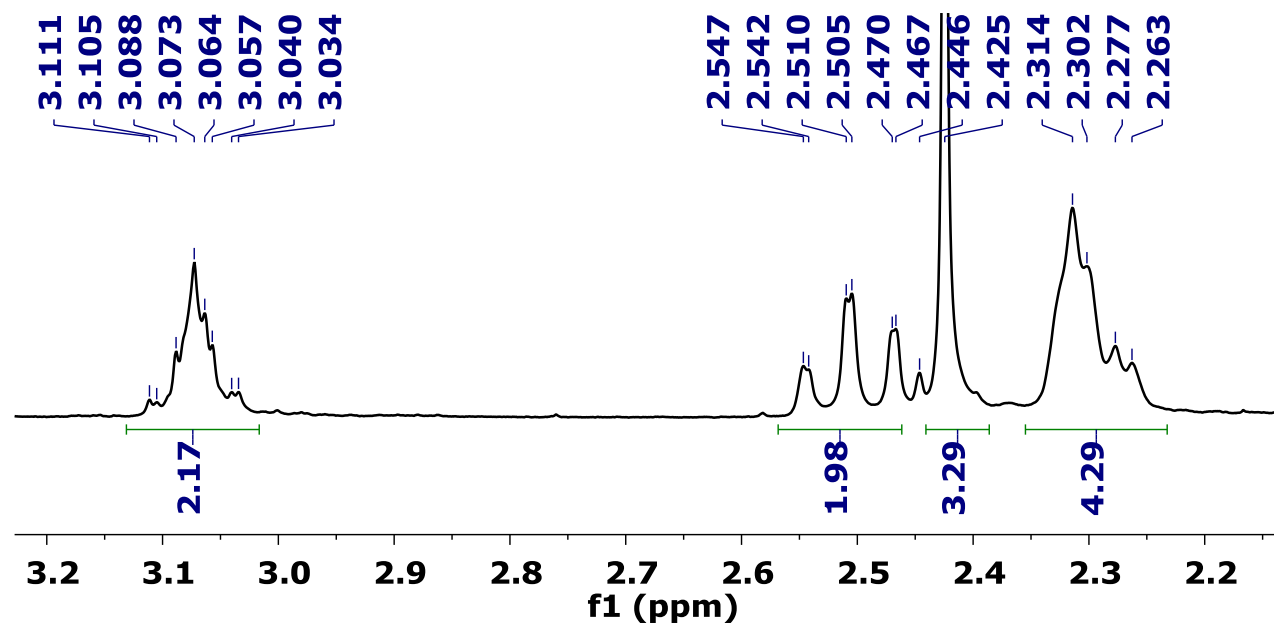
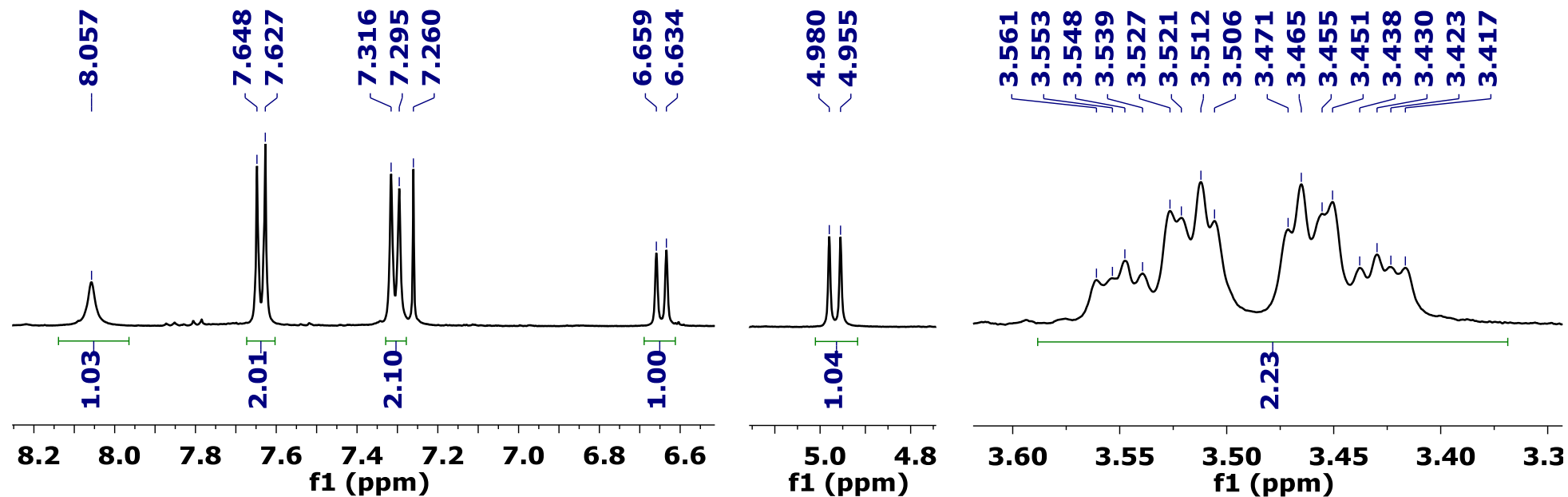


Product 3ai

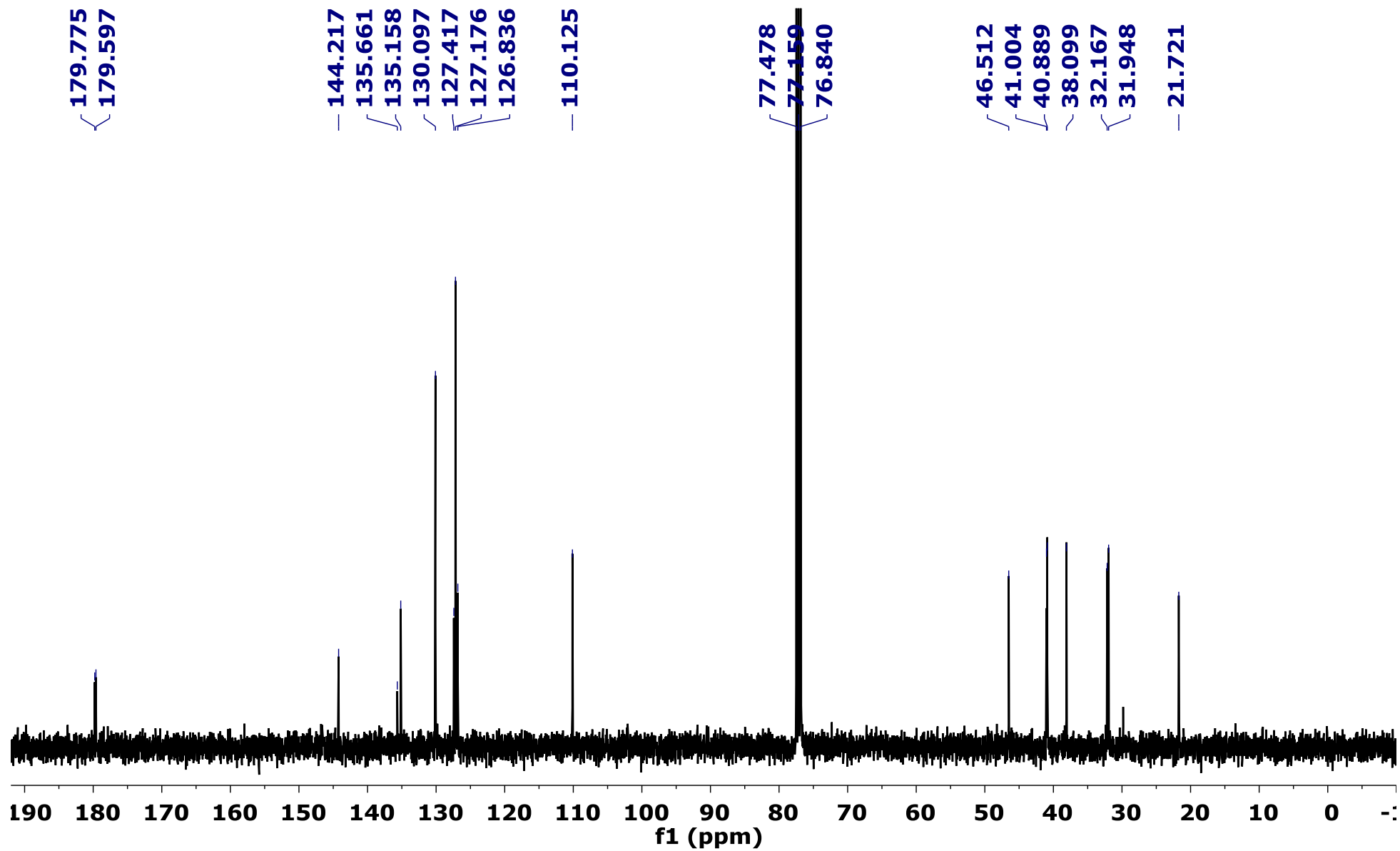


^1H NMR (400 MHz, CDCl_3)

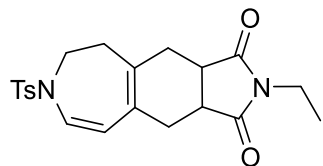




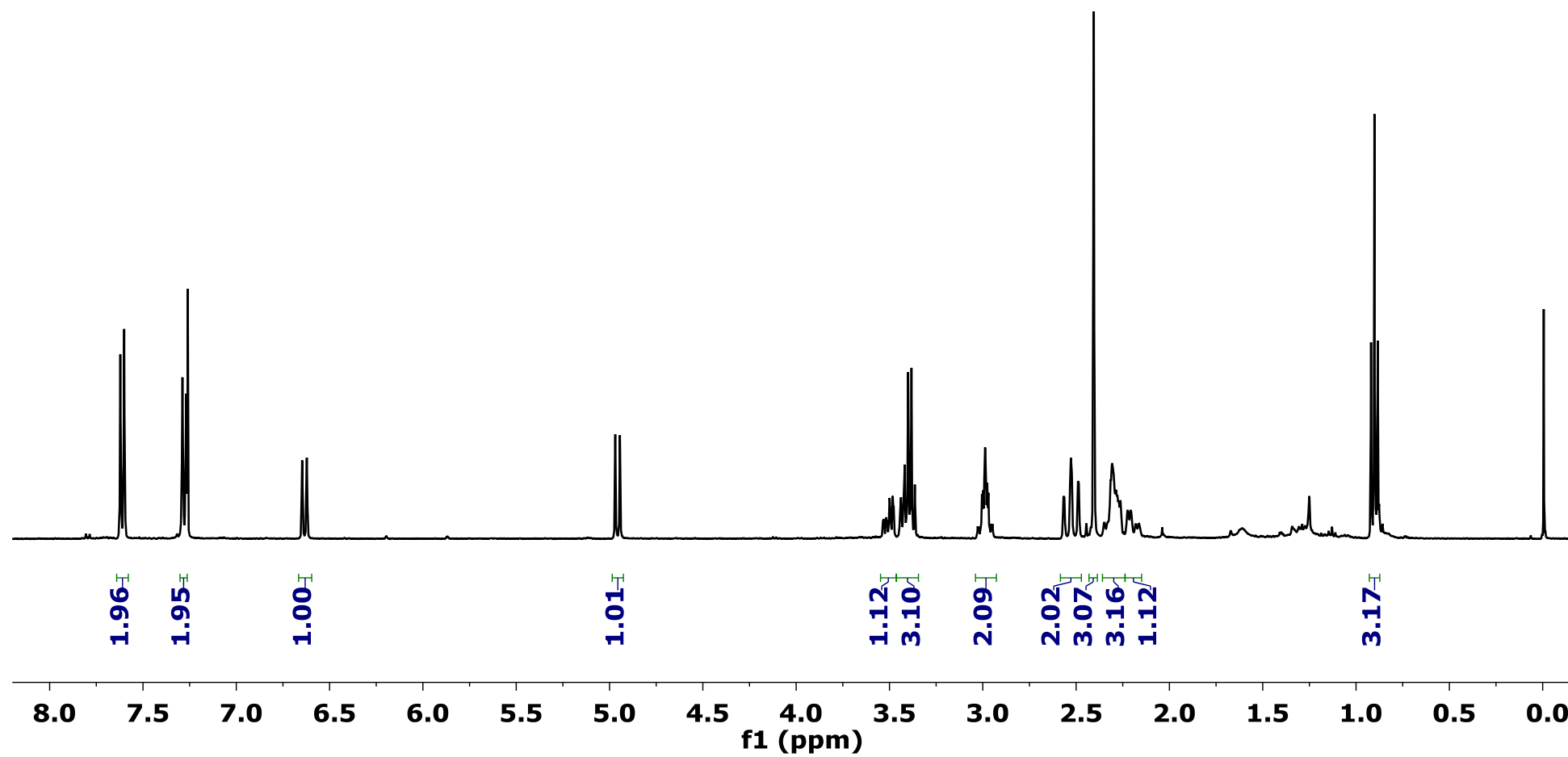
¹³C NMR (101 MHz, CDCl₃)

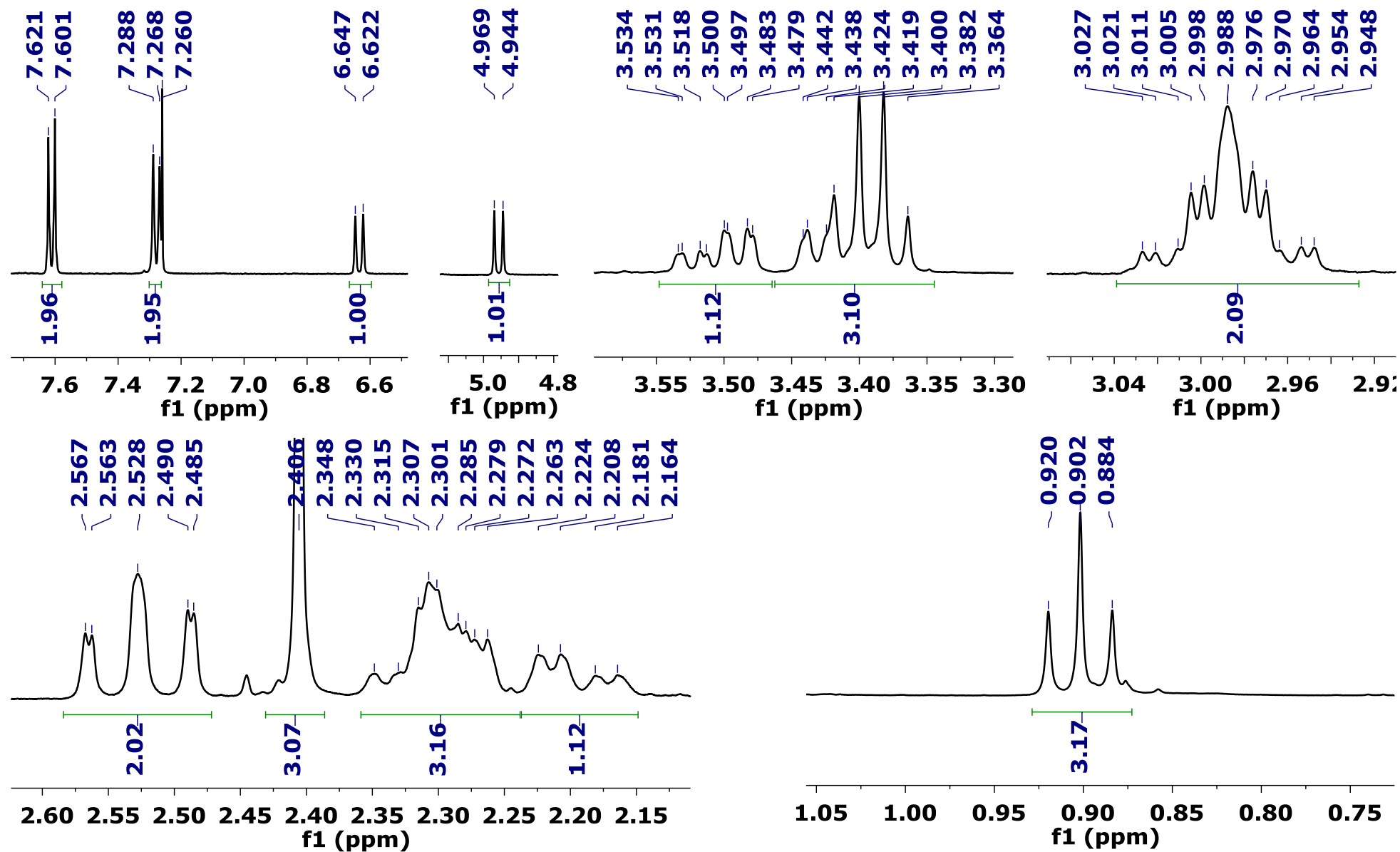


Product 3aj

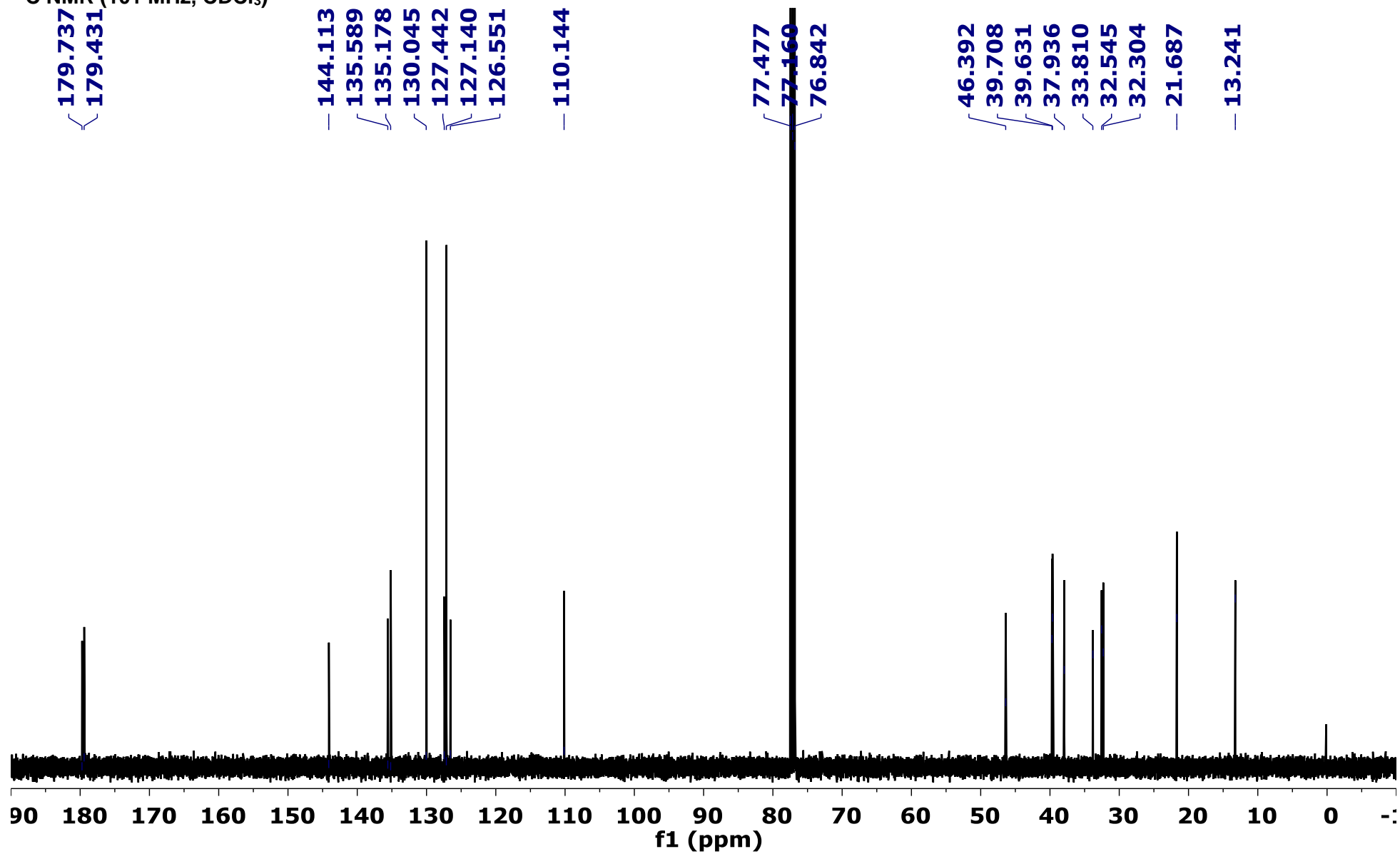


^1H NMR (400 MHz, CDCl_3)

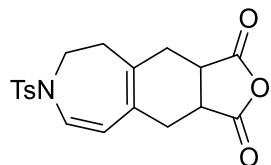




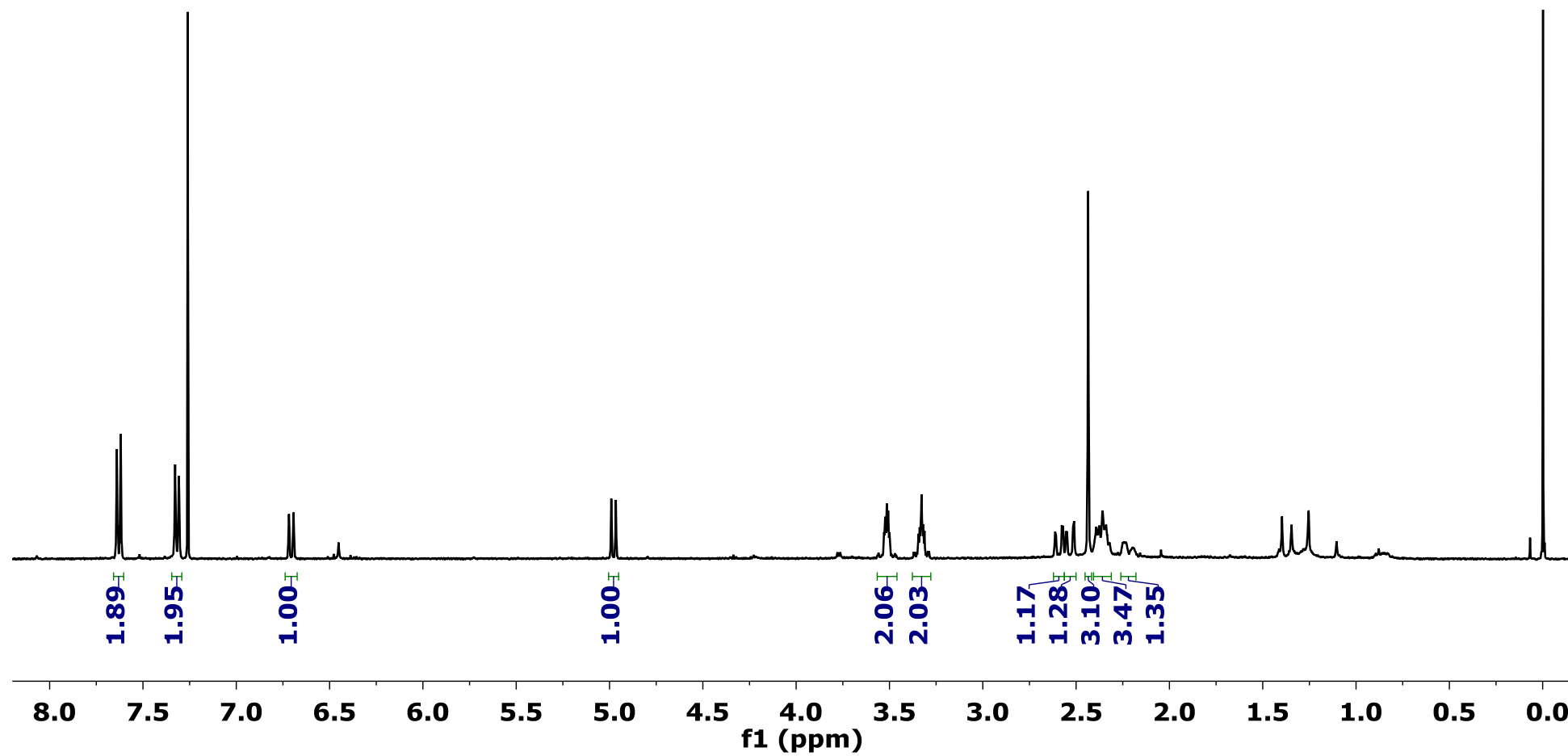
¹³C NMR (101 MHz, CDCl₃)

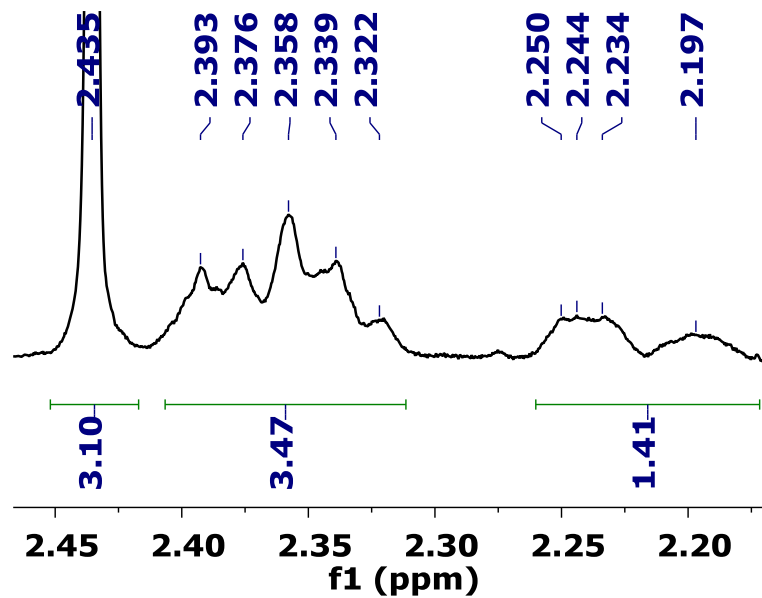
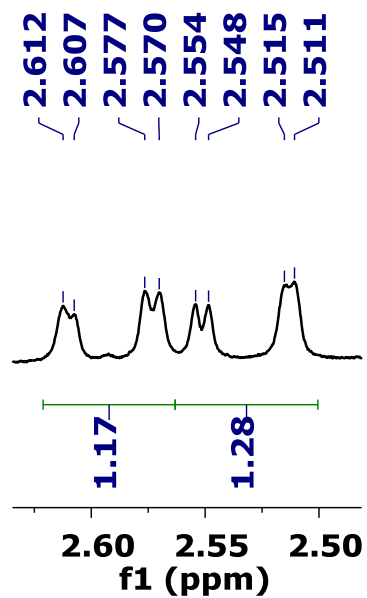
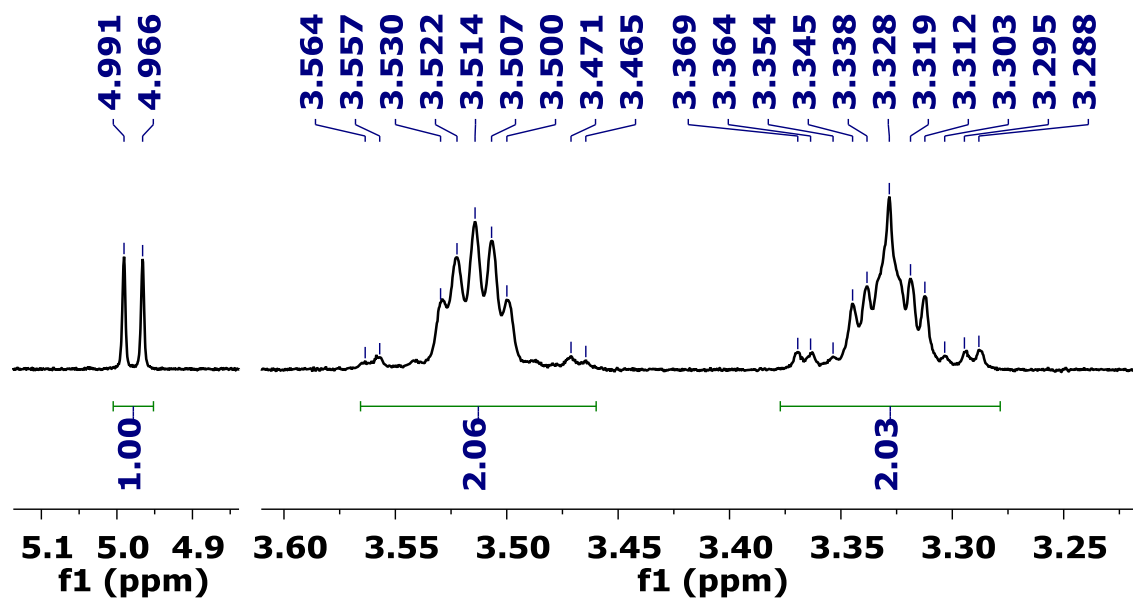
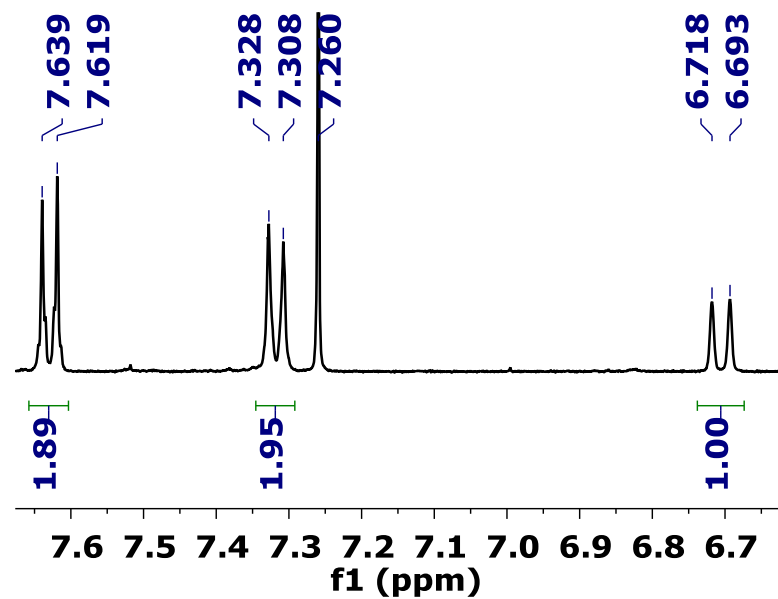


Product 3ak

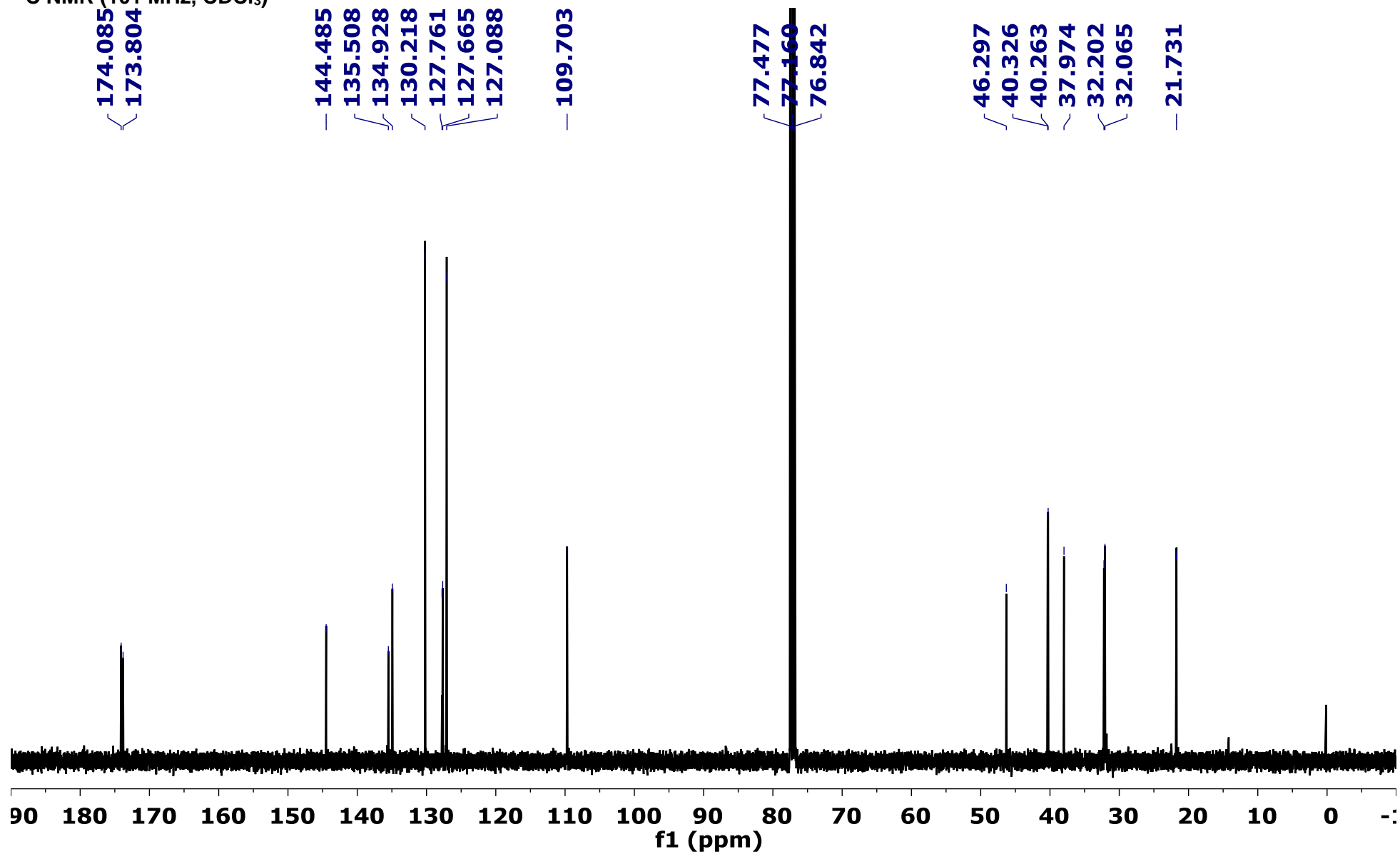


^1H NMR (400 MHz, CDCl_3)

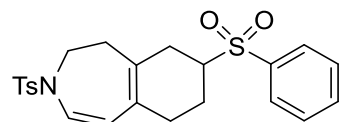




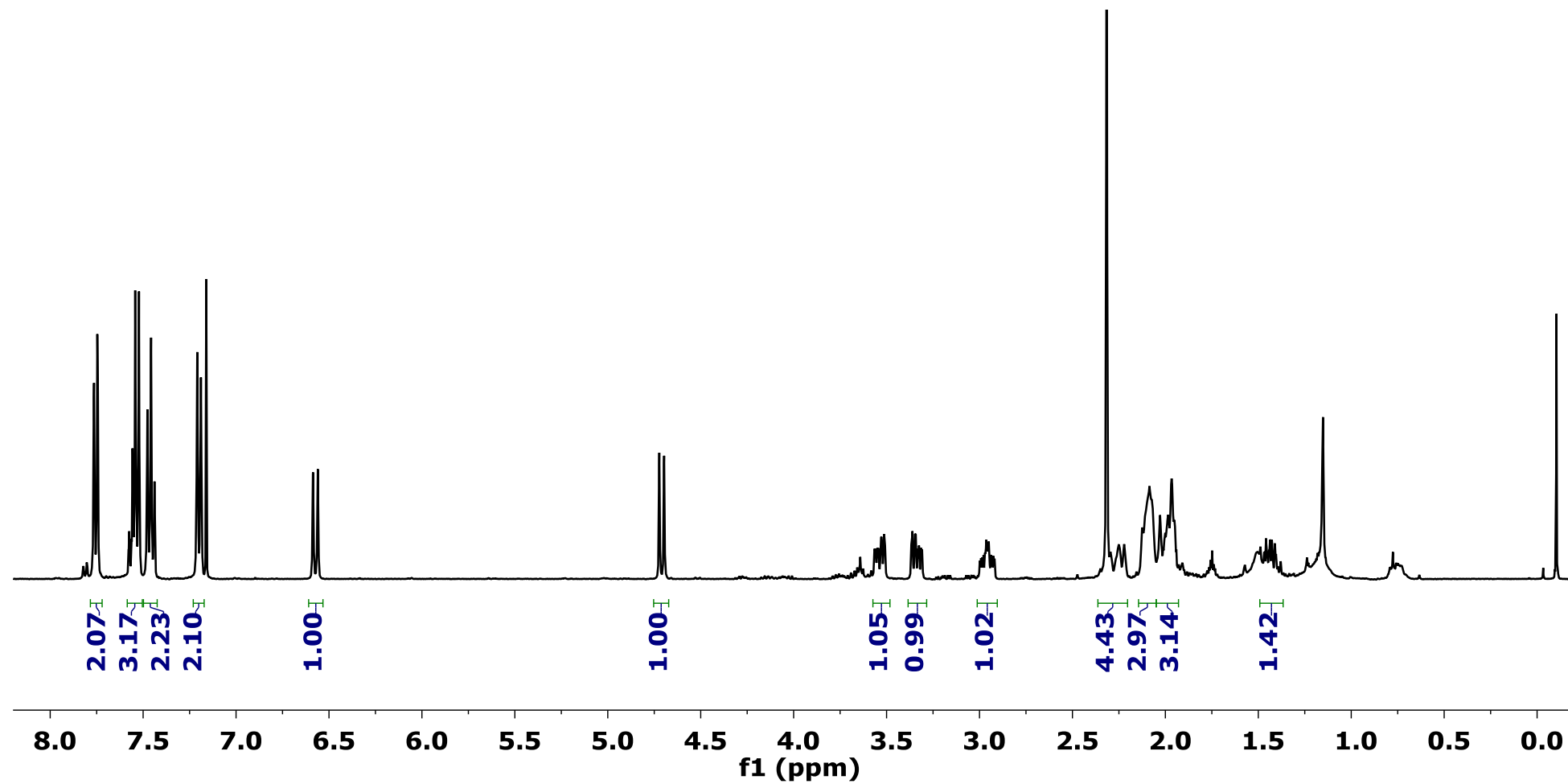
¹³C NMR (101 MHz, CDCl₃)

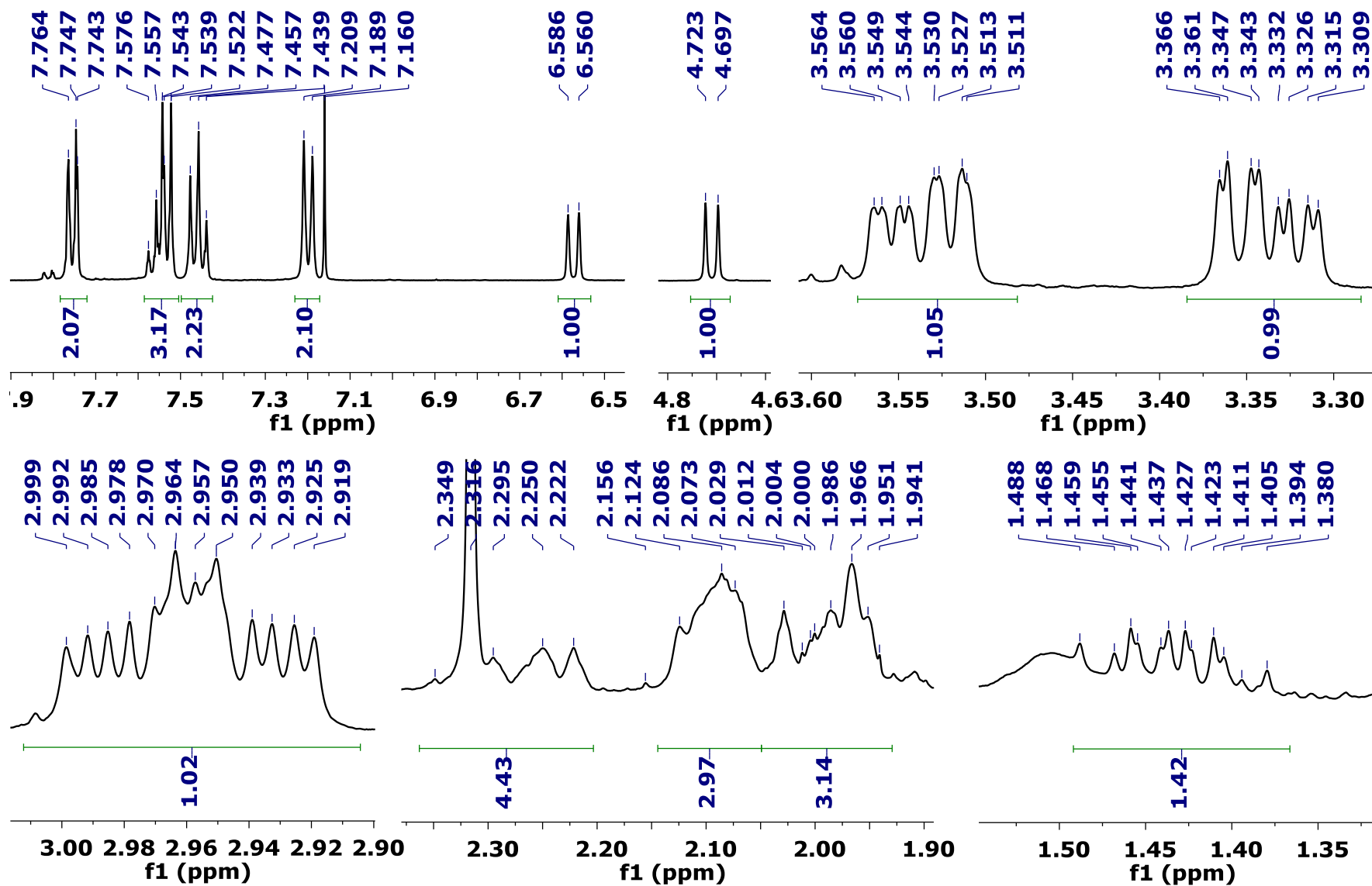


Product 3al

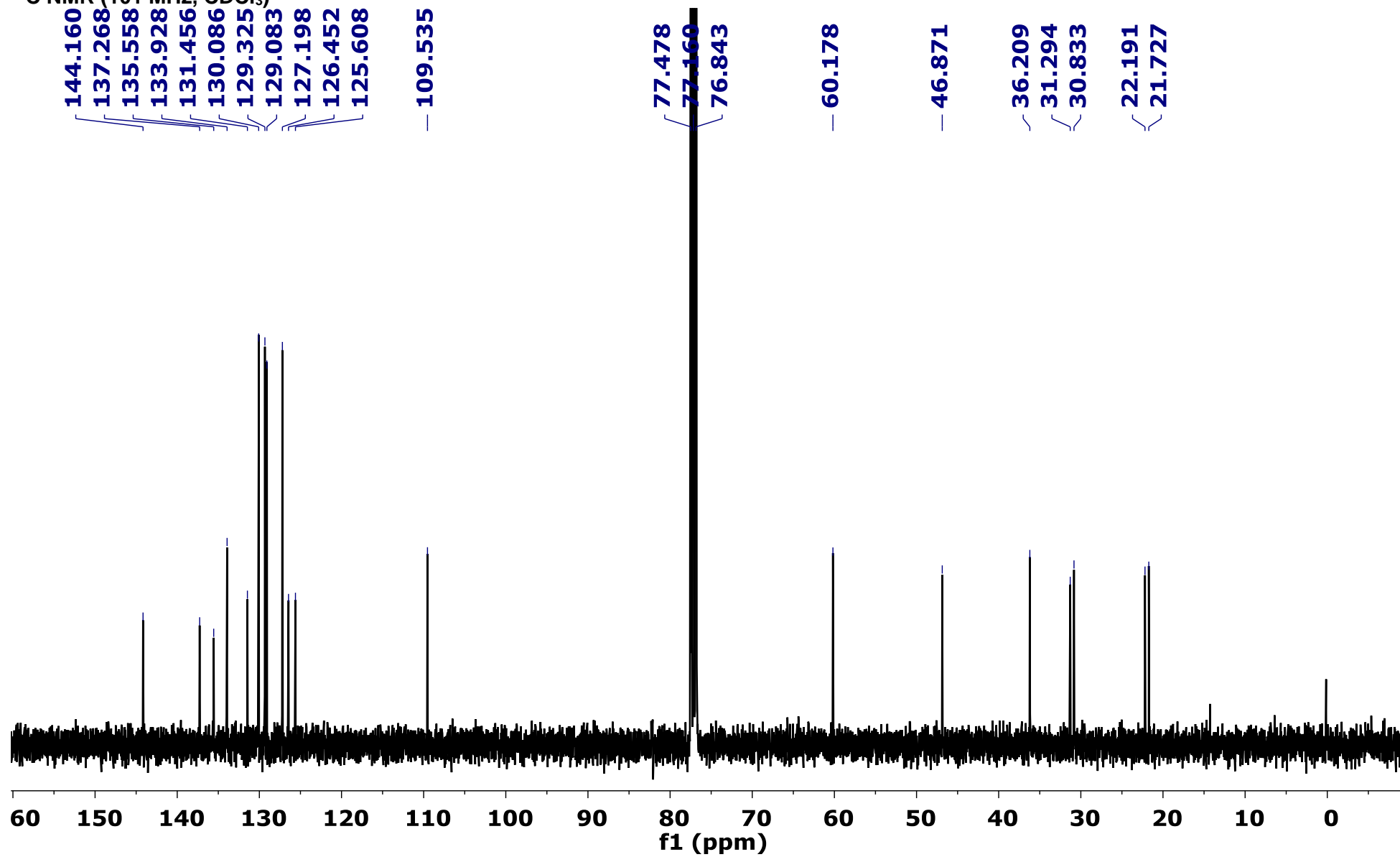


^1H NMR (400 MHz, CDCl_3)

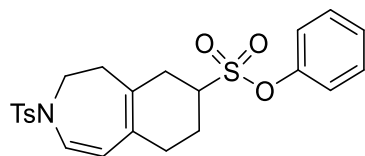




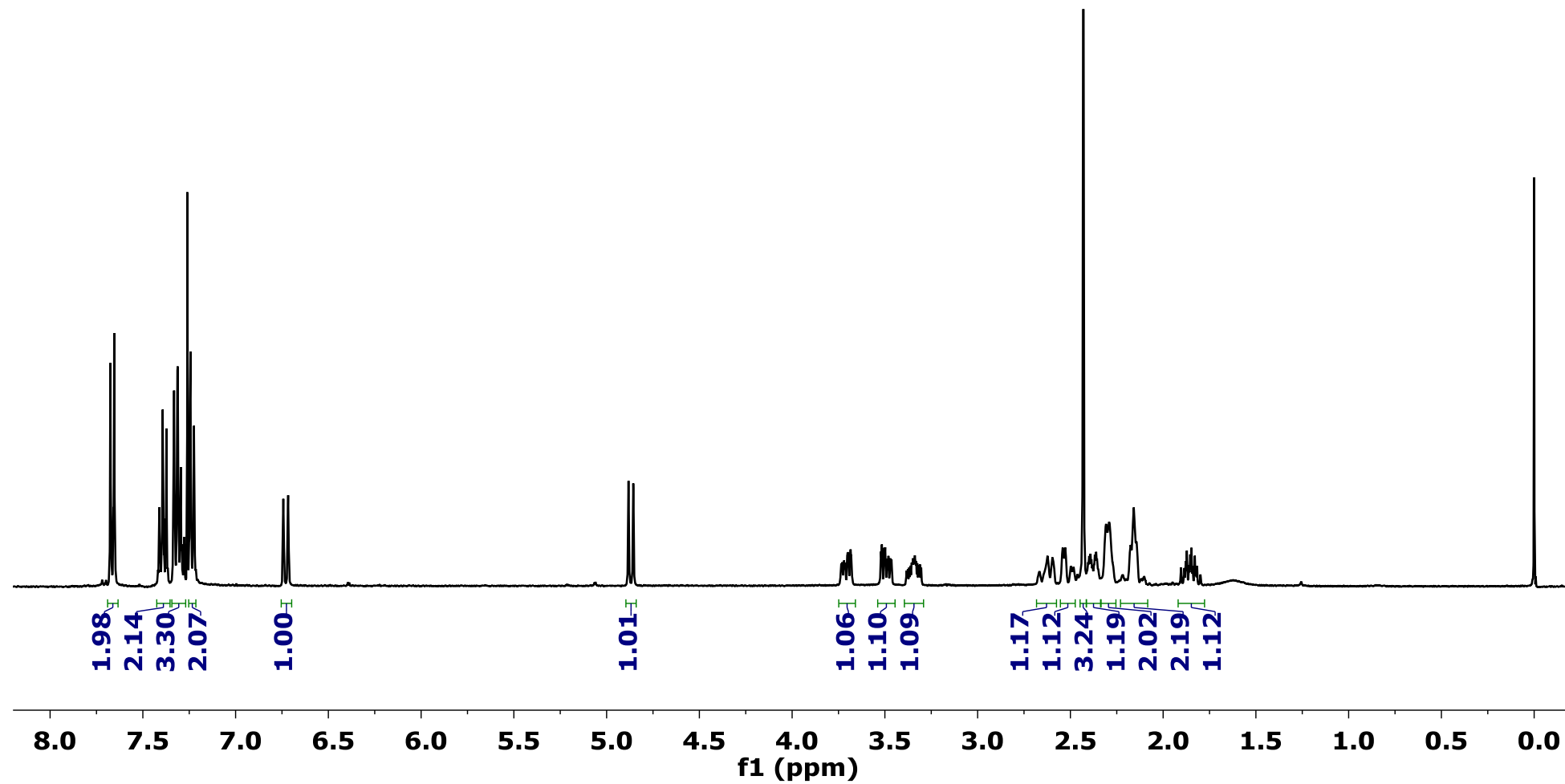
¹³C NMR (101 MHz, CDCl₃)

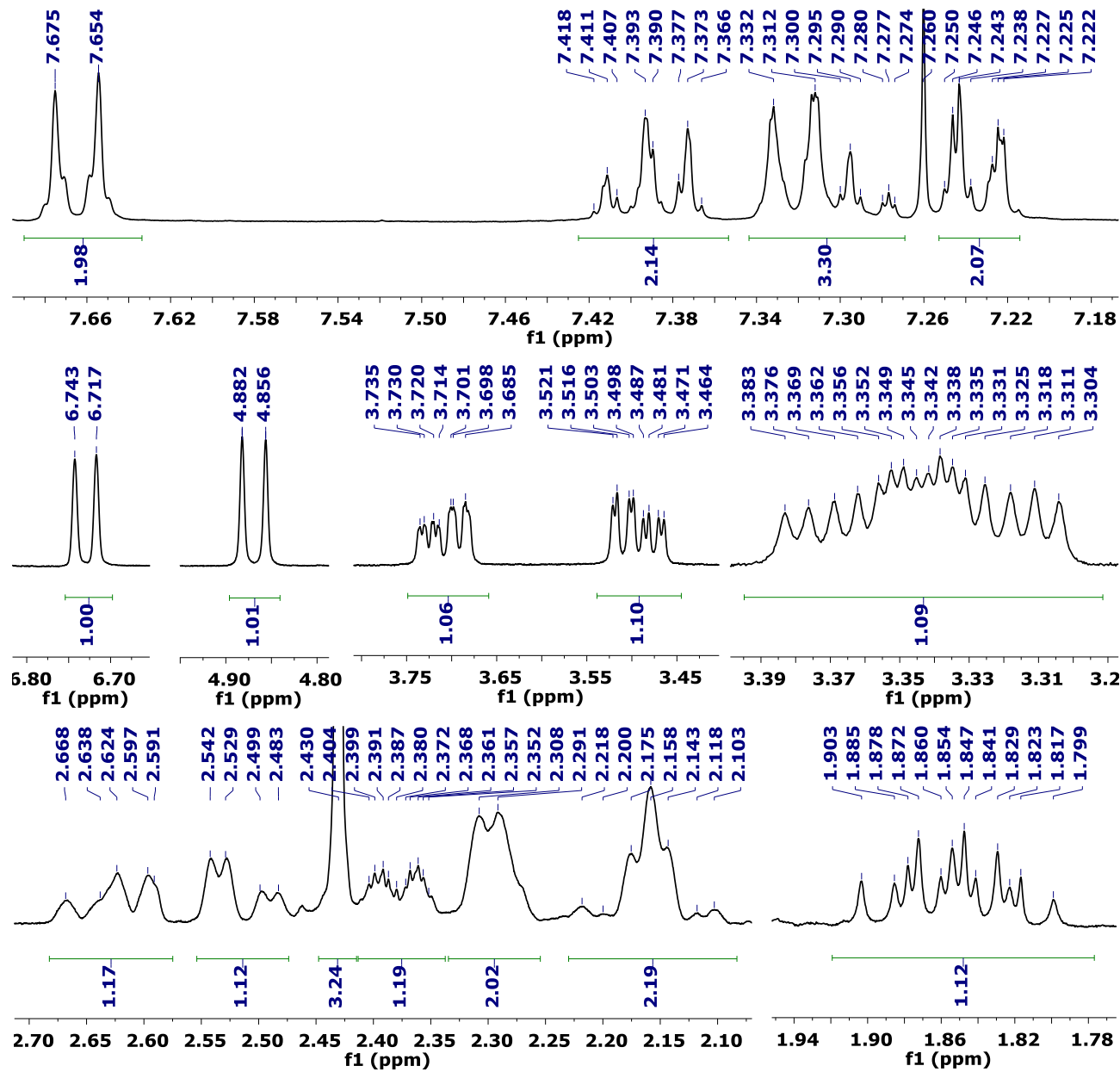


Product 3am

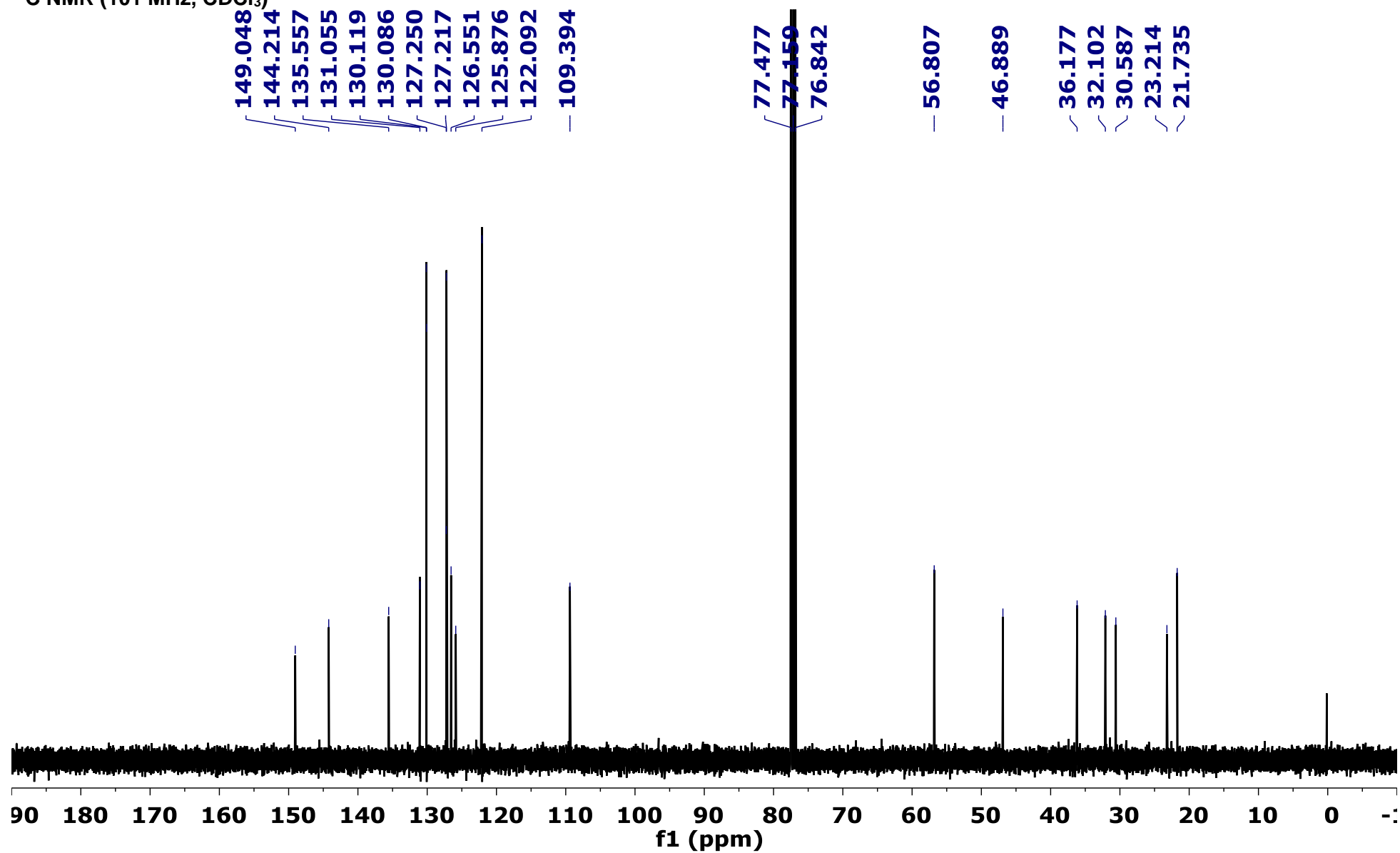


^1H NMR (400 MHz, CDCl_3)

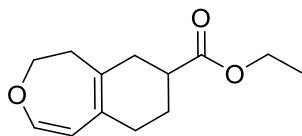




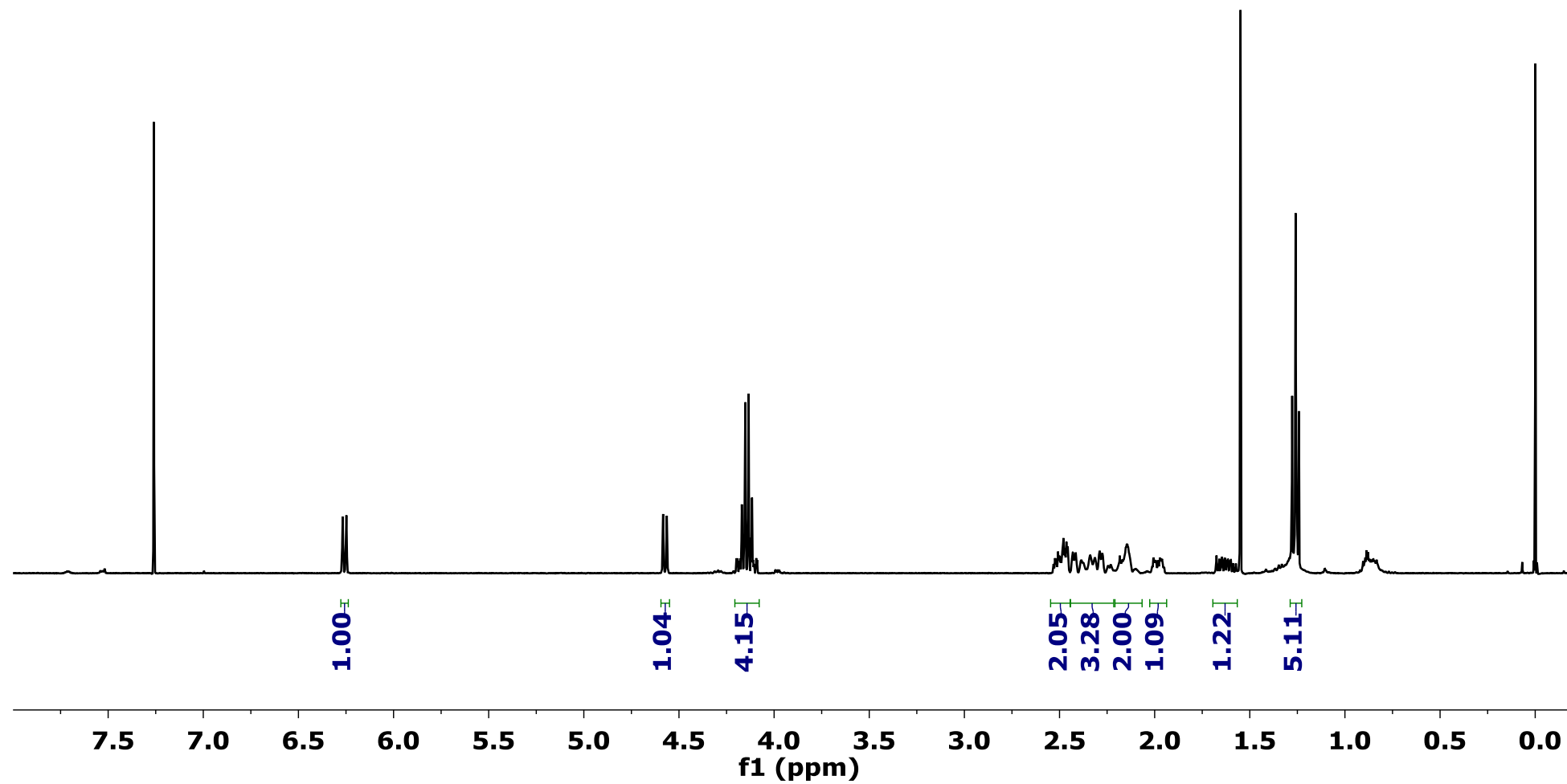
¹³C NMR (101 MHz, CDCl₃)

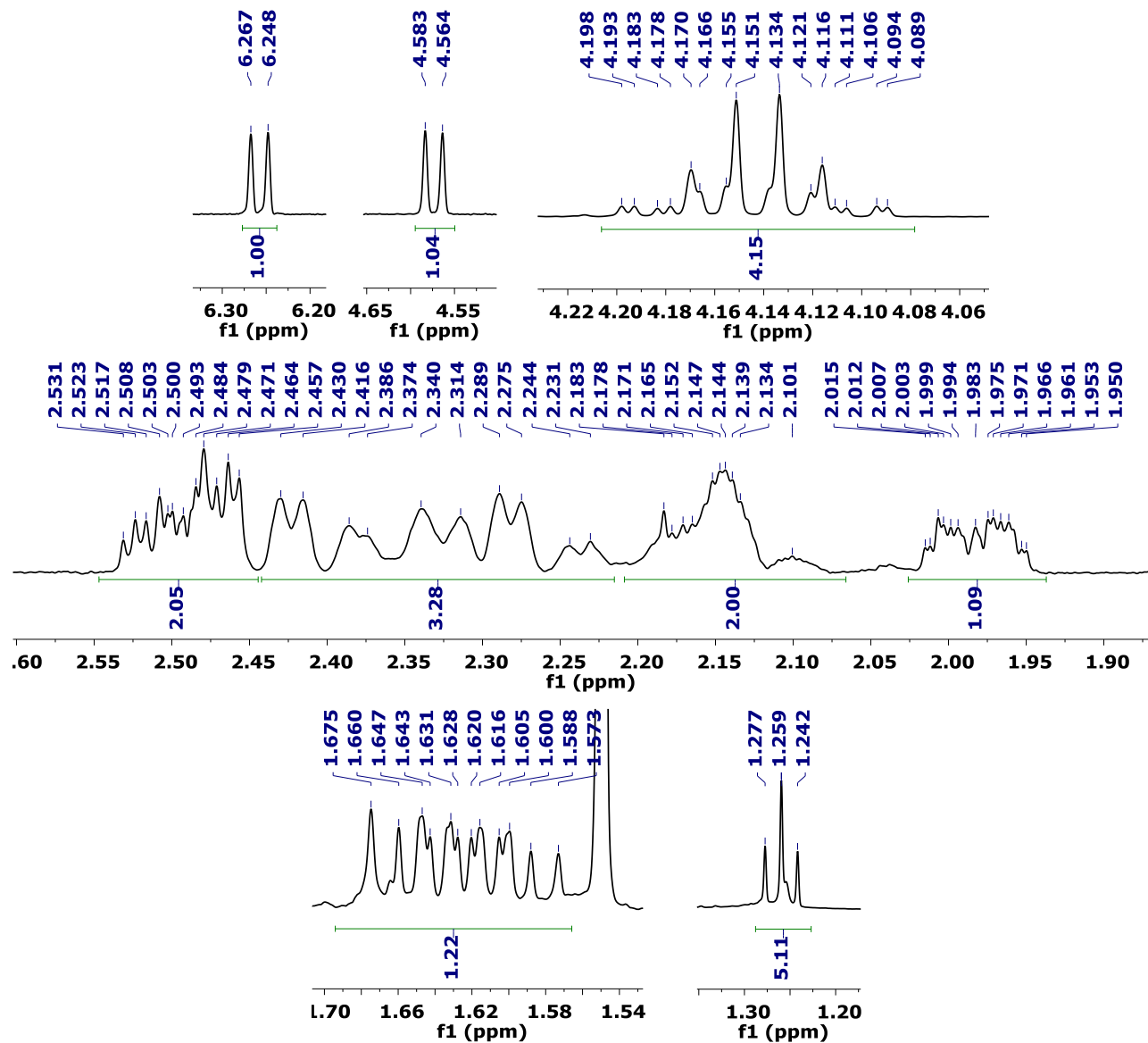


Product 3ba

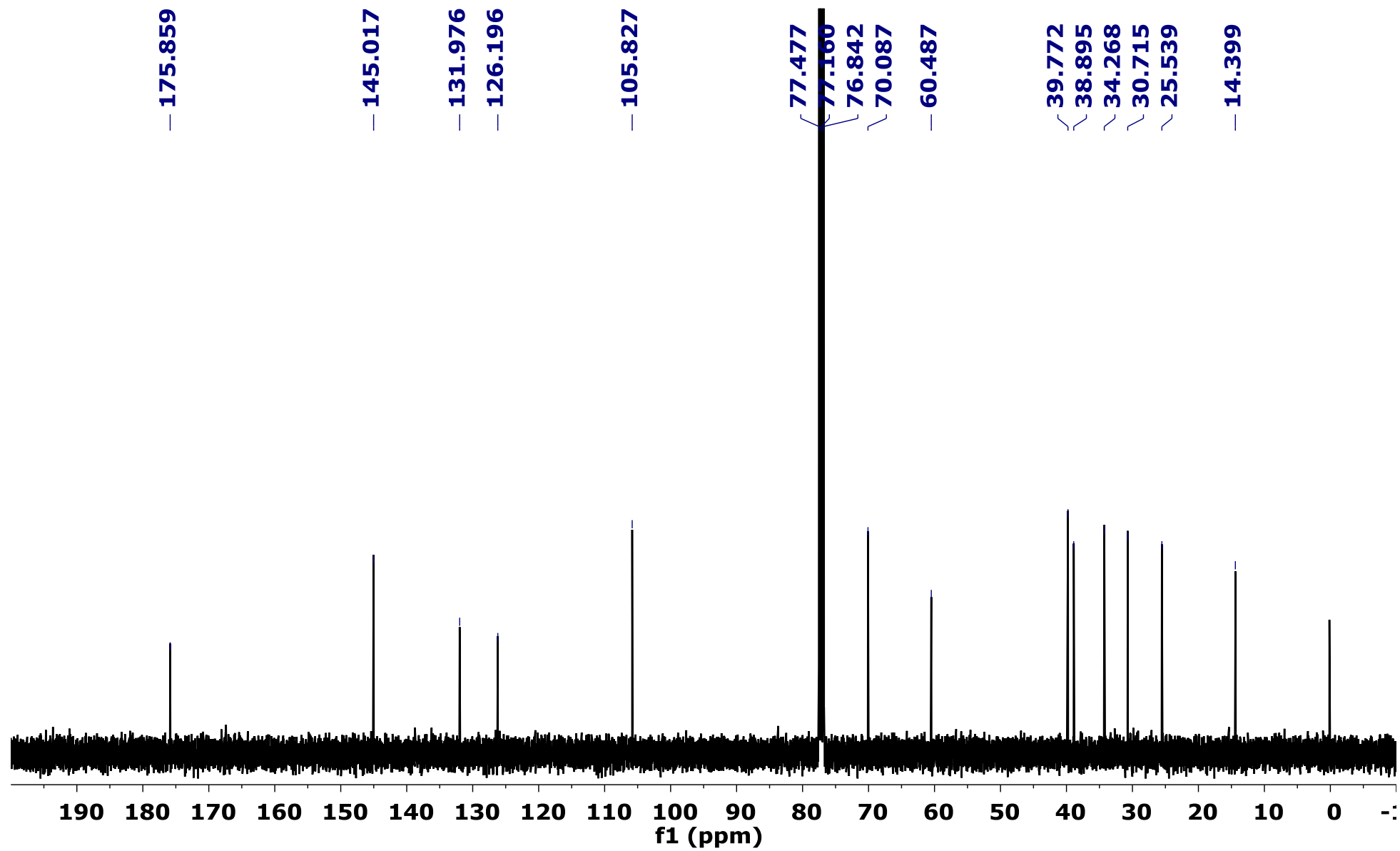


^1H NMR (400 MHz, CDCl_3)

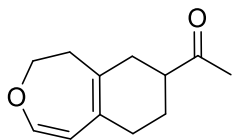




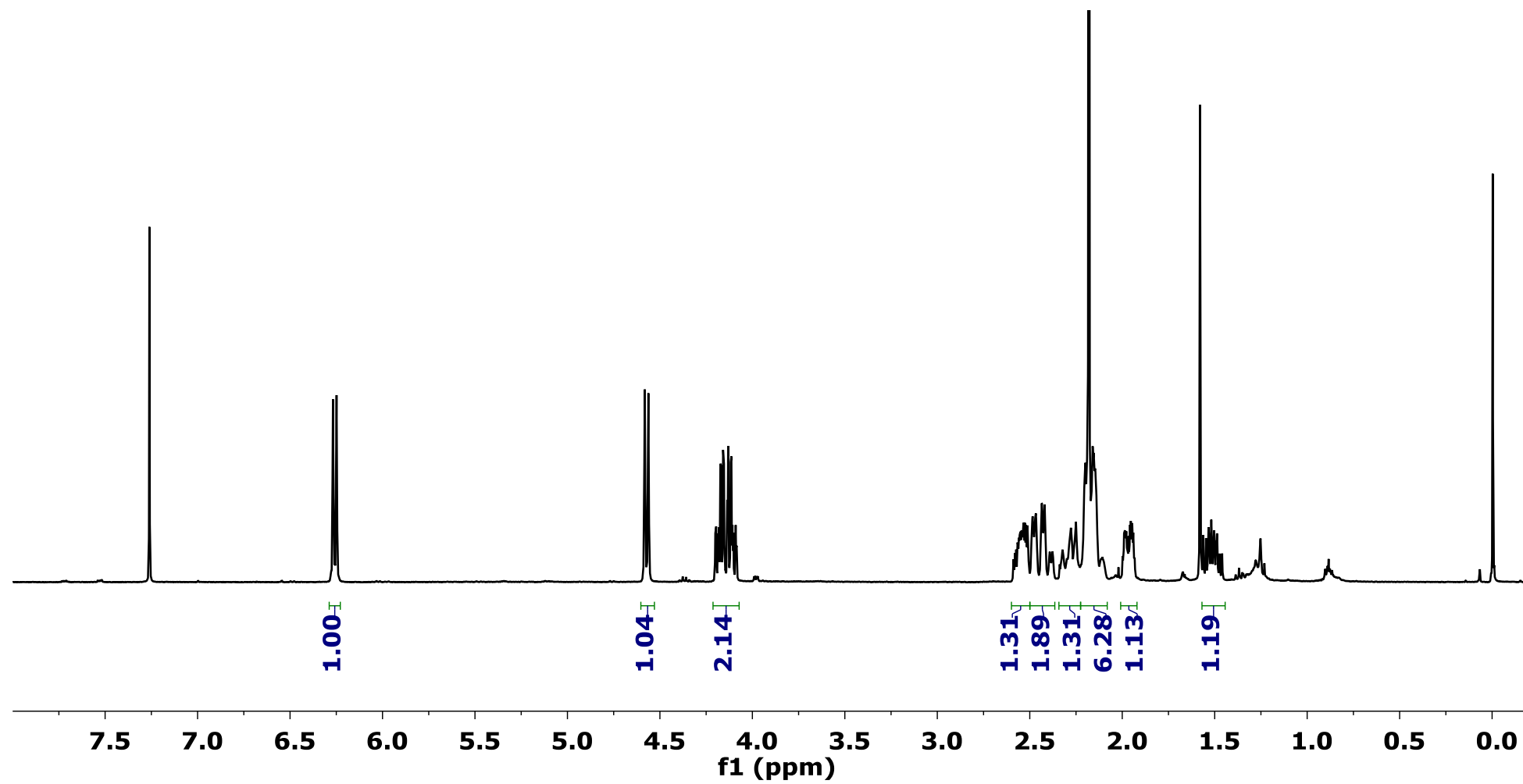
¹³C NMR (101 MHz, CDCl₃)

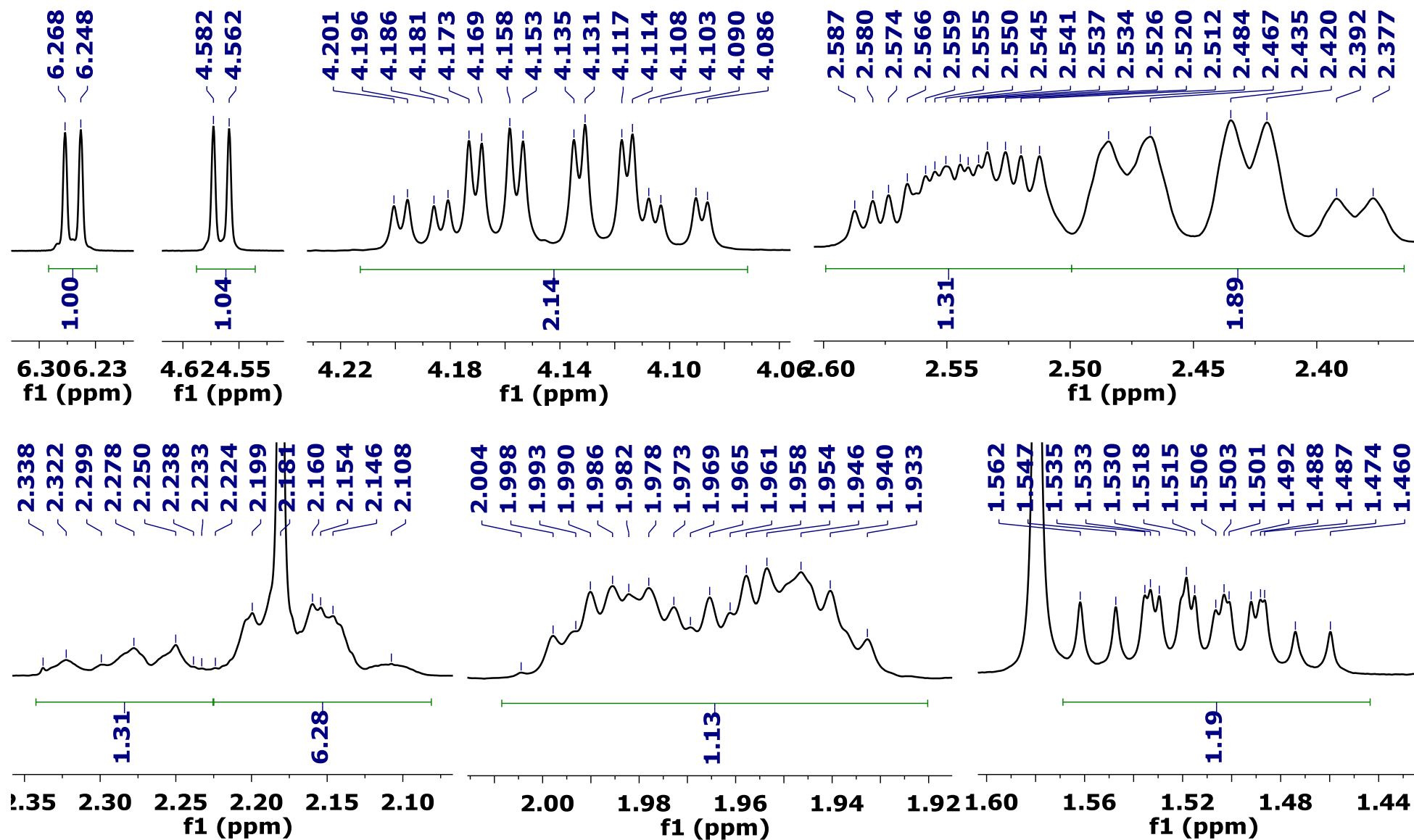


Product 3bg

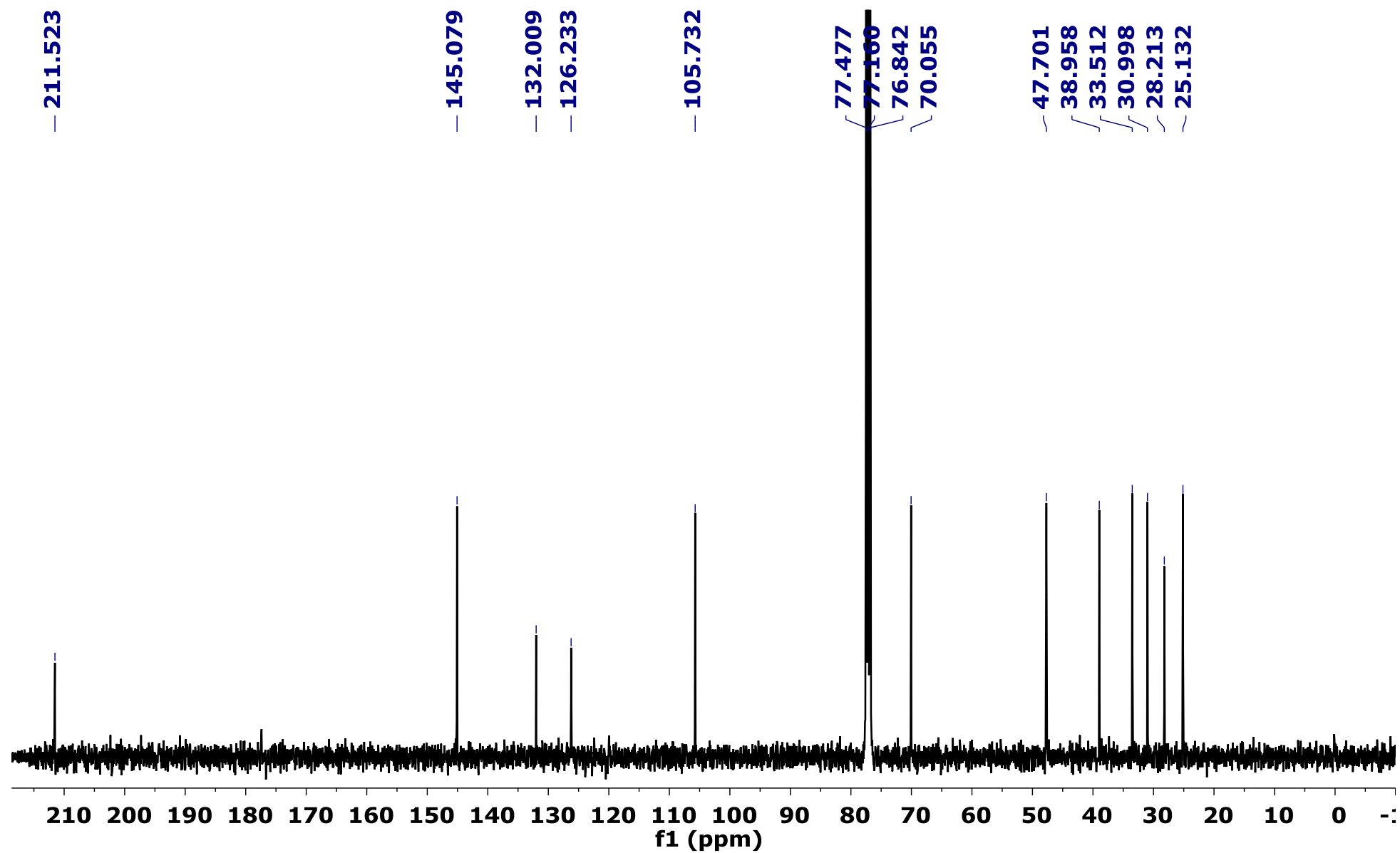


^1H NMR (400 MHz, CDCl_3)

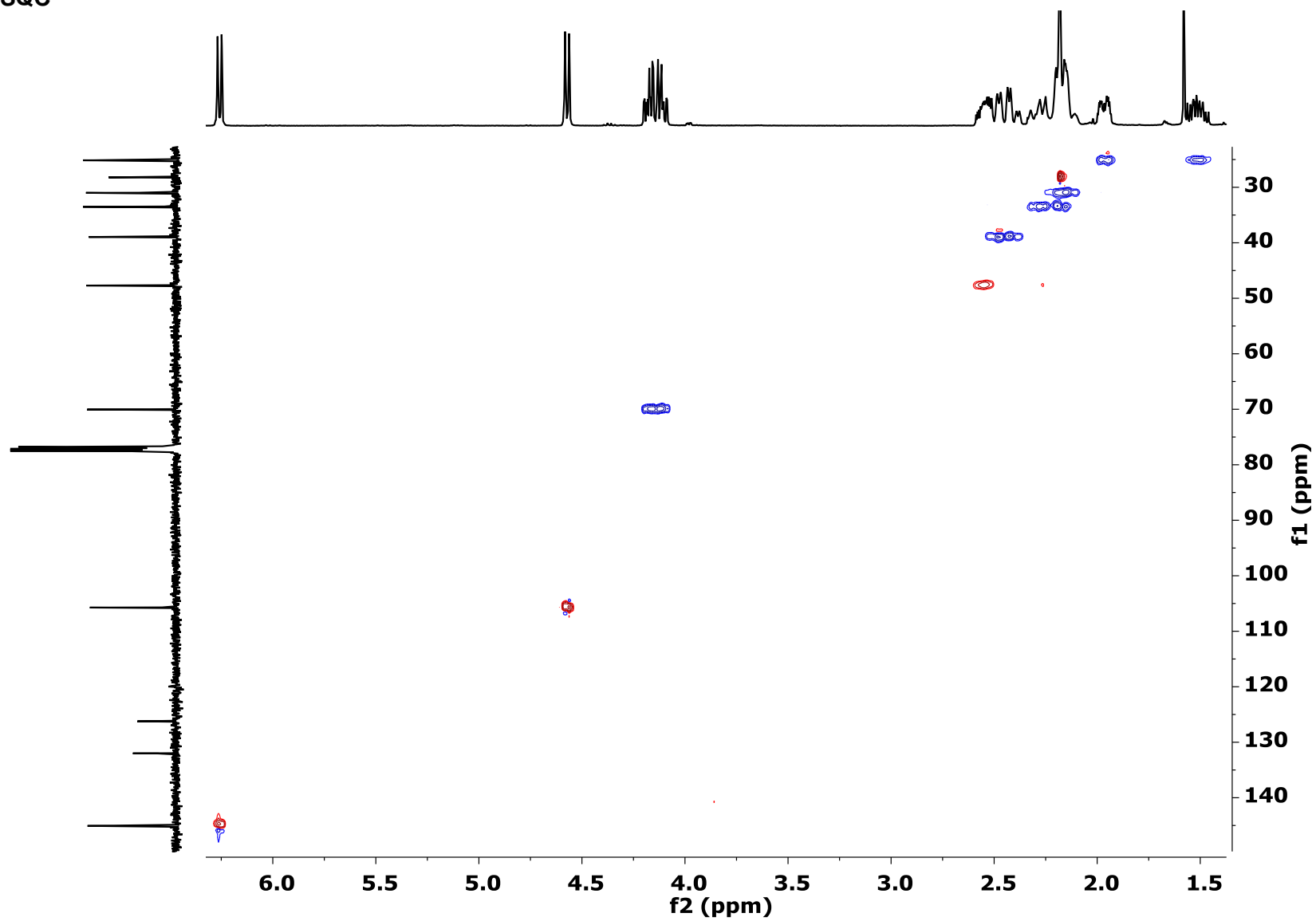




¹³C NMR (101 MHz, CDCl₃)

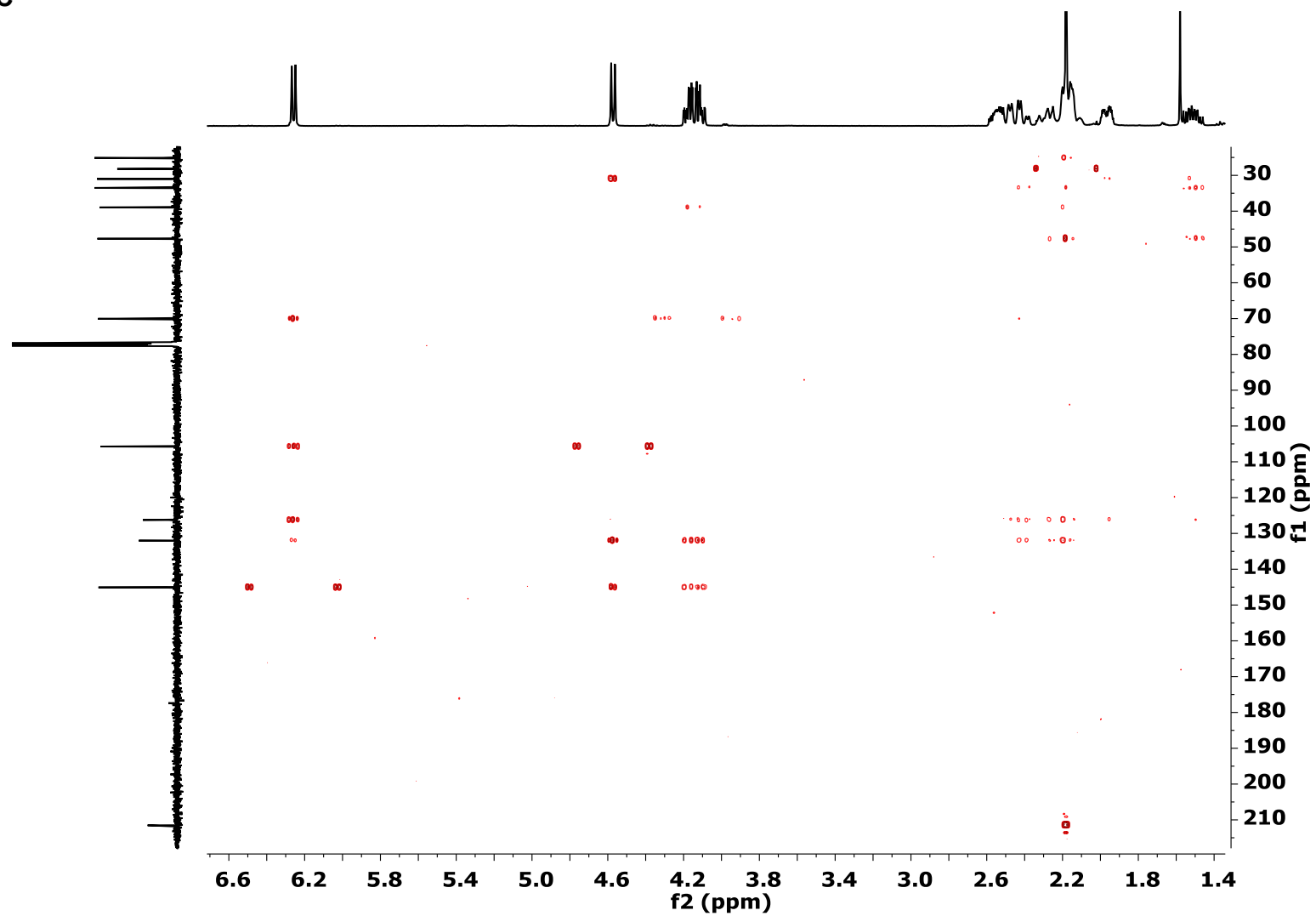


2D NMR HSQC

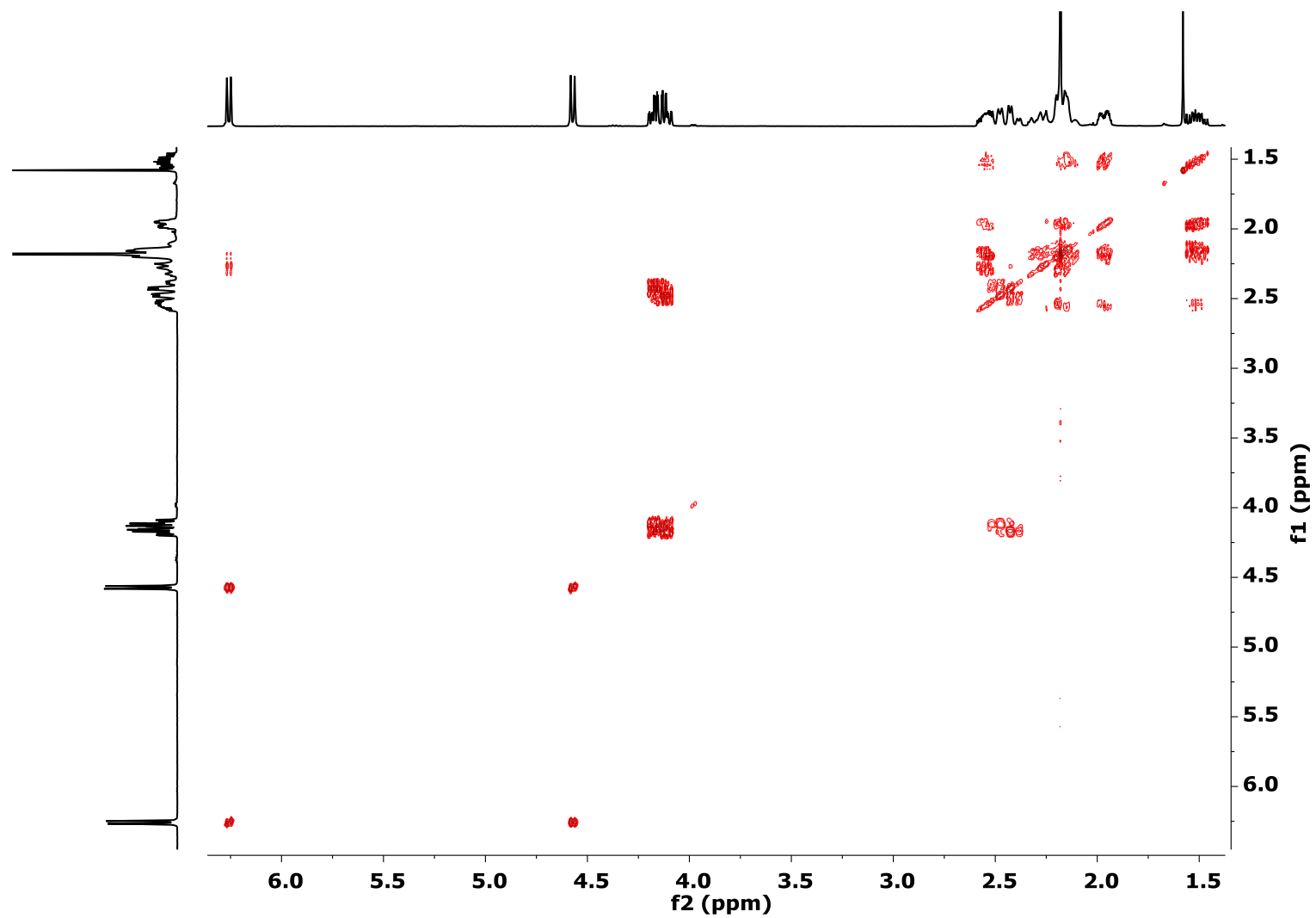


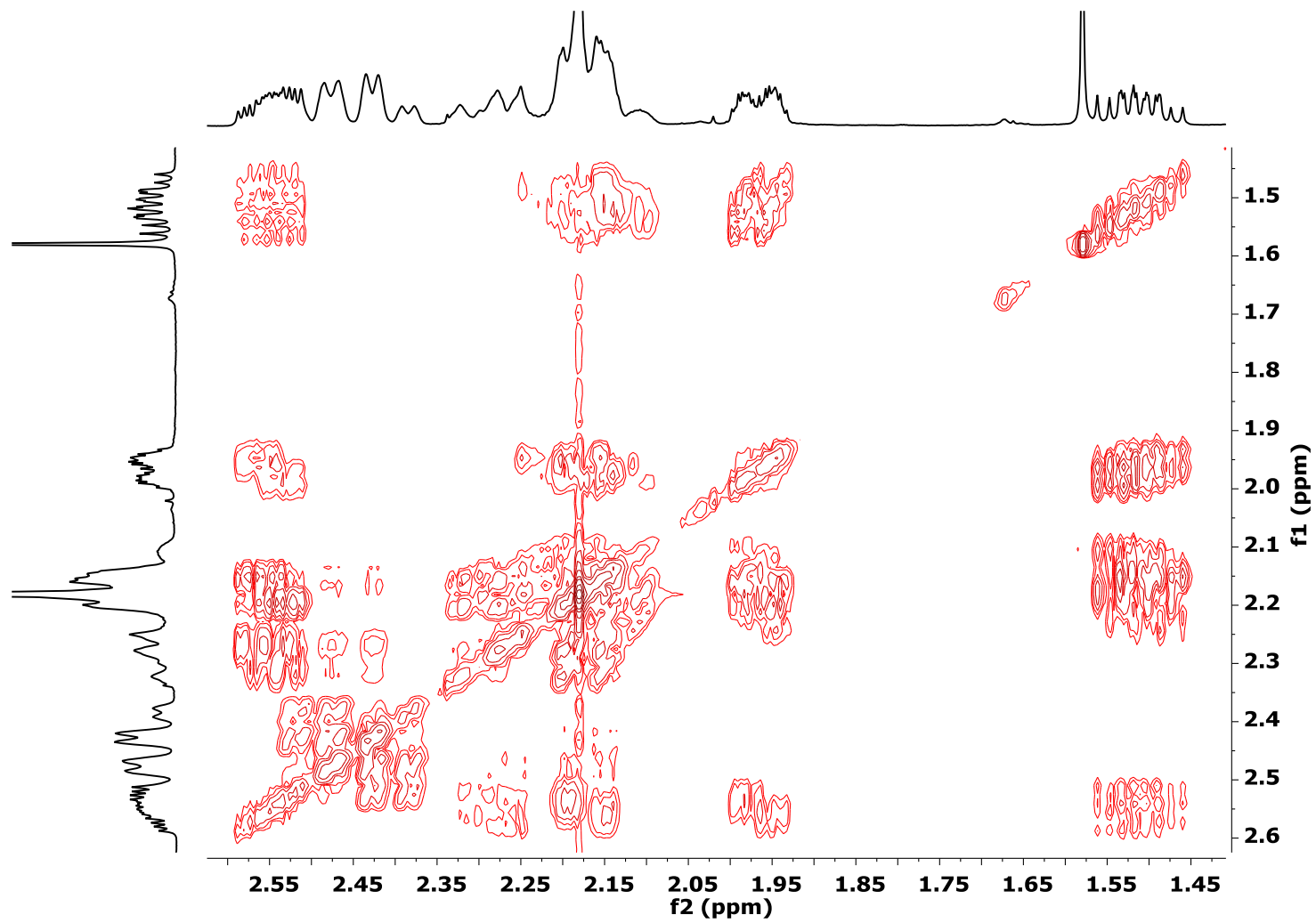
S80

2D NMR HMBC

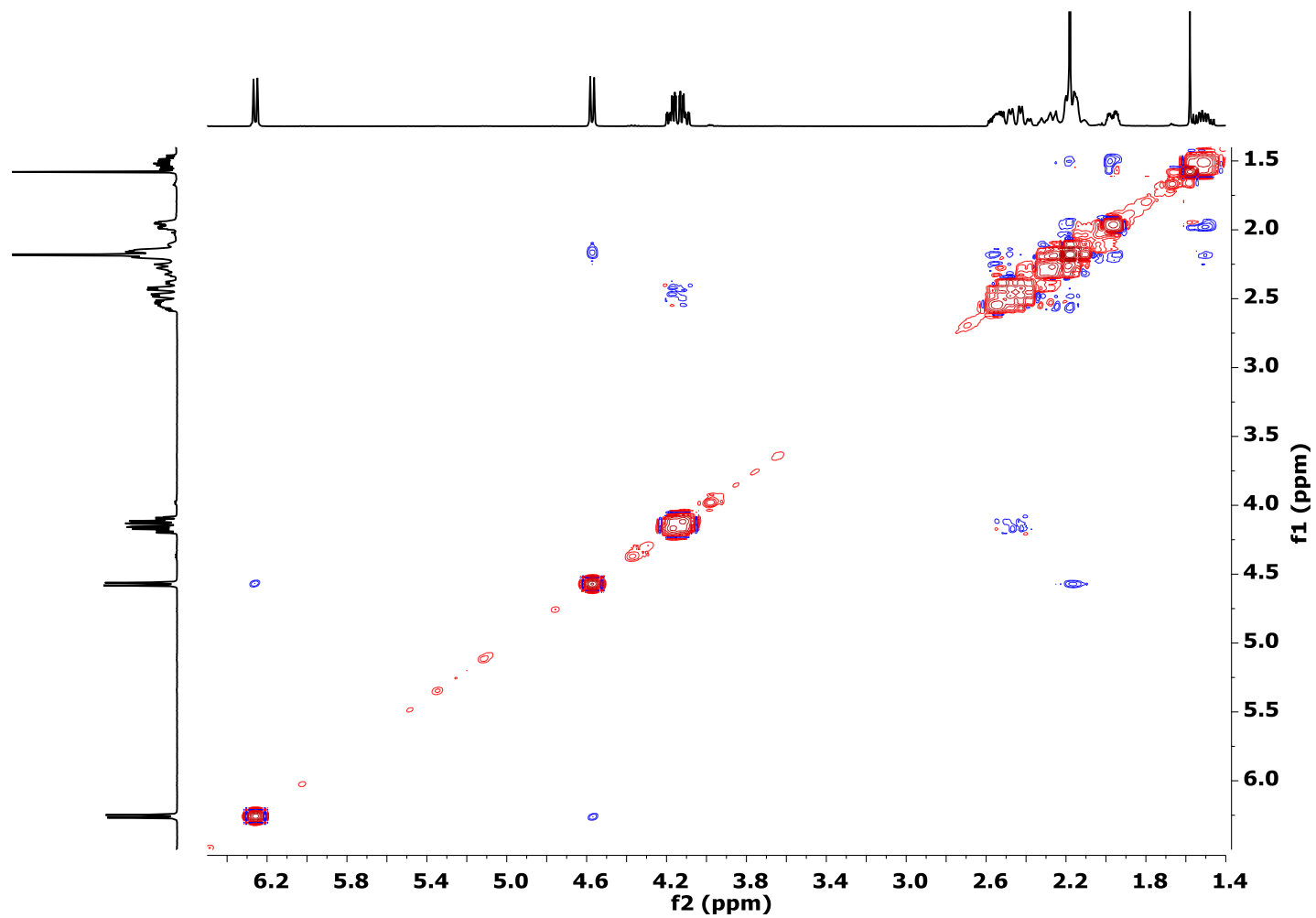


2D NMR COSY

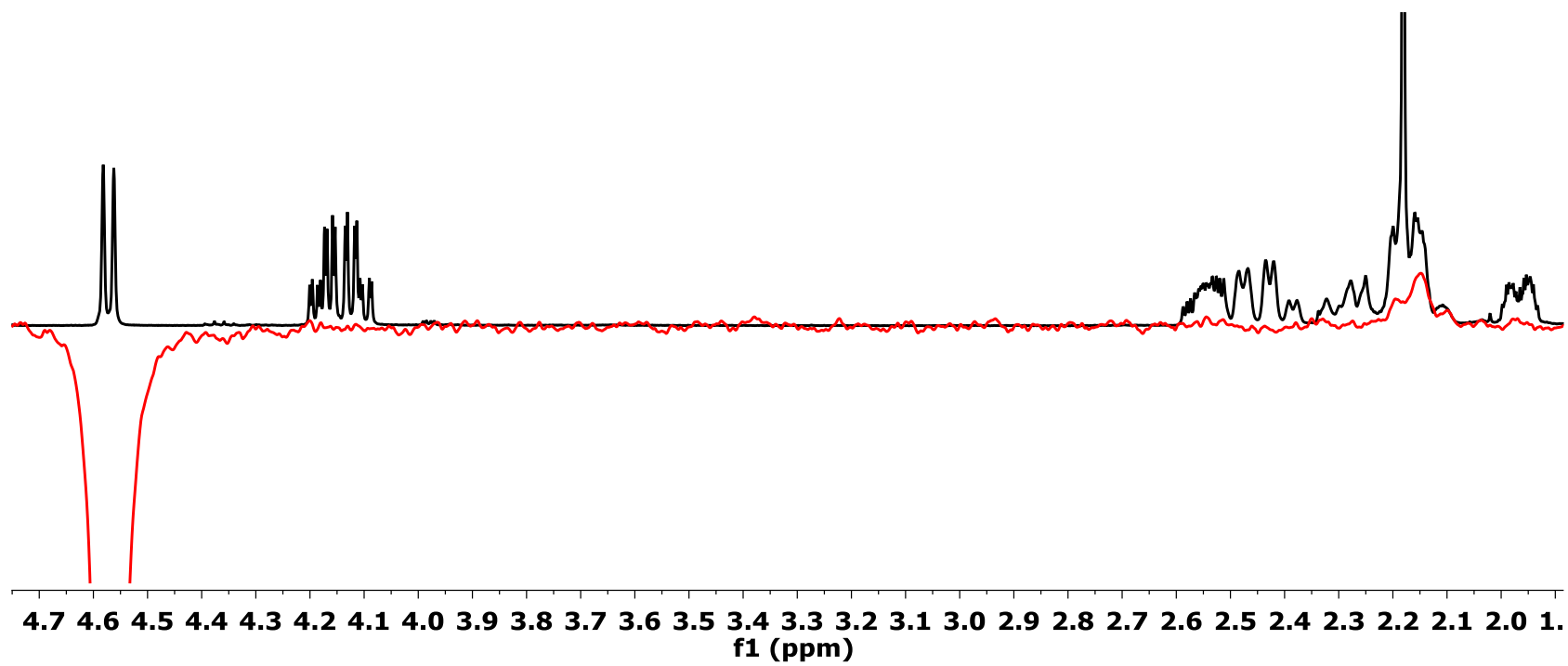




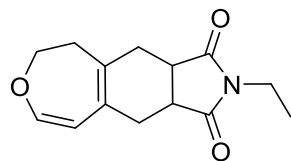
2D NMR NOESY



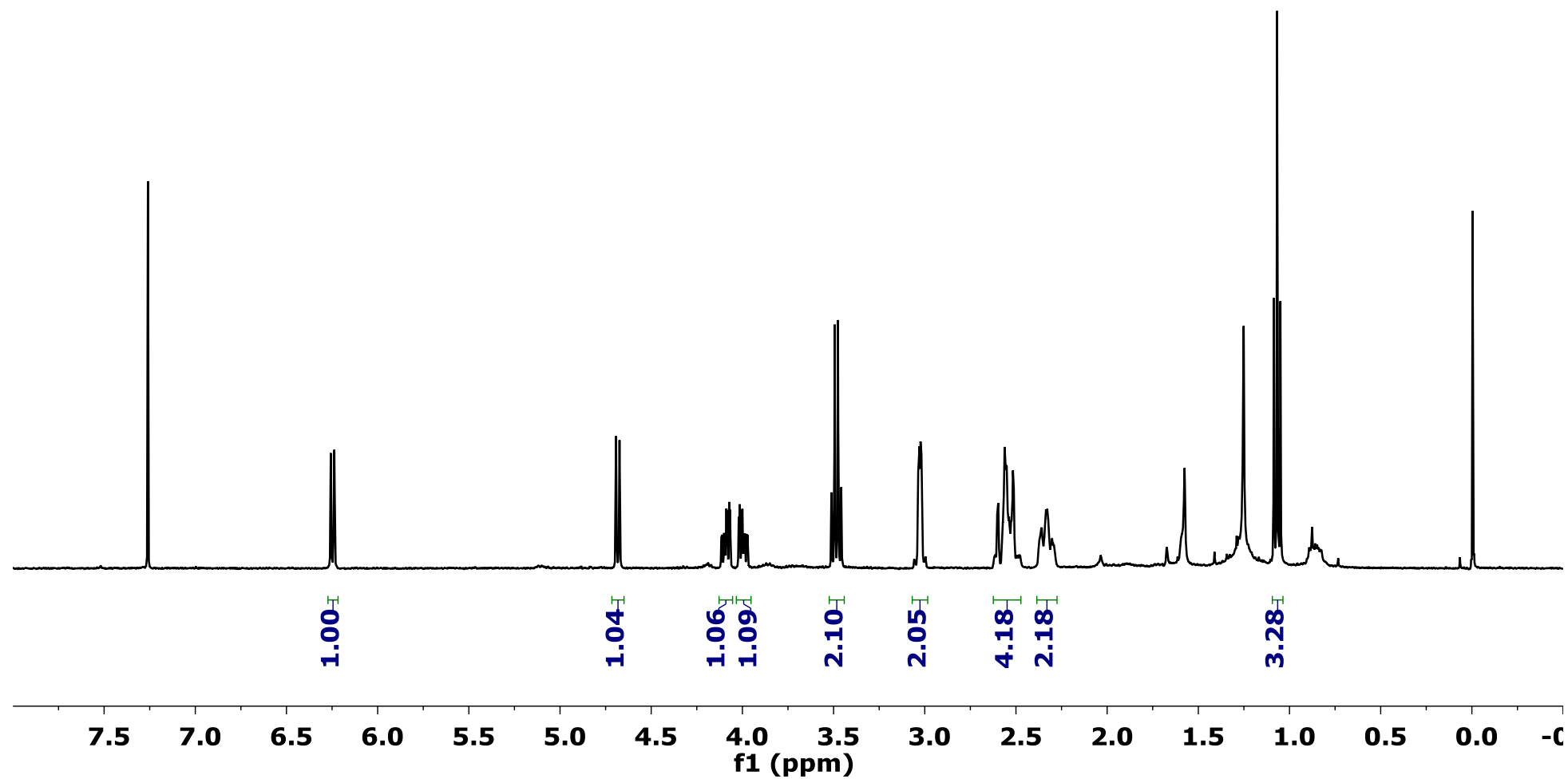
1D NMR SELECTIVE NOESY

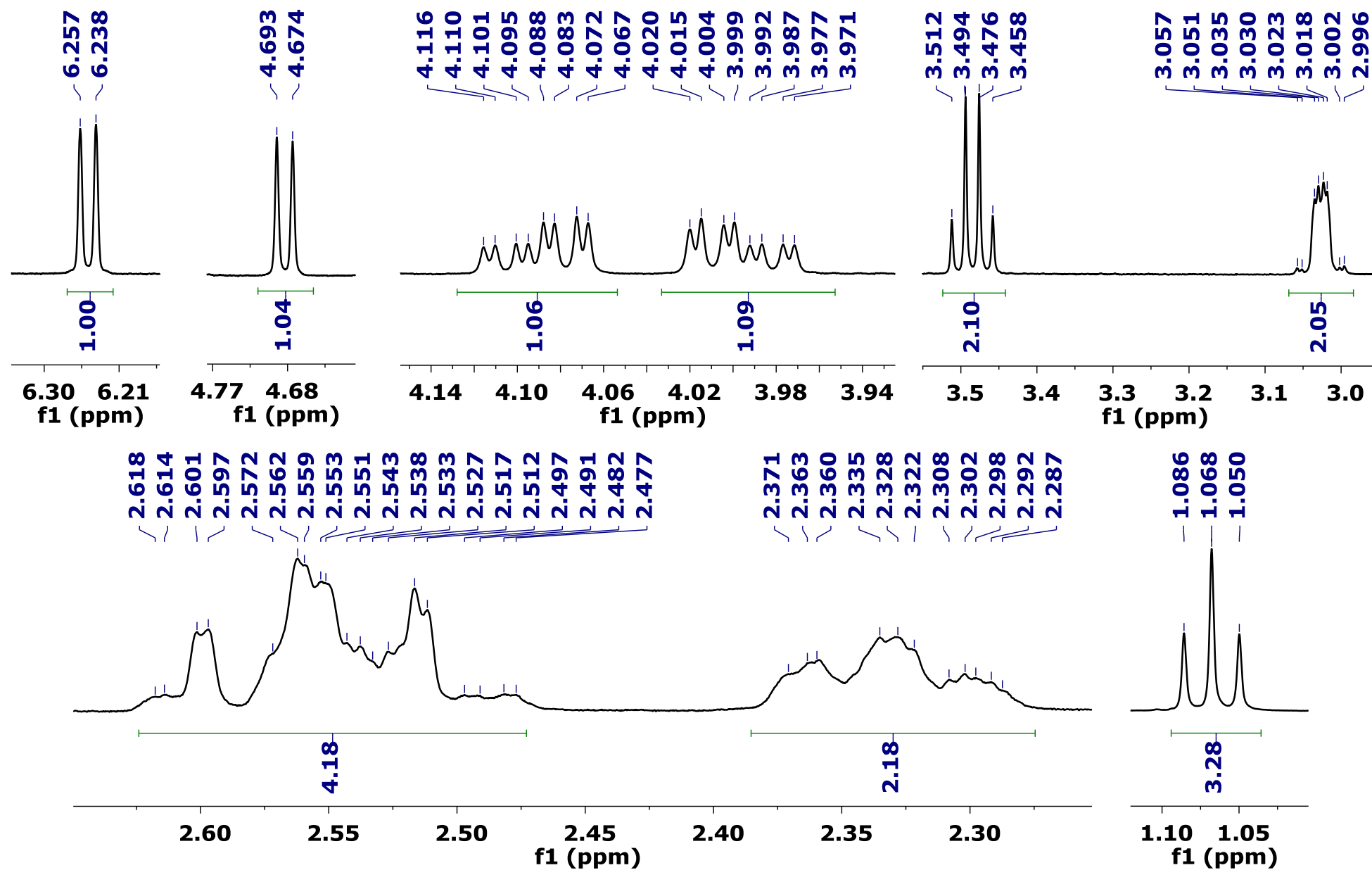


Product 3bj

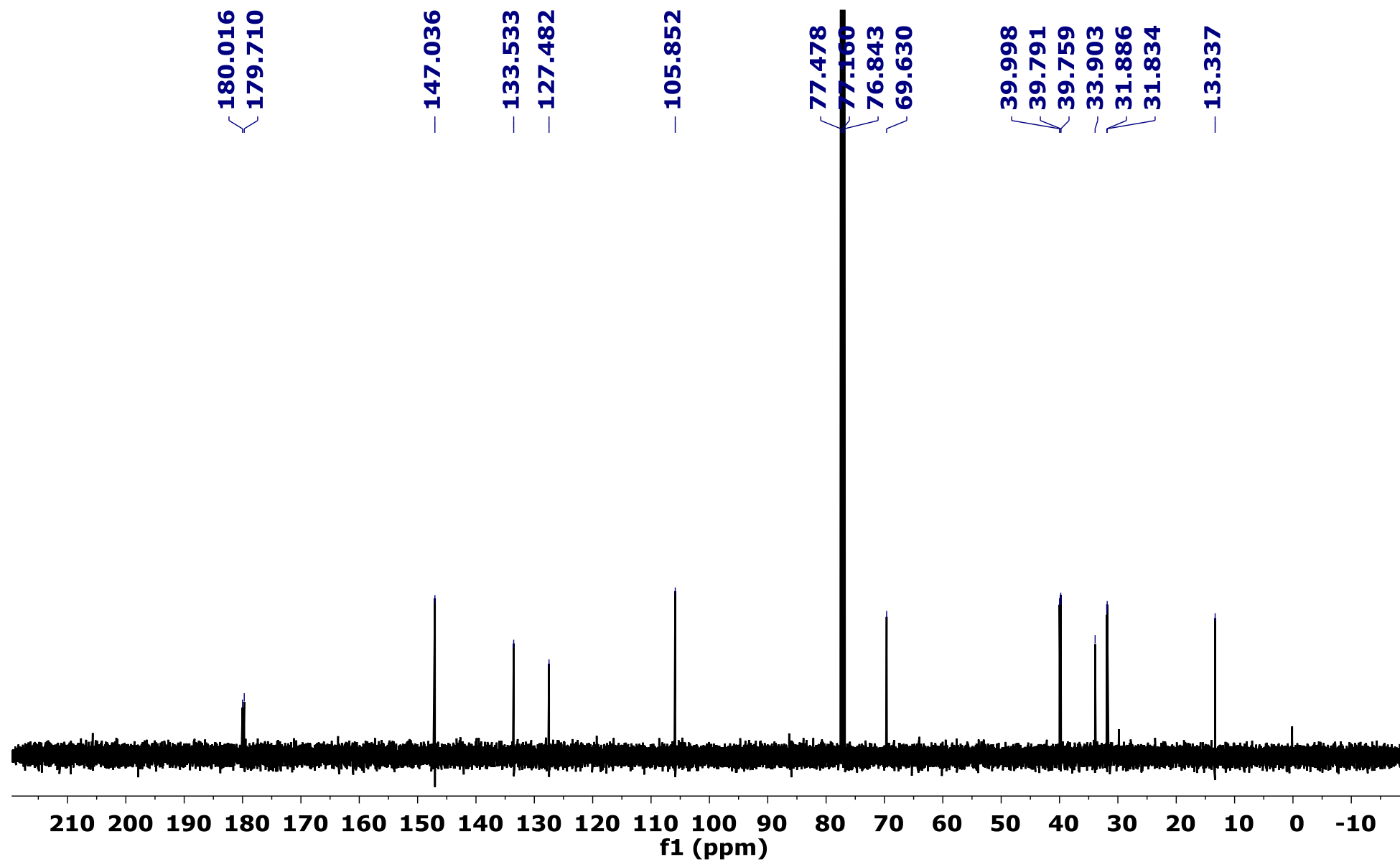


^1H NMR (400 MHz, CDCl_3)



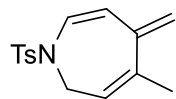


¹³C NMR (101 MHz, CDCl₃)

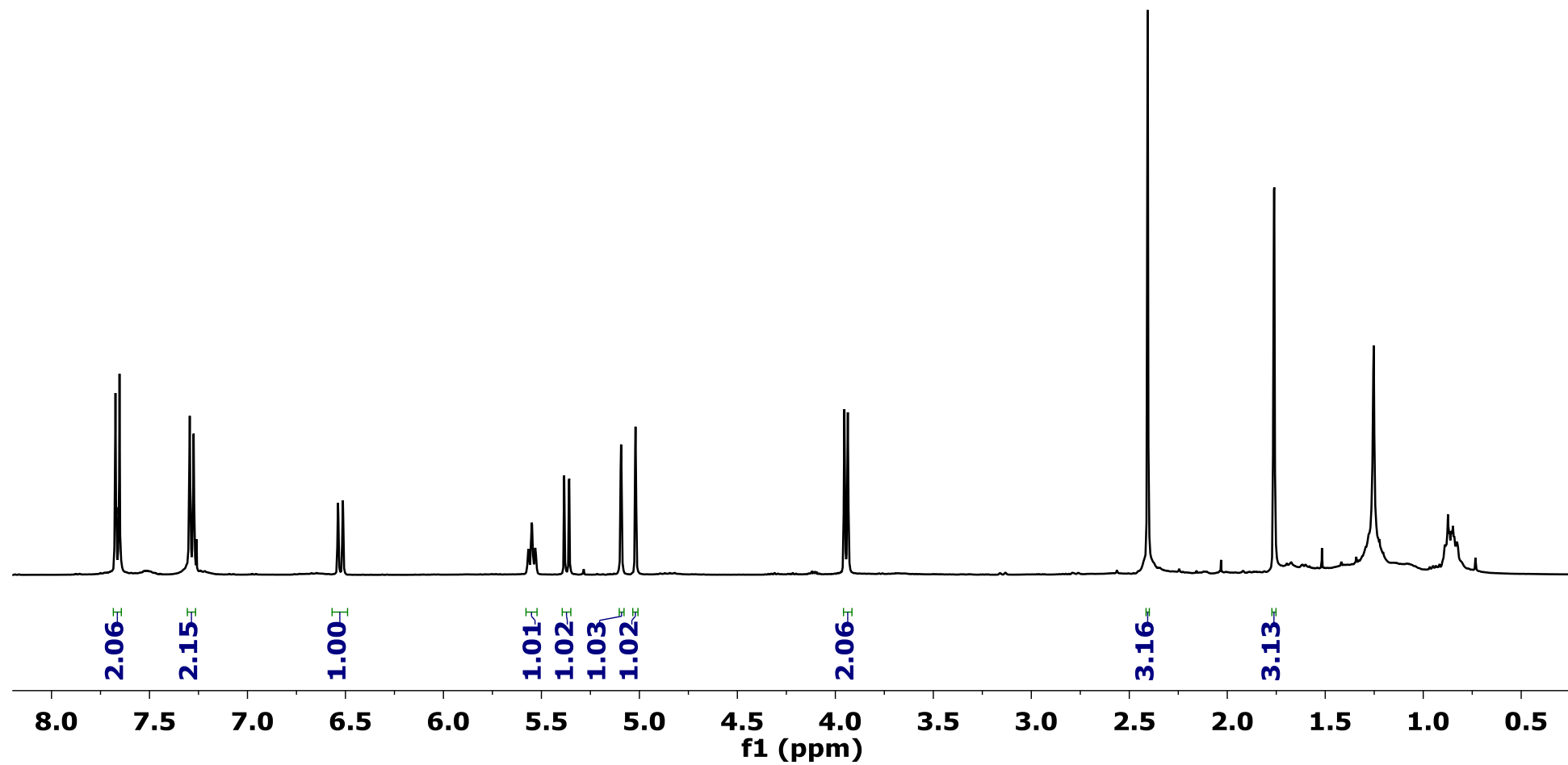


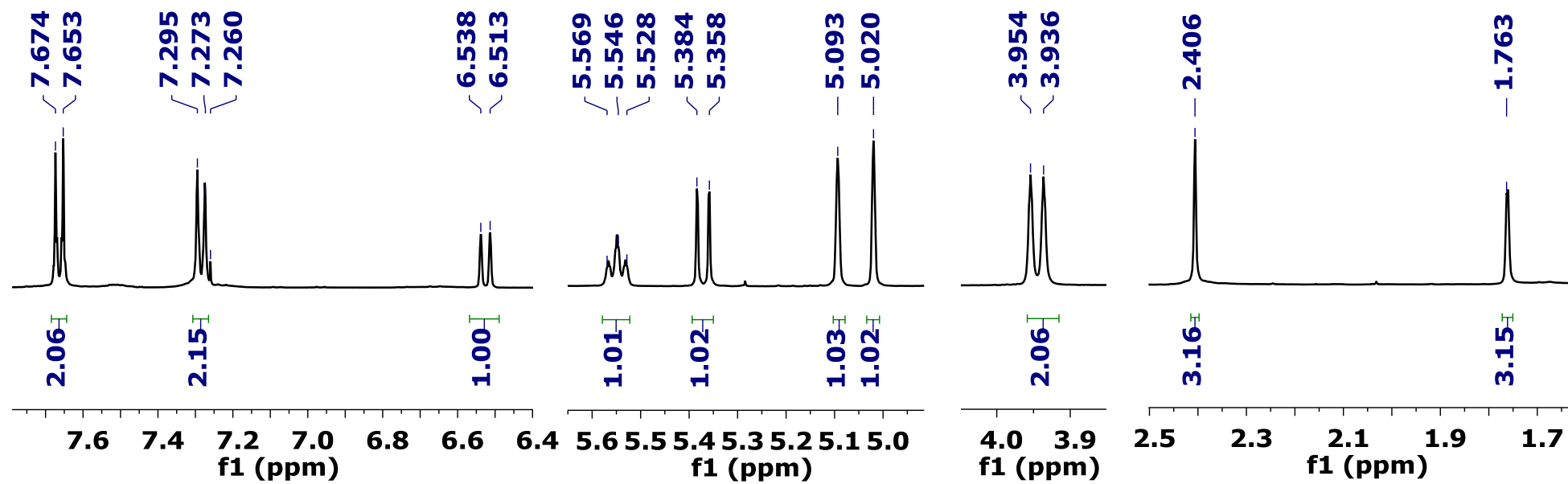
S88

Product 4a

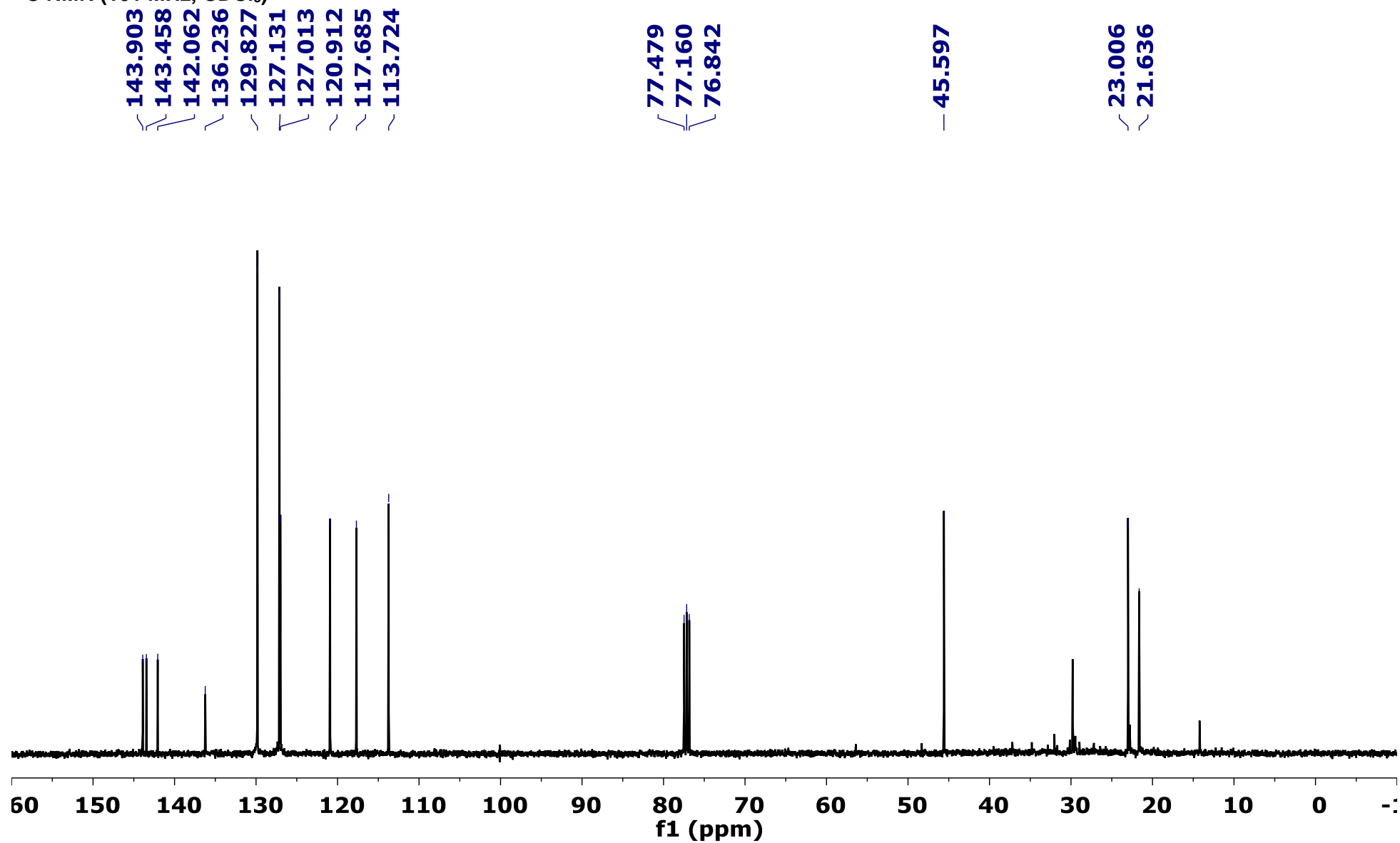


^1H NMR (400 MHz, CDCl_3)

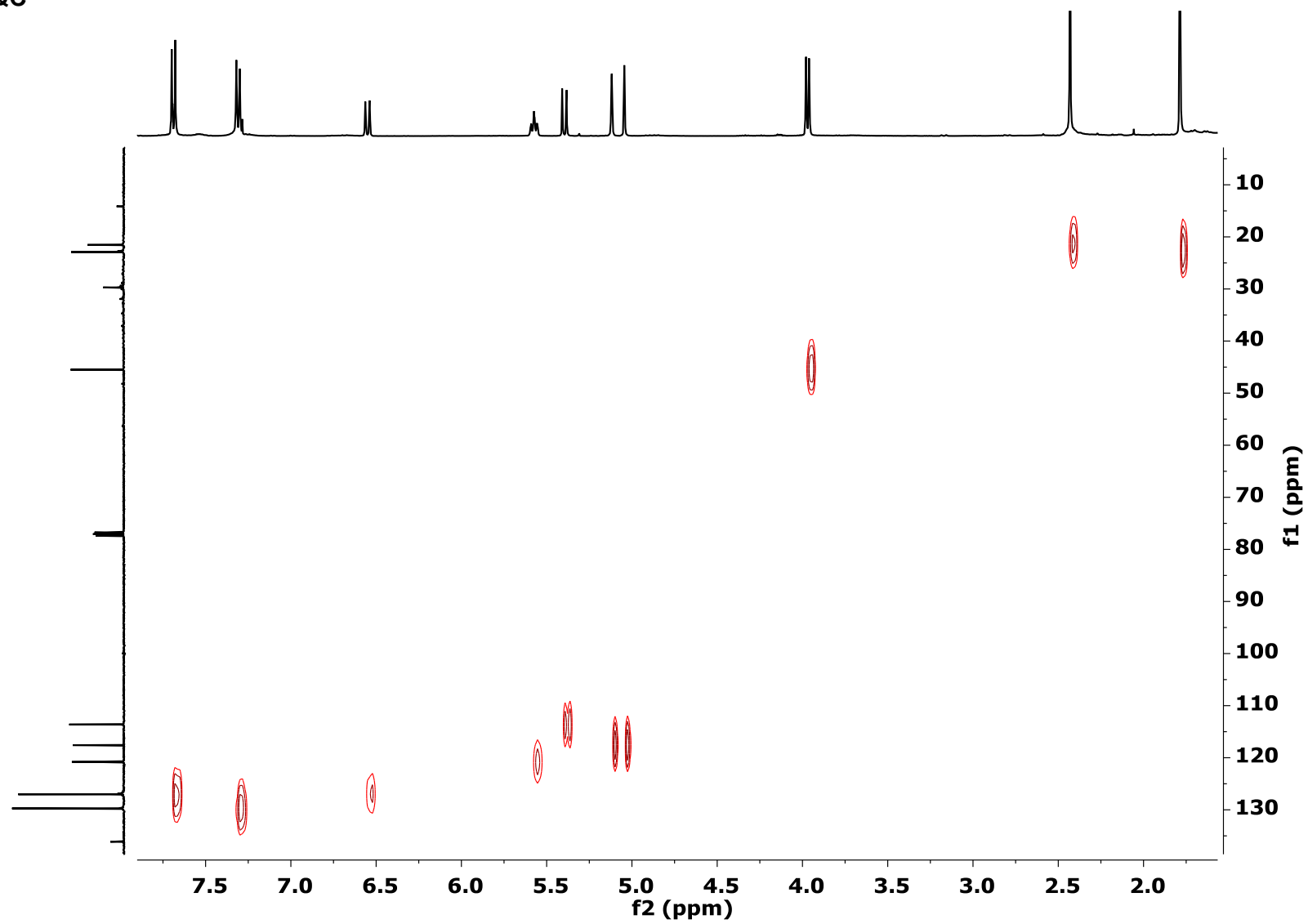




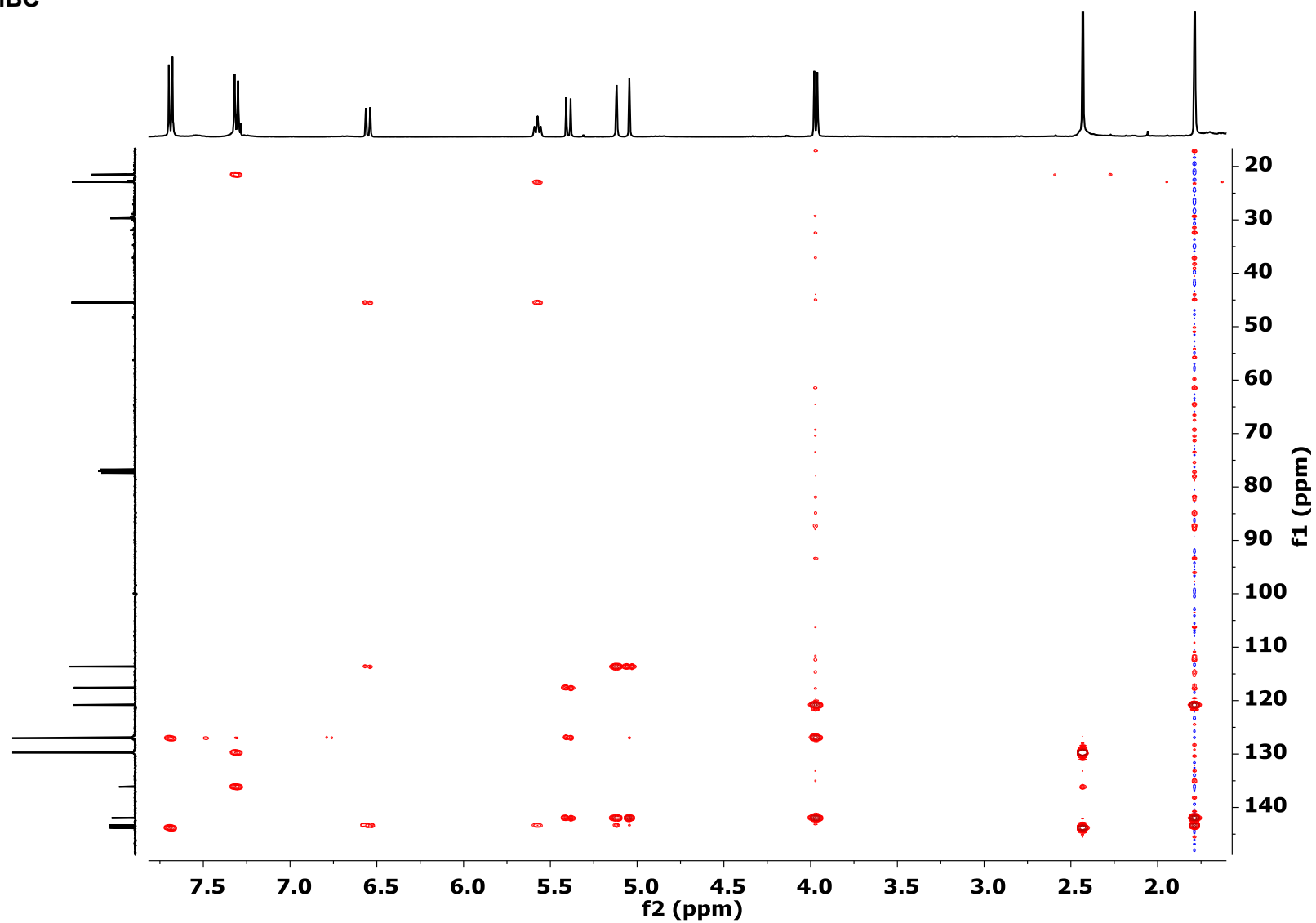
¹³C NMR (101 MHz, CDCl₃)



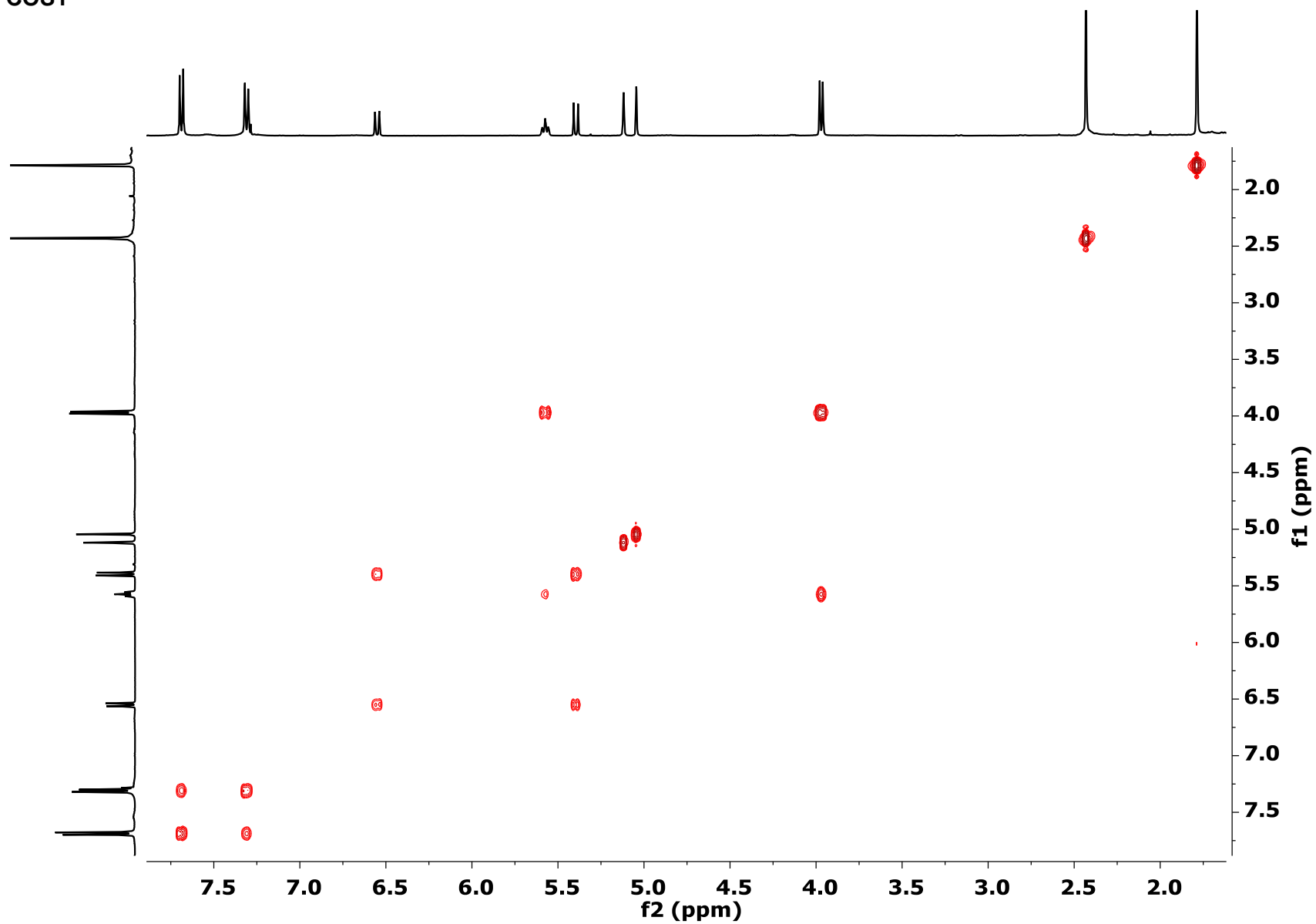
2D NMR HSQC



2D NMR HMBC

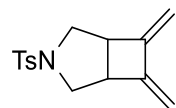


2D NMR COSY

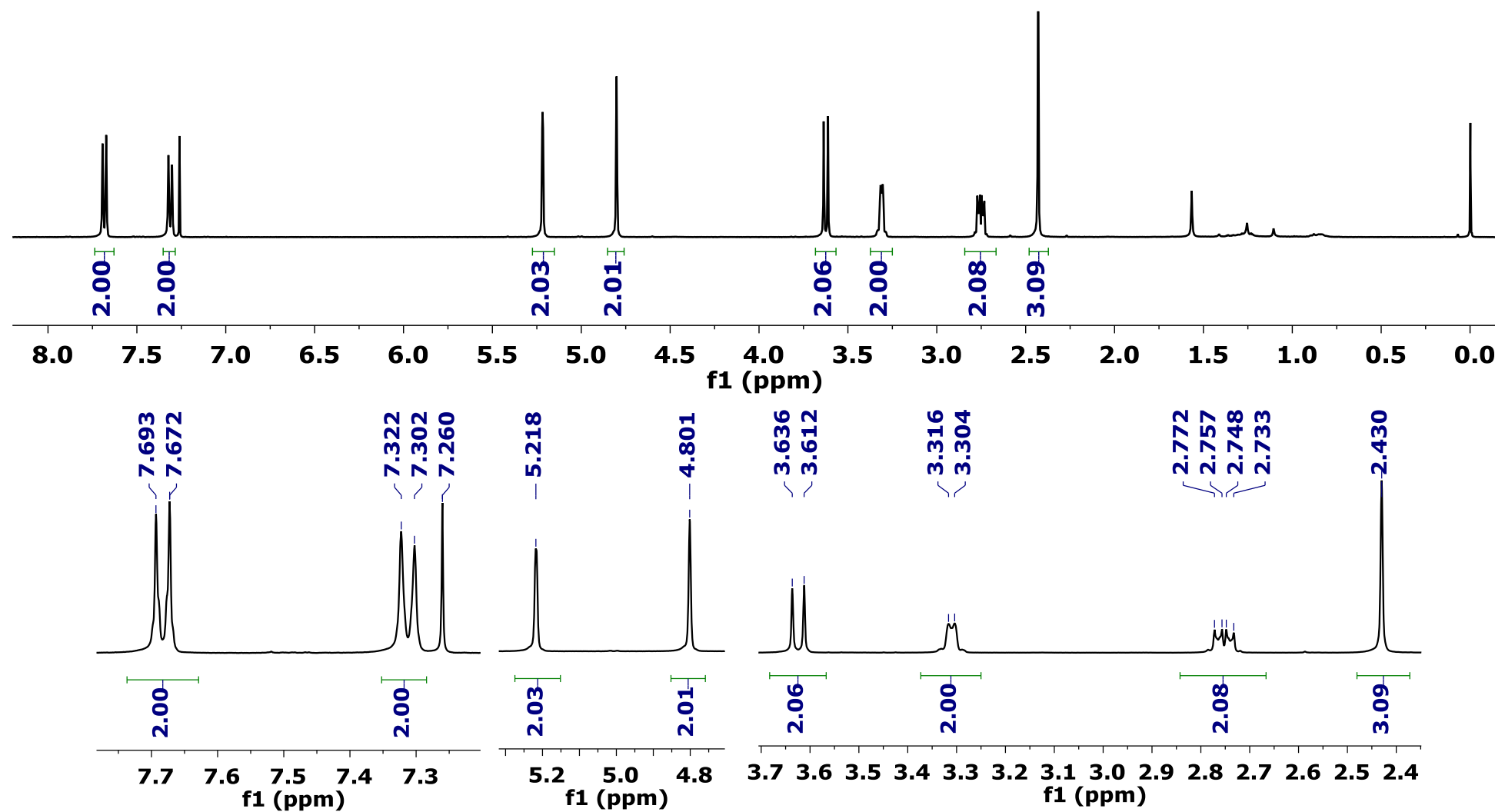


S94

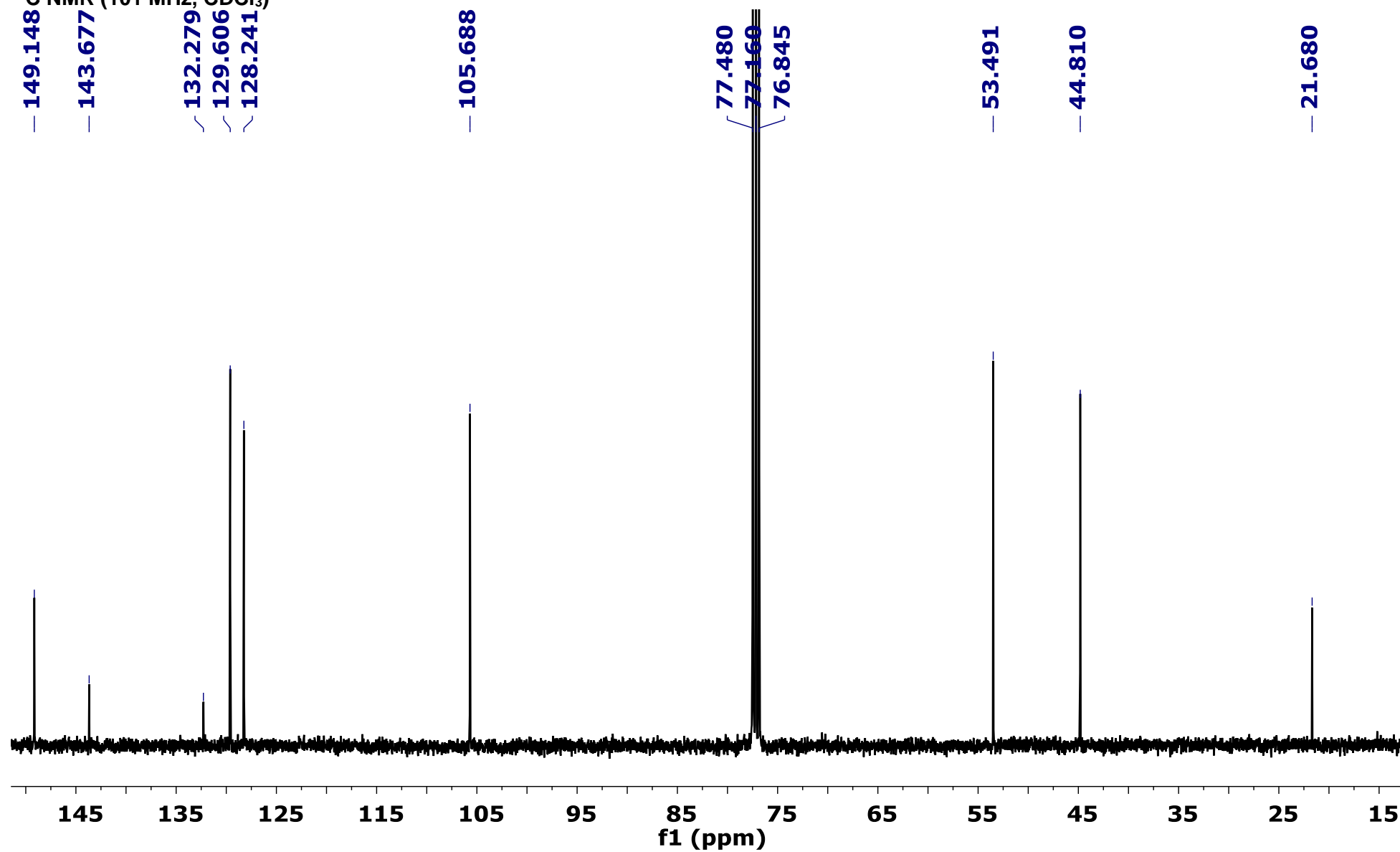
Product 5a



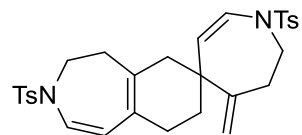
^1H NMR (400 MHz, CDCl_3)



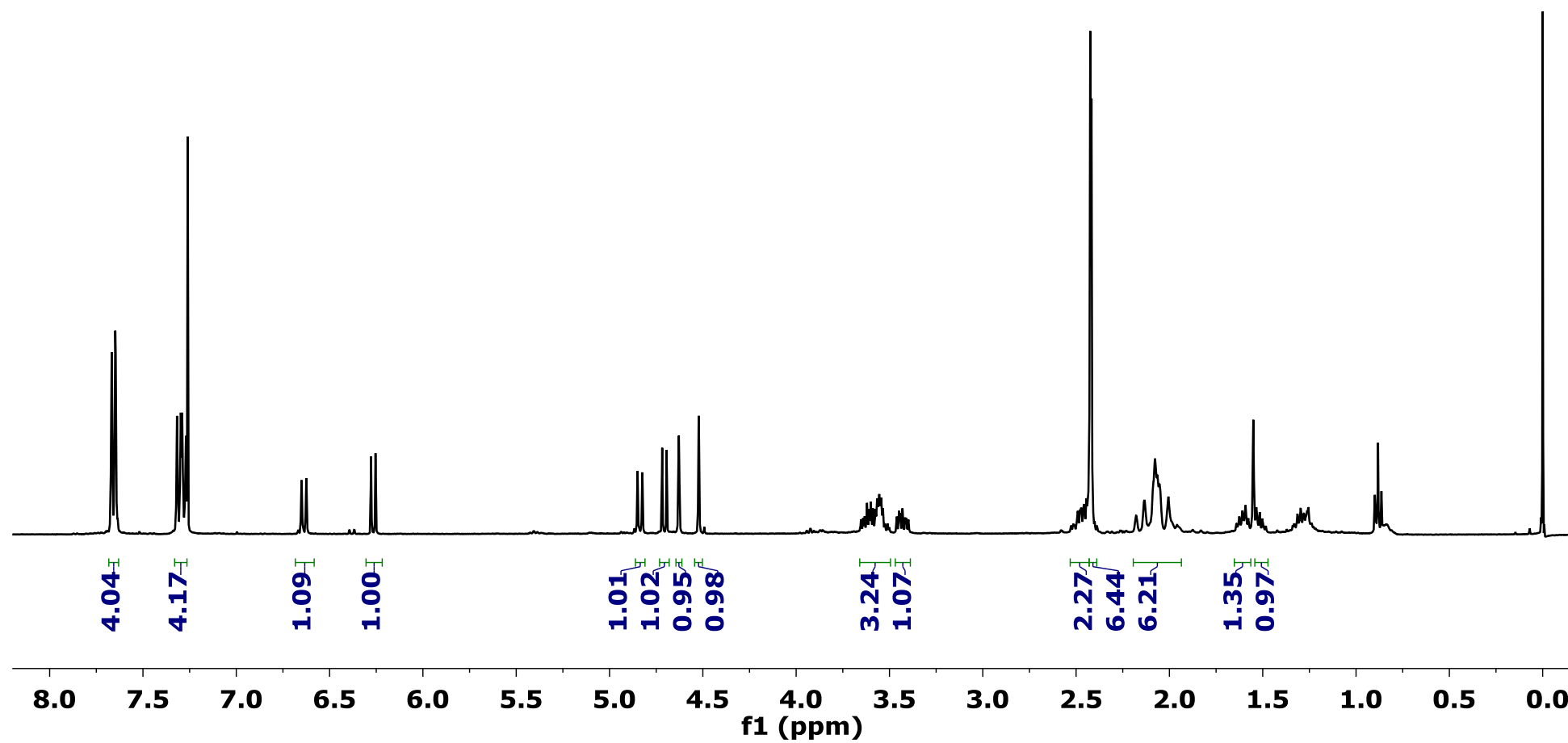
¹³C NMR (101 MHz, CDCl₃)

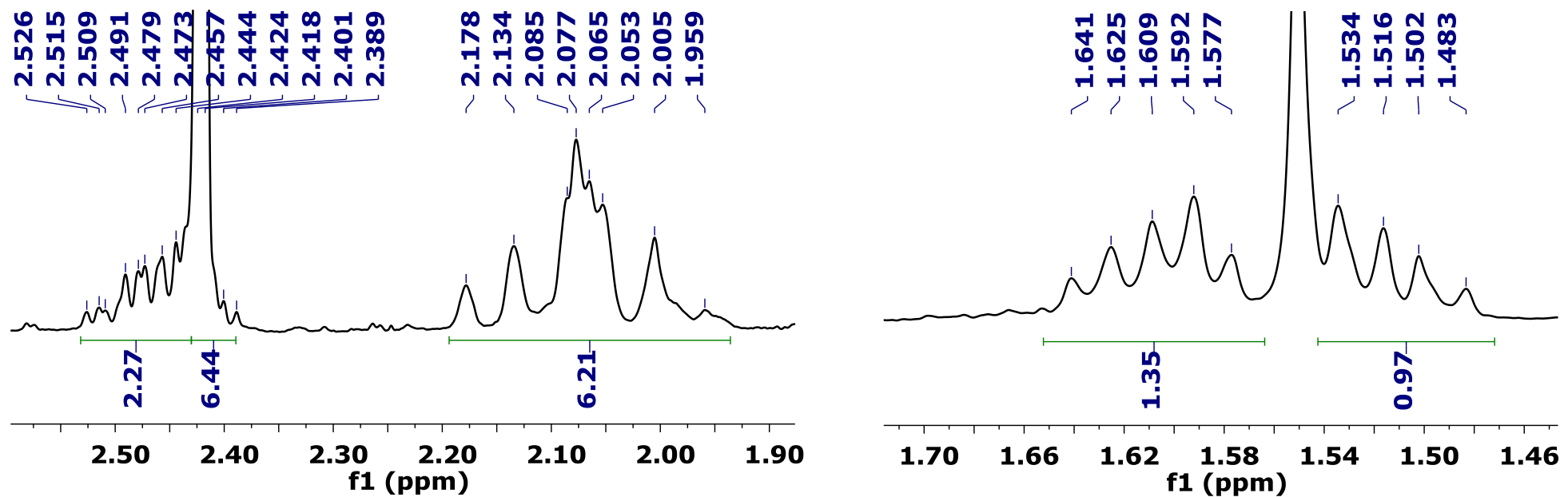
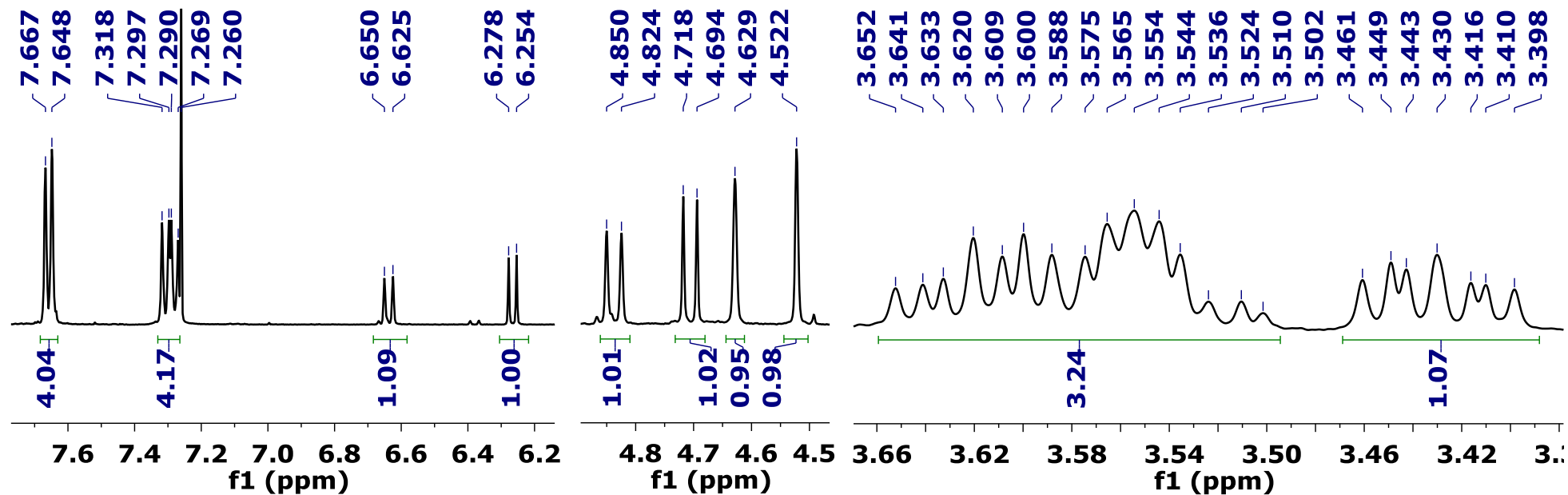


Product 6a

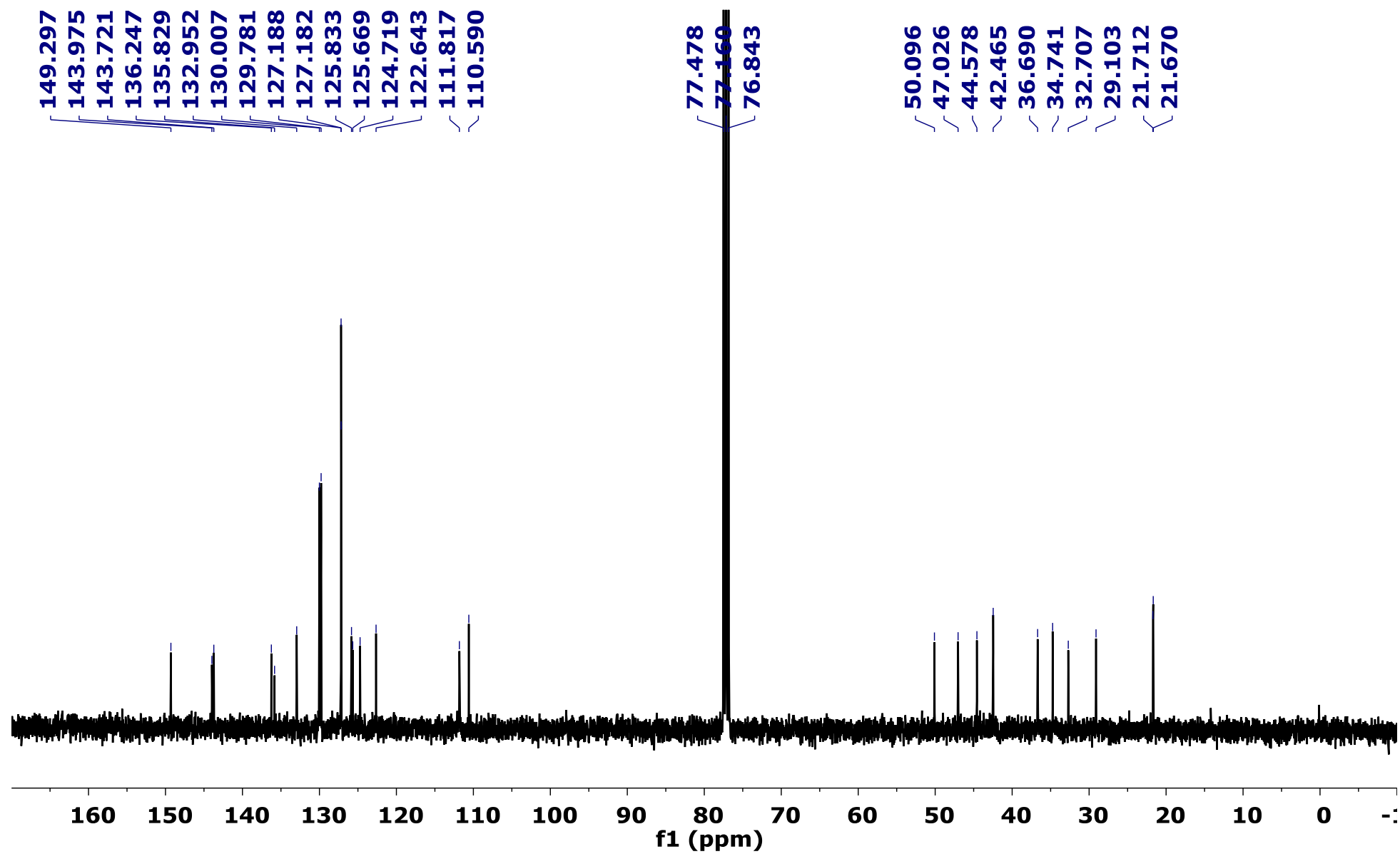


^1H NMR (400 MHz, CDCl_3)

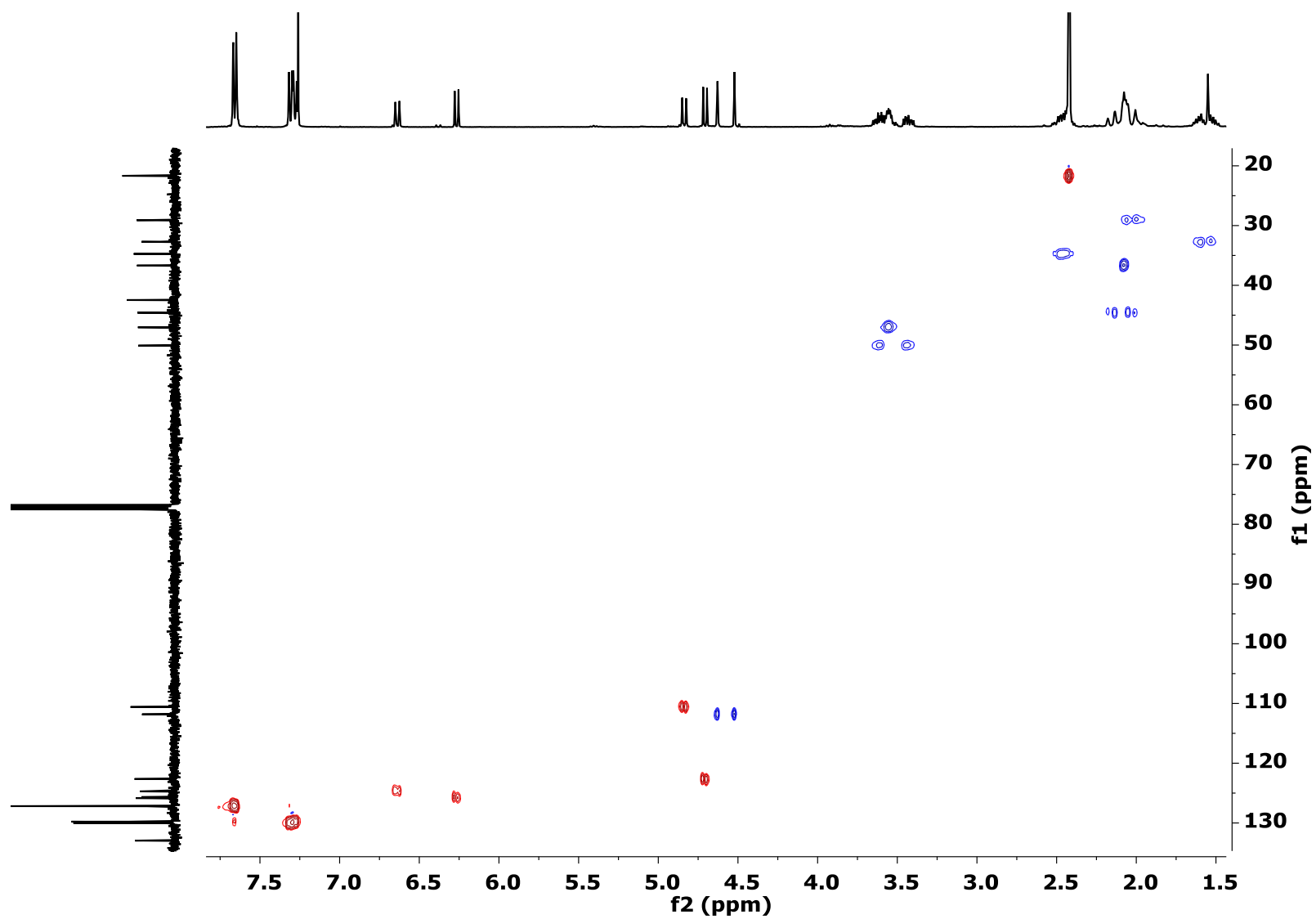




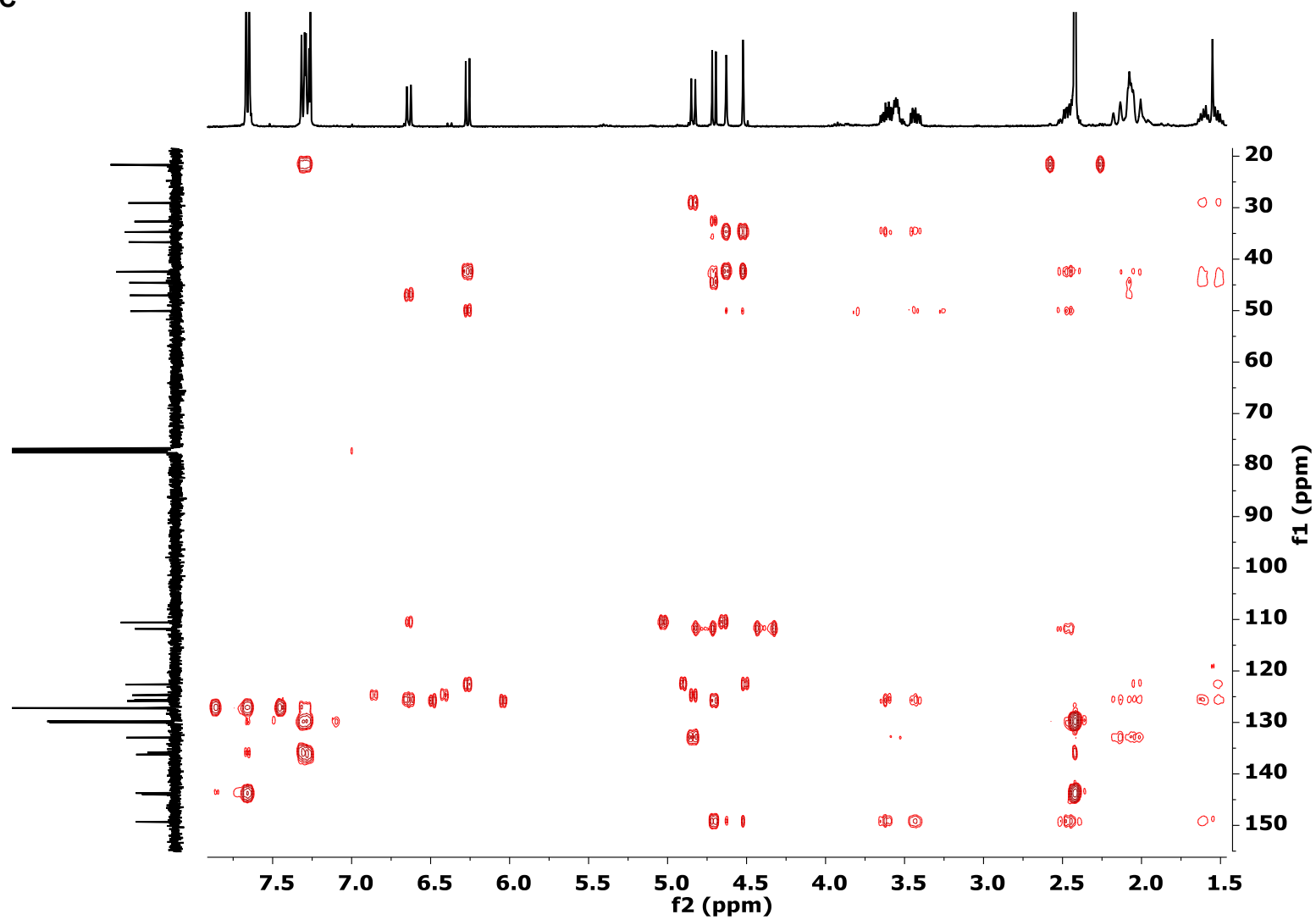
¹³C NMR (101 MHz, CDCl₃)



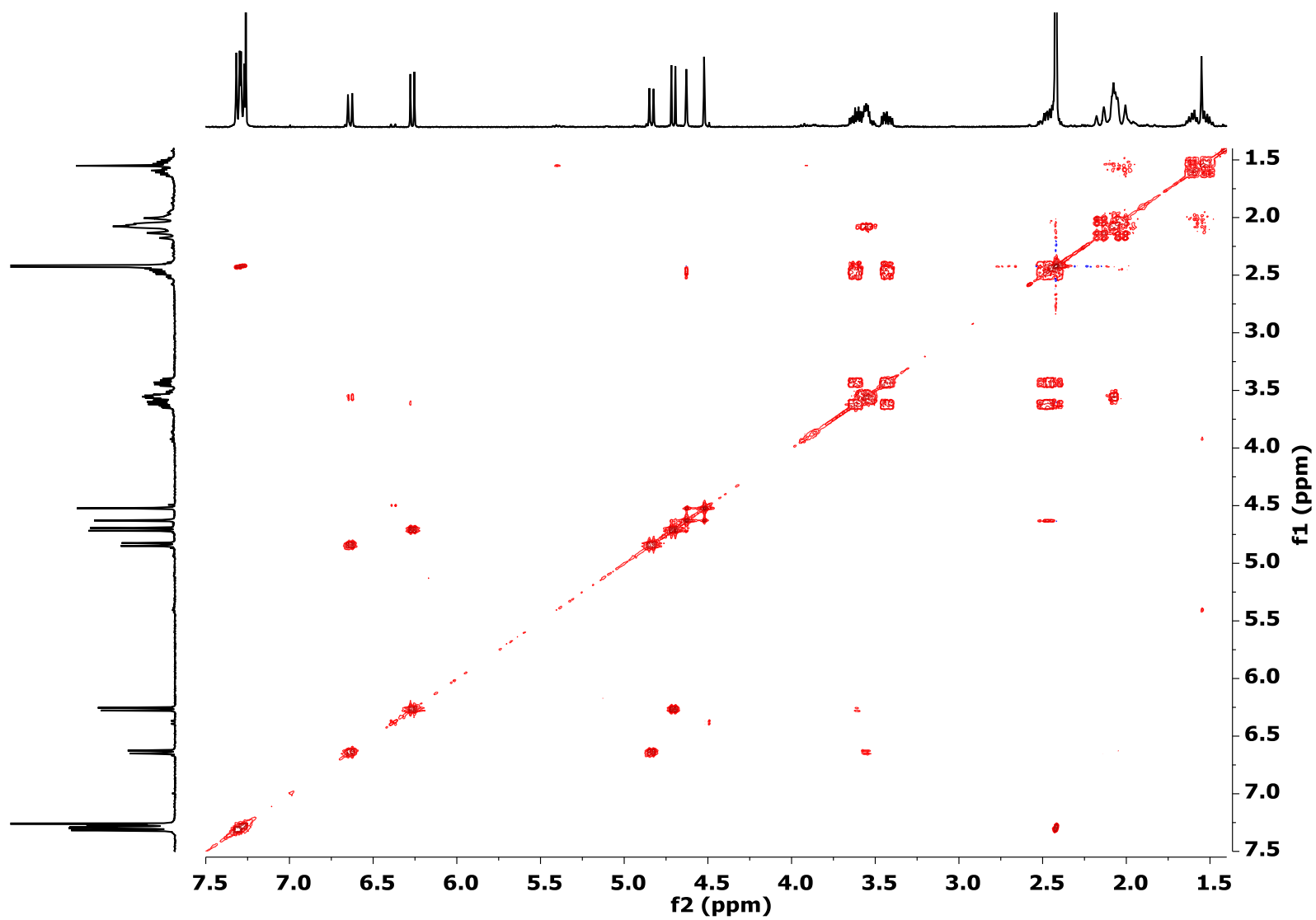
2D NMR HSQC



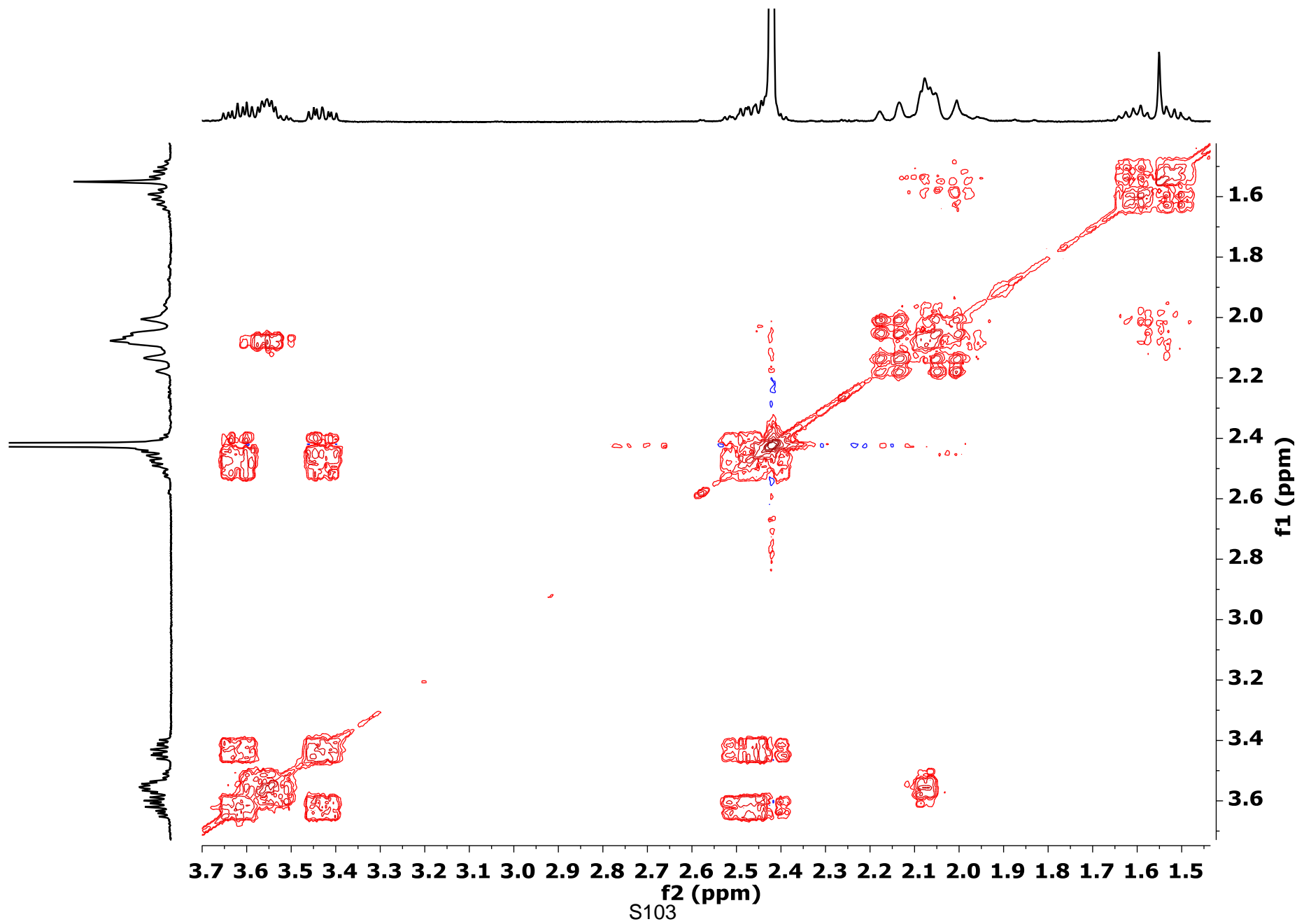
2D NMR HMBC



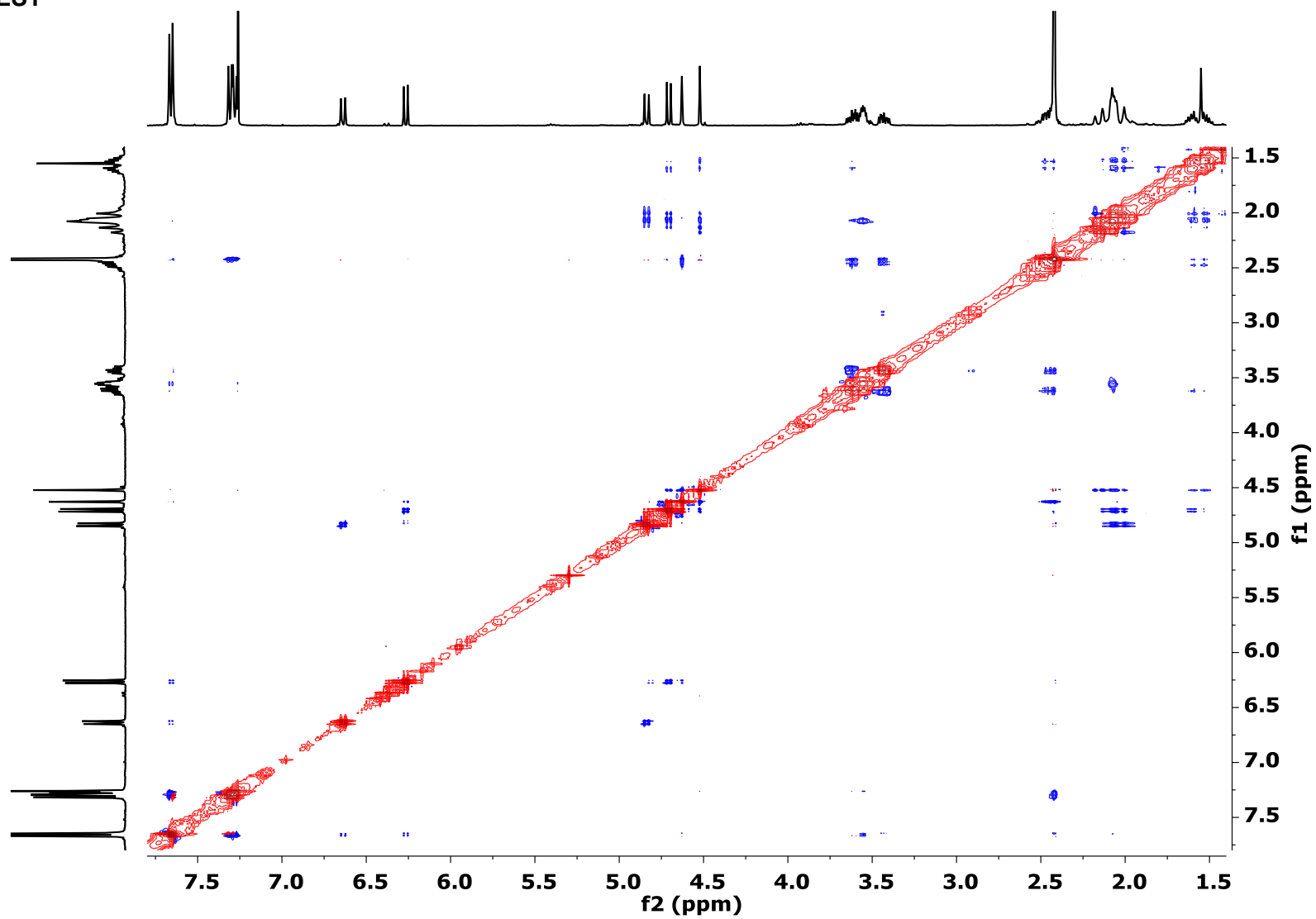
2D NMR COSY

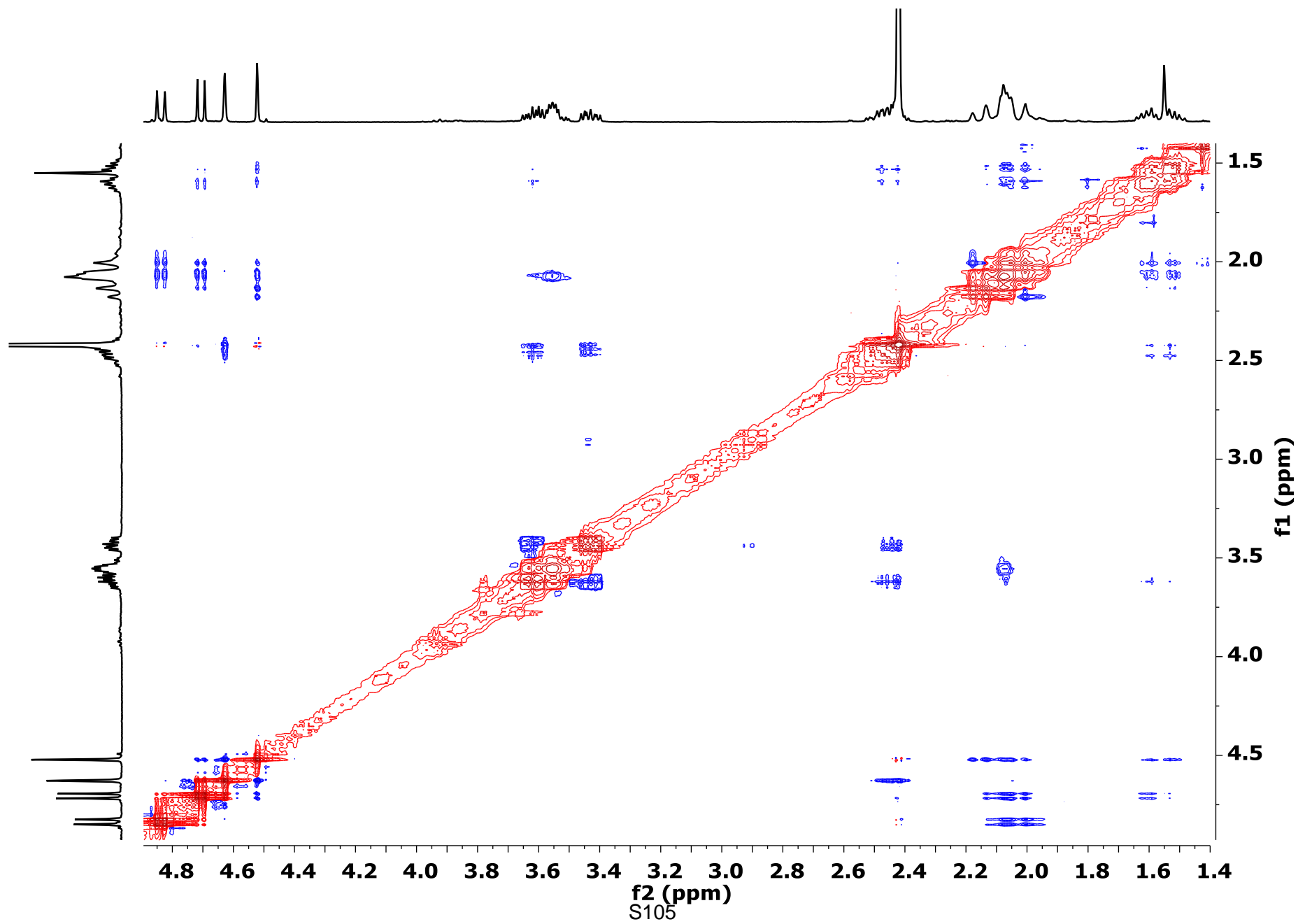


S102



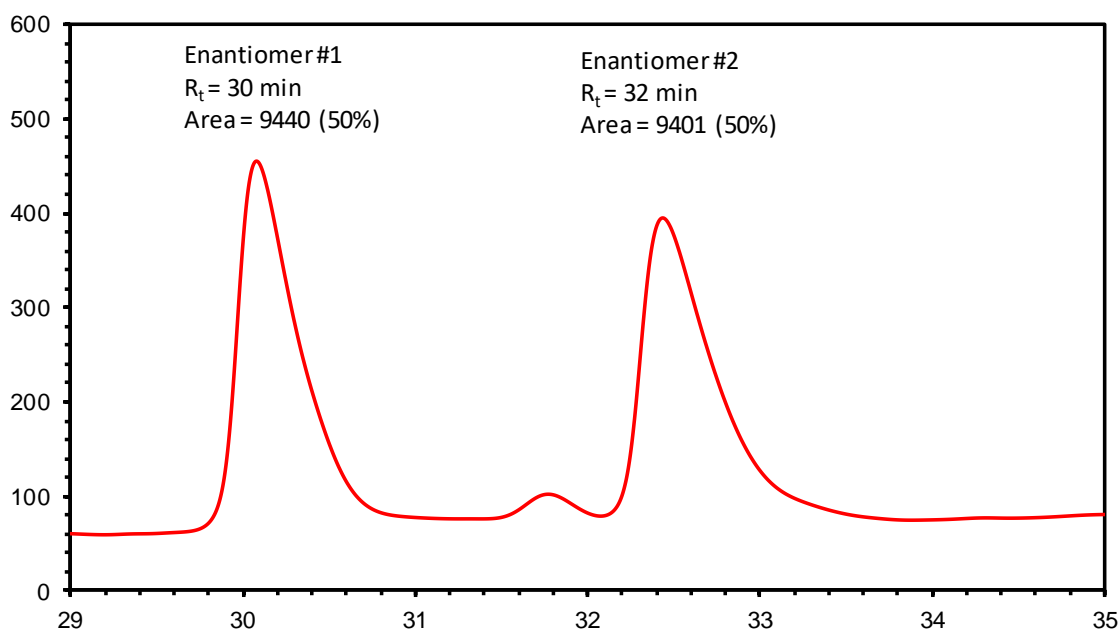
2D NMR NOESY





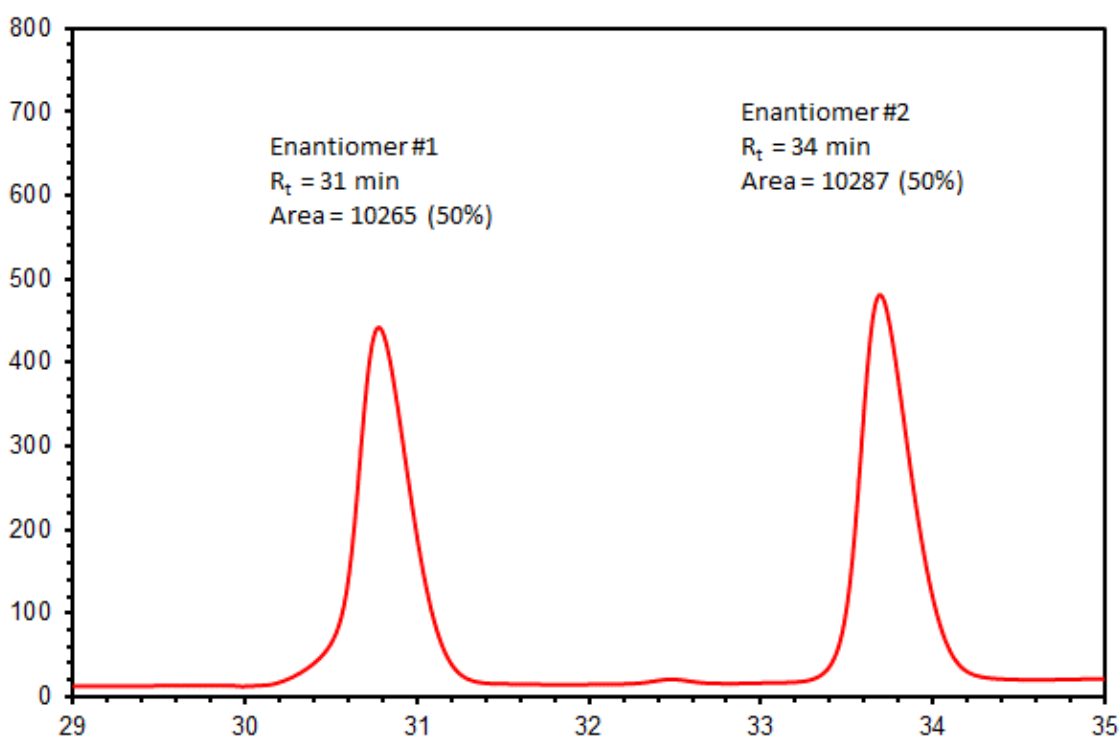
HPLC

Figure S1. HPLC trace of compound 3aa obtained using (\pm)-BINAP as a phosphine ligand.



Conditions: Chiralpak IA column (4.6 x 250 mm, 5 μ m); 1 mL/min flow rate; 100% hexane \rightarrow 20% 2-propanol in hexane; 40 min.; $\lambda = 254$ nm.

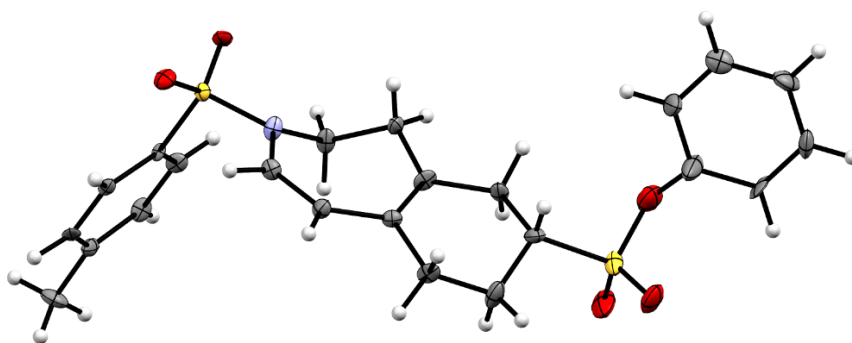
Figure S2. HPLC trace of compound 3aa obtained under optimal conditions, using (*R*)-DTBM-Segphos as a phosphine ligand.



Conditions: Chiralpak IA column (4.6 x 250 mm, 5 μ m); 1 mL/min flow rate; 100% hexane \rightarrow 20% 2-propanol in hexane; 40 min.; $\lambda = 254$ nm.

Crystal structure of compound 3am

Figure S3: ORTEP representation of compound 3am with probability level of 30%.



Colourless needle-like crystals of **3am** were grown at 2-6 °C using a layered solution approach. The bottom solution layer, contained within a long straight tube, consisted of the compound **3am** dissolved in CH₂Cl₂. Pentane was carefully placed on top using a syringe. The X-ray intensity data were measured on a three-circle diffractometer system equipped with a Ceramic x-ray tube (Mo K α , λ = 0.71073 Å) and a doubly curved silicon crystal Bruker Triumph monochromator.

A total of 546 frames were collected. The total exposure time was 9.10 hours. The frames were integrated with the Bruker SAINT software package using a narrow-frame algorithm. The integration of the data using a **monoclinic** unit cell yielded a total of **15117** reflections to a maximum θ angle of **27.55°** (**0.77** Å resolution), of which **4959** were independent (average redundancy **3.048**, completeness = **98.7%**, R_{int} = **4.56%**, R_{sig} = **5.51%**) and **4430** (**89.33%**) were greater than $2\sigma(F^2)$. The final cell constants of a = **11.7010(15)** Å, b = **7.8929(11)** Å, c = **11.8094(14)** Å, β = **94.717(4)°**, volume = **1087.0(2)** Å³, are based upon the refinement of the XYZ-centroids of **8874** reflections above $20\sigma(I)$ with **6.214°** < 2θ < **54.22°**. Data were corrected for absorption effects using the Multi-Scan method (SADABS). The ratio of minimum to maximum apparent transmission was **0.619**. The calculated minimum and maximum transmission coefficients (based on crystal size) are **0.9080** and **0.9780**.

The structure was solved and refined using the Bruker SHELXTL Software Package, using the space group **P 1 21 1**, with Z = **2** for the formula unit, **C₂₃H₂₅NO₅S₂**. The final anisotropic full-matrix least-squares refinement on F^2 with **270** variables converged at $R1$ = **12.75%**, for the observed data and $wR2$ = **33.18%** for all data. The goodness-of-fit was **1.109**. The largest peak in the final difference electron density synthesis was **2.362** e⁻/Å³ and the largest hole was **-0.894** e⁻/Å³ with an RMS deviation of **0.176** e⁻/Å³. On the basis of the final model, the calculated density was **1.404** g/cm³ and $F(000)$, **484** e⁻.

Table S2. Sample and crystal data for 3am.

Identification code	vilavadri1_2on	
Chemical formula	C ₂₃ H ₂₅ NO ₅ S ₂	
Formula weight	459.56 g/mol	
Temperature	100(2) K	
Wavelength	0.71073 Å	
Crystal size	0.080 x 0.100 x 0.350 mm	
Crystal habit	colorless needle	
Crystal system	monoclinic	
Space group	P 1 21 1	
Unit cell dimensions	a = 11.7010(15) Å	α = 90°
	b = 7.8929(11) Å	β = 94.717(4)°
	c = 11.8094(14) Å	γ = 90°
Volume	1087.0(2) Å ³	
Z	2	
Density (calculated)	1.404 g/cm ³	
Absorption coefficient	0.281 mm ⁻¹	
F(000)	484	

Table S3. Data collection and structure refinement for 3am.

Diffractometer	Bruker D8 QUEST ECO three-circle diffractometer	
Radiation source	Ceramic x-ray tube (Mo Kα, λ = 0.71073 Å)	
Theta range for data collection	3.11 to 27.55°	
Index ranges	-15 ≤ h ≤ 15, -10 ≤ k ≤ 10, -13 ≤ l ≤ 15	
Reflections collected	15117	
Independent reflections	4959 [R(int) = 0.0456]	
Coverage of independent reflections	98.7%	
Absorption correction	Multi-Scan	
Max. and min. transmission	0.9780 and 0.9080	
Structure solution technique	direct methods	
Structure solution program	SHELXT 2014/5 (Sheldrick, 2014)	
Refinement method	Full-matrix least-squares on F ²	
Refinement program	SHELXL-2017/1 (Sheldrick, 2017)	
Function minimized	Σ w(F _o ² - F _c ²) ²	
Data / restraints / parameters	4959 / 1 / 270	
Goodness-of-fit on F ²	1.109	
Final R indices	4430 data; I > 2σ(I)	R1 = 0.1275, wR2 = 0.3229
	all data	R1 = 0.1388, wR2 = 0.3318
Weighting scheme	w = 1/[σ ² (F _o ²) + (0.1482P) ² + 10.0620P] where P = (F _o ² + 2F _c ²)/3	
Absolute structure parameter	0.3(3)	
Largest diff. peak and hole	2.362 and -0.894 eÅ ⁻³	

R.M.S. deviation from mean 0.176 eÅ⁻³

Table S4. Atomic coordinates and equivalent isotropic atomic displacement parameters (Å²) for 3am.

U(eq) is defined as one third of the trace of the orthogonalized U_{ij} tensor.

	x/a	y/b	z/c	U(eq)
S22	0.7508(2)	0.7786(4)	0.4966(2)	0.0187(5)
S8	0.3208(2)	0.2537(5)	0.9766(2)	0.0328(8)
O7	0.2231(11)	0.3852(16)	0.9631(11)	0.055(3)
O9	0.2747(11)	0.0761(16)	0.9868(11)	0.054(3)
O10	0.3974(10)	0.299(2)	0.0674(9)	0.067(4)
O23	0.6954(7)	0.9390(11)	0.5040(9)	0.033(2)
O24	0.7636(8)	0.7001(12)	0.3889(7)	0.0304(19)
N16	0.6753(9)	0.6437(13)	0.5674(9)	0.026(2)
C1	0.1129(5)	0.3162(18)	0.9130(8)	0.081(9)
C2	0.0361(7)	0.2471(16)	0.9841(6)	0.043(4)
C3	0.9196(6)	0.2440(14)	0.9501(7)	0.041(3)
C4	0.8797(5)	0.3100(14)	0.8451(8)	0.045(4)
C5	0.9565(8)	0.3791(13)	0.7740(6)	0.037(3)
C6	0.0731(7)	0.3822(16)	0.8080(7)	0.050(4)
C11	0.3904(11)	0.272(2)	0.8482(10)	0.035(3)
C12	0.4224(10)	0.4510(14)	0.8256(12)	0.027(2)
C13	0.5061(11)	0.4671(14)	0.7322(10)	0.024(2)
C14	0.5154(10)	0.6445(15)	0.6939(11)	0.025(2)
C15	0.6381(10)	0.7007(14)	0.6792(11)	0.027(2)
C17	0.6890(10)	0.4717(15)	0.5488(10)	0.024(2)
C18	0.6430(11)	0.3379(16)	0.6040(10)	0.026(2)
C19	0.5647(10)	0.3317(14)	0.6954(9)	0.021(2)
C20	0.5449(13)	0.1513(16)	0.7395(11)	0.031(3)
C21	0.4875(14)	0.1507(18)	0.8506(13)	0.041(3)
C25	0.8875(8)	0.7910(13)	0.5702(7)	0.0132(17)
C26	0.9767(10)	0.7015(13)	0.5319(9)	0.021(2)
C27	0.0861(10)	0.7148(15)	0.5913(11)	0.026(2)
C28	0.1024(10)	0.8117(17)	0.6897(11)	0.032(3)
C29	0.0115(10)	0.9051(15)	0.7243(10)	0.025(2)
C30	0.9029(10)	0.8939(14)	0.6667(10)	0.023(2)
C31	0.2176(11)	0.8270(19)	0.7568(12)	0.037(3)

Computational methods

Geometries of all stationary points were optimized without symmetry constraint with the Gaussian 09 program⁶ using the DFT B3LYP hybrid exchange-correlation functional.^{7–9} The all-electron cc-pVDZ basis set^{10,11} was employed for non-metal atoms and the cc-pVDZ-PP basis set¹⁰ containing an effective core relativistic pseudopotential was used for Rh. The electronic energy was improved by performing single point energy calculations with the cc-pVTZ (cc-pVTZ-PP for Rh) basis set and the M06L functional¹¹ and including solvent effects corrections computed with the solvent model based on density (SMD) continuum solvation.¹² To mimic the experimental solvent mixture with a molar fraction ratio of 76:24 of THF:CH₂Cl₂, the values of the solvent descriptors used in the SMD solvation model were re-defined on the basis of a linear behavior with the molar fraction. Using the “Solvent=(Generic,Read)” options of the Gaussian09 SCRF keyword, the solvent mixture was defined employing the following solvent descriptors: Dynamic Dielectric Constant=1.410; Static Dielectric Constant=1.4085; Abraham’s hydrogen bond acidity=0.02424; Abraham’s hydrogen bond basicity=0.3758; Surface Tension=39.3697; Carbon Aromaticity=0; Electronegativity Halogenicity=0.1617. The D3 Grimme energy corrections for dispersion¹³ with the original damping function were added in all B3LYP/cc-pVDZ-PP and M06L/cc-pVTZ-PP calculations. Analytical Hessians were computed to determine the nature of stationary points (one and zero imaginary frequencies for TSs and minima, respectively) and to calculate unscaled zero-point energies (ZPEs) as well as thermal corrections and entropy effects using the standard statistical-mechanics relationships for an ideal gas.¹⁴ These two latter terms were computed at 313.15 K and 1 atm to provide the reported relative Gibbs energies. As a summary, the reported Gibbs energies contain electronic energies including solvent effects calculated at the M06L-D3/cc-pVTZ-PP//B3LYP-D3/cc-pVDZ-PP level together with gas phase thermal and entropic contributions computed at 313.15 K and 1 atm with the B3LYP-D3/cc-pVDZ-PP method. The catalytic species employed for computational modelling is [Rh(BINAP)]⁺, noted as **[Rh]** in figures for simplification purposes. All stationary points were unambiguously confirmed by IRC calculations.

Figure S4. Molecular structures of (a) **TS A1A2**, (b) **TS A2A3**, (c) **TS A3A4**, (d) **TS A3'B1**, (e) **TS A5-3aa'** and (f) **TS A5-3aa**. Distances are given in Angstroms (Å). Hydrogen atoms not shown for clarity.

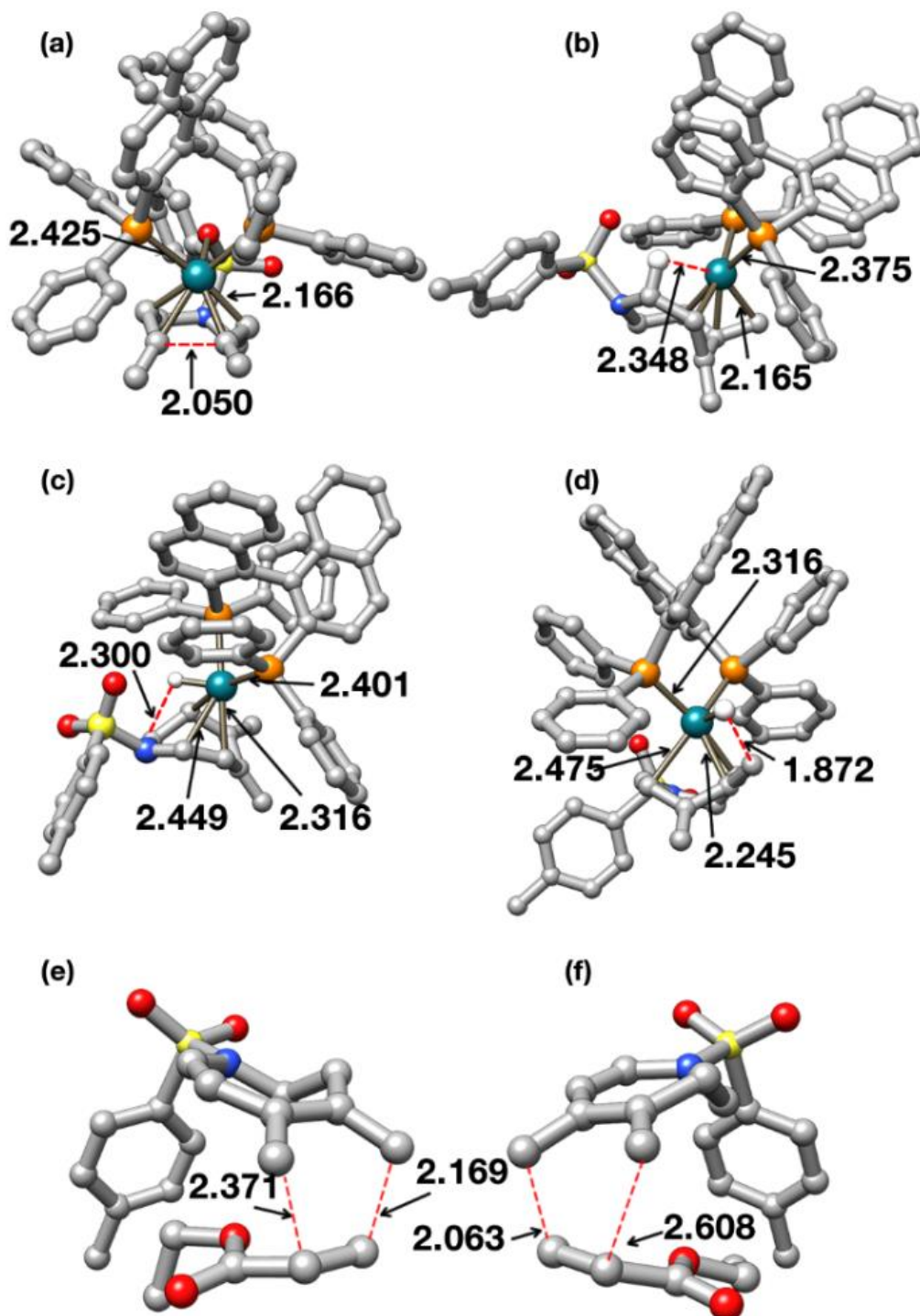


Figure S5. M06L-D3/cc-pVTZ-PP/SMD(76% THF, 24% CH₂Cl₂)/B3LYP-D3/cc-pVDZ-PP Gibbs energy profile for the tandem cycloisomerisation/Diels-Alder cycloaddition of 1,5-bisallene **1a** and ethyl acrylate catalysed by [Rh(BINAP)]⁺. **Alternative reaction path:** Diels-Alder cycloaddition involving intermediate **A4**.

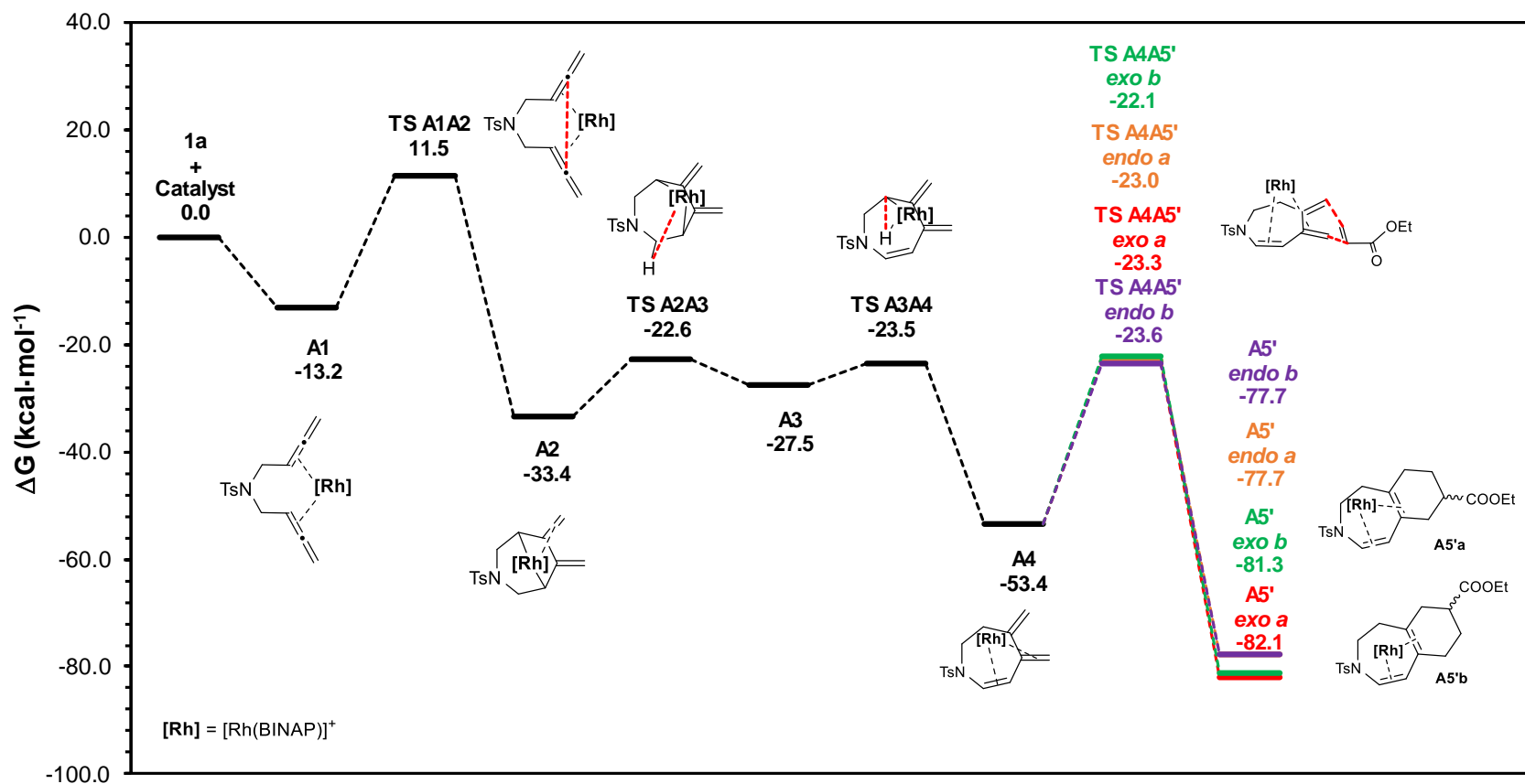


Figure S6. M06L-D3/cc-pVTZ-PP/SMD(76% THF, 24% CH₂Cl₂)/B3LYP-D3/cc-pVDZ-PP Gibbs energy profile for the tandem cycloisomerisation/Diels-Alder cycloaddition of 1,5-bisallene **1a** and ethyl acrylate catalysed by [Rh(BINAP)]⁺. **Alternative reaction path:** Diels-Alder cycloaddition involving intermediate **A3**.

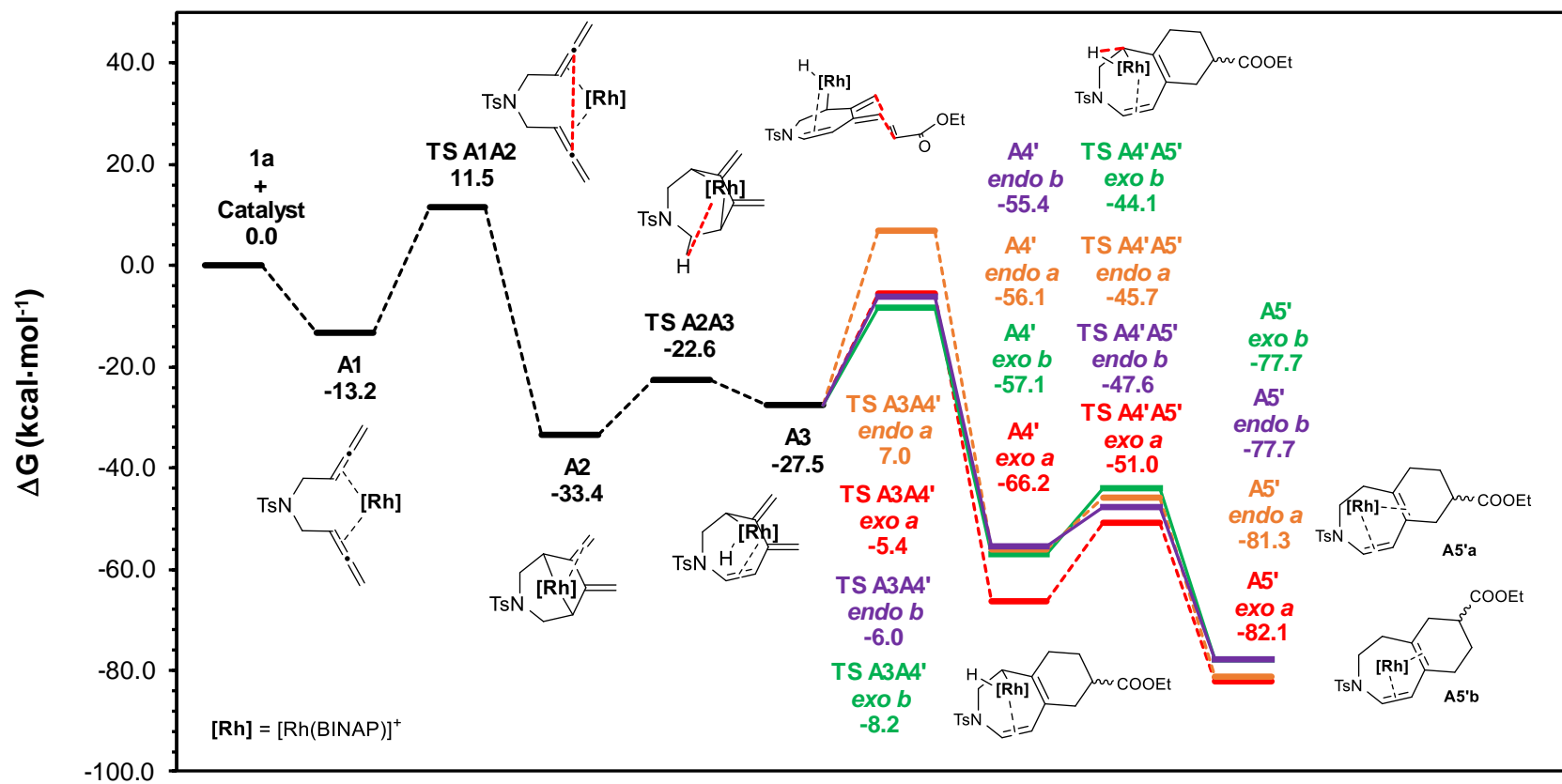


Figure S7. M06L-D3/cc-pVTZ-PP/SMD(76% THF, 24% CH₂Cl₂)/B3LYP-D3/cc-pVDZ-PP Gibbs energy profile for the tandem cycloisomerisation/Diels-Alder cycloaddition of 1,5-bisallene **1a** and ethyl acrylate catalysed by [Rh(BINAP)]⁺. **Alternative reaction path:** Diels-Alder cycloaddition involving intermediate **A2**.

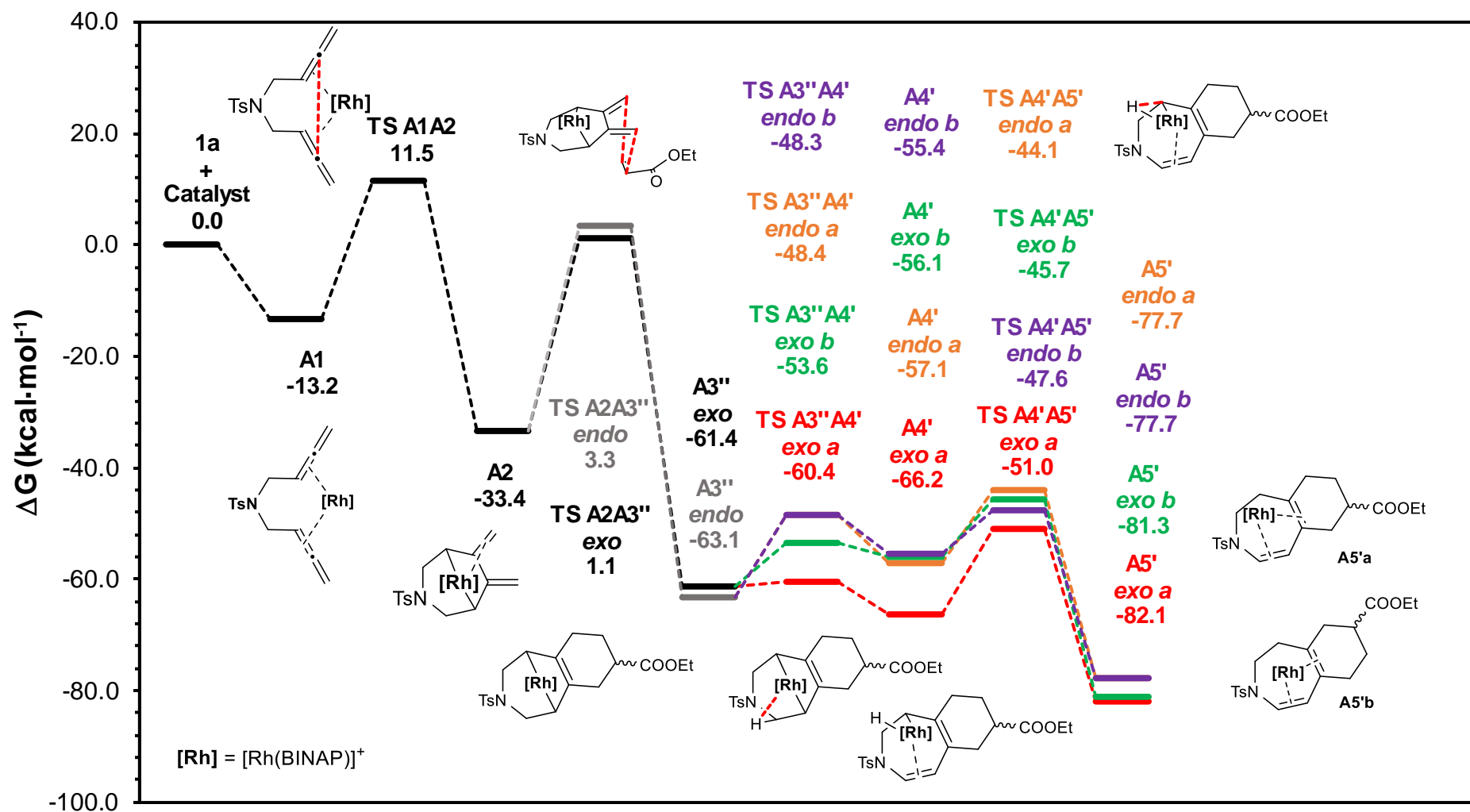
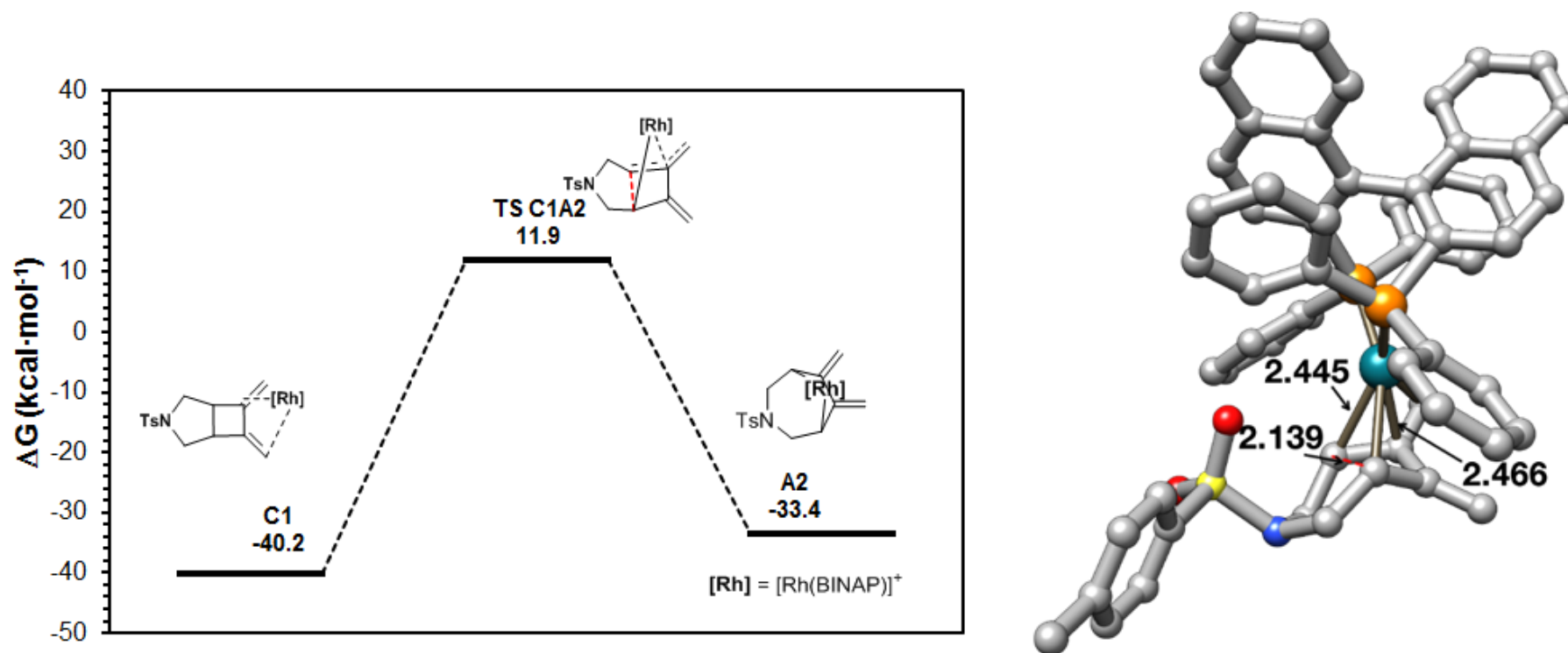


Figure S8. (a) M06L-D3/cc-pVTZ-PP/SMD(76% THF, 24% CH₂Cl₂)/B3LYP-D3/cc-pVDZ-PP Gibbs energy profile for the transformation of intermediate **C1** into intermediate **A2** catalysed by [Rh(BINAP)]⁺. (b) Molecular structure of **TS C1A2**. Distances are indicated in Angstroms (Å). ΔG relative to **1a** + catalyst. Hydrogen atoms suppressed for clarity.



Intermediate **C1** (Chart 1) has to surmount a Gibbs energy barrier of 52.1 kcal/mol (**TS C1A2**) in order to be transformed into **A2**. The backward process is not energetically feasible either (**TS A2C1**, $\Delta G^\ddagger = 45.3$ kcal/mol). Taken together, all these results show that the byproduct **5a** must be formed by a completely independent mechanism involving a Rh(I)-catalyzed [2+2] cycloaddition of the internal C=C bonds of 1,5-bisallene **1a**.¹⁵

Computational data

All DFT data obtained within this study are provided through the following link:

<https://iochem.udg.edu:8443/browse/review-collection/100/660/236d90b68e822f98633662d5>

References

- (1) Hashmi, A. S. K.; Häffner, T.; Rudolph, M.; Rominger, F. Gold Catalysis: Domino Reaction of En-Diynes to Highly Substituted Phenols. *Chem. - A Eur. J.* **2011**, *17*, 8195–8201.
- (2) Kang, S.-K.; Baik, T.-G.; Kulak, A. N.; Ha, Y.-H.; Lim, Y.; Park, J. Palladium-Catalyzed Carbocyclization/Silastannylation and Distannylation of Bis(Allenenes). *J. Am. Chem. Soc.* **2000**, *122*, 11529–11530.
- (3) Lu, P.; Ma, S. Observation of New Cycloisomerization Pattern of 1,5-Bisallenenes. Catalyst and Substituent Effects. *Org. Lett.* **2007**, *9*, 2095–2097.
- (4) Lu, P.; Kuang, J.; Ma, S. Carbon-Carbon Double-Bond Isomerization and Diels-Alder Reaction of Dimethyl 5-Methylene-4-Isopropylidene-2-Cycloheptene-1,1-Dicarboxylate with Dienophiles. *Synlett* **2010**, *2010*, 227–230.
- (5) Kawamura, T.; Inagaki, F.; Narita, S.; Takahashi, Y.; Hirata, S.; Kitagaki, S.; Mukai, C. Rhodium(I)-Catalyzed Intramolecular Carbonylative [2+2+1] Cycloadditions and Cycloisomerizations of Bis(Sulfonylallene)s. *Chem. - A Eur. J.* **2010**, *16*, 5173–5183.
- (6) Gaussian 09, Revision E.01, Frisch, M. J.; Trucks, G. W.; Schlegel, H. B.; Scuseria, G. E.; Robb, M. A.; Cheeseman, J. R.; Scalmani, G.; Barone, V.; Mennucci, B.; Petersson, G. A.; Nakatsuji, H.; Caricato, M.; Li, X.; Hratchian, H. P.; Izmaylov, A. F.; Bloino, J.; Zheng, G.; Sonnenberg, J. L.; Hada, M.; Ehara, M.; Toyota, K.; Fukuda, R.; Hasegawa, J.; Ishida, M.; Nakajima, T.; Honda, Y.; Kitao, O.; Nakai, H.; Vreven, T.; Montgomery, J. A., Jr.; Peralta, J. E.; Ogliaro, F.; Bearpark, M.; Heyd, J. J.; Brothers, E.; Kudin, K. N.; Staroverov, V. N.; Kobayashi, R.; Normand, J.; Raghavachari, K.; Rendell, A.; Burant, J. C.; Iyengar, S. S.; Tomasi, J.; Cossi, M.; Rega, N.; Millam, J. M.; Klene, M.; Knox, J. E.; Cross, J. B.; Bakken, V.; Adamo, C.; Jaramillo, J.; Gomperts, R.; Stratmann, R. E.; Yazyev, O.; Austin, A. J.; Cammi, R.; Pomelli, C.; Ochterski, J. W.; Martin, R. L.; Morokuma, K.; Zakrzewski, V. G.; Voth, G. A.; Salvador, P.; Dannenberg, J. J.; Dapprich, S.; Daniels, A. D.; Farkas, Ö.; Foresman, J. B.; Ortiz, J. V.; Cioslowski, J.; Fox, D. J. Gaussian, Inc., Wallingford CT, 2009.
- (7) Stephens, P. J.; Devlin, F. J.; Chabalowski, C. F.; Frisch, M. J. Ab Initio Calculation of Vibrational Absorption and Circular Dichroism Spectra Using Density Functional Force Fields. *J. Phys. Chem.* **1994**, *98*, 11623–11627.
- (8) Becke, A. D. Density-functional Thermochemistry. III. The Role of Exact Exchange. *J. Chem. Phys.* **1993**, *98*, 5648–5652.
- (9) Lee, C.; Yang, W.; Parr, R. G. Development of the Colle-Salvetti Correlation-Energy Formula into a Functional of the Electron Density. *Phys. Rev. B* **1988**, *37*, 785–789.
- (10) Dunning, T. H. Gaussian Basis Sets for Use in Correlated Molecular Calculations. I. The

Atoms Boron through Neon and Hydrogen. *J. Chem. Phys.* **1989**, *90*, 1007–1023.

- (11) Woon, D. E.; Dunning, T. H. Gaussian Basis Sets for Use in Correlated Molecular Calculations. III. The Atoms Aluminum through Argon. *J. Chem. Phys.* **1993**, *98*, 1358–1371.
- (12) Marenich, A. V.; Cramer, C. J.; Truhlar, D. G. Universal Solvation Model Based on Solute Electron Density and on a Continuum Model of the Solvent Defined by the Bulk Dielectric Constant and Atomic Surface Tensions. *J. Phys. Chem. B* **2009**, *113*, 6378–6396.
- (13) Grimme, S.; Antony, J.; Ehrlich, S.; Krieg, H. A Consistent and Accurate Ab Initio Parametrization of Density Functional Dispersion Correction (DFT-D) for the 94 Elements H-Pu. *J. Chem. Phys.* **2010**, *132*, 154104.
- (14) Atkins, P.; De Paula, J. *The Elements of Physical Chemistry*, 3rd ed.; Oxford University Press: Oxford, 2006.